RÉPUBLIQUE DU CAMEROUN
Paix-Travail-Patrie
* * * * * * * * * *
UNIVERSITÉ DE YAOUNDÉ I
* * * * * * * * * *
CENTRE DE RECHERCHE ET DE FORMATION DOCTORALE EN SCIENCES TECHNOLOGIE ET GÉOSCIENCES
* * * * * * * * *
UNITÉ DE RECHERCHE ET DE FORMATION DOCTORALE EN PHYSIQUE ET APPLICATIONS
BP : 812 Yaoundé
Email : crfd@uy1.uninet.cm

REPUBLIC OF CAMEROON
Peace-Work-Fatherland
* * * * * * * * *
UNIVERSITY OF YAOUNDE I
* * * * * * * * *
POSTGRADUATE SCHOOL OF SCIENCE TECHNOLOGY AND GEOSCIENCES
* * * * * * * * *
RESEARCH AND POSTGRADUATE TRAINING UNIT FOR PHYSICS AND APPLICATIONS
P.O. Box : 812 Yaounde
Web Site : www.uy1researchstg.cm

SELF-ORGANIZATION OF DISSIPATIVE SOLITONS IN NONLINEAR METAMATERIALS BEYOND THE SLOWLY VARYING ENVELOPE APPROXIMATION

THÈSE

Présentée en vue de l'obtention du diplôme de Doctorat/Ph.D de

Physique Option : Mécanique, Matériaux et Structures

Par :

MEGNE TIAM Laure

***Matricule :* 10W1318**

Master en Physique, Option Mécanique et Matériaux

Sous la direction de :

KOFANE TIMOLEON Crépin

Professeur

Le 5 juin 2023

REPUBLIC OF CAMEROON **UNIVERSITY OF YAOUNDE I**

REPUBLIQUE DU CAMEROUN ***UNIVERSITE DE YAOUNDE I***

FACULTY OF SCIENCE

FACULTE DES SCIENCES

DEPARTMENT OF PHYSICS

DEPARTEMENT DE PHYSIQUE

Laboratory of Mechanics, Materials and Structures

Laboratoire de Mécanique, Matériaux et Structures

SELF-ORGANIZATION OF DISSIPATIVE SOLITONS IN NONLINEAR METAMATERIALS BEYOND THE SLOWLY VARYING ENVELOPE APPROXIMATION

Submitted in Partial Fulfillment of the award

for the Degree of Doctor of Philosophy in Physics

Laboratry: **Mechanics, Material and Structures**

Option: **Mechanics and Complex Systems**

by

MEGNE TIAM LAURE

M. Sc. in Physics

Registration Number: ***10W1318***

Under the Supervision of:

KOFANE Timoléon Crépin

Professor, UYI

Academic year 2022

Contents

List of Figures

Dedications

My first and foremost dedication is devoted to our almighty **God** who takes care of us every day and guides us on the straight way.

To my late grandfather **Mr. TAFO Gerôme**,and grandmother **Mrs. SIDZE Marie**.

To my father **Mr. TIAM Jean**, and his wife Mrs.TIAM born **METIAVE Chantale**.

To my daugher **Mrs. FONGANG BOGHE Eva Manuella**.

Acknowledgments

Firstly, I would like to express my sincere gratitude to **God** almighty who gave me the life, the opportunity and the knowledge to reach and to end with the PhD study level.

I have furthermore to thank the persons responsible of the Faculty of Sciences, and the Research and postgraduate training unit for physics and applications who gave and confirmed the permission to go ahead with my thesis.

I would like to express all my gratitude and my deep appreciation to my thesis supervisor, Professor KOFANE Timoléon Crépin, for his unfailing availability, his remarks, his advice and above all his rigor in his work despite his various occupations of all kinds. As a teacher, its works on soliton's theories , "chaos" and their applications, earned him in 2014 the first ever continental price **Kwame Nkrumah** of the African Union. I was totally new to the field of solitary wave research in nonlinear metamaterials, but the vast knowledge of him inspired me a lot and his competence in this field helped me to quickly grasp the concepts. He never gave me too much pressure at work and always gave me the freedom to work. I express my sincere gratitude to him for his constant encouragement, motivation and friendly nature that gives me the courage to consult him at at any time. I owe him a deep respect for his collaboration and his help during this thesis work. Apart from a guide he is a wonderful person and I am lucky to have his support during my research term. Her helping attitude, her sincerity in her work, her unwavering courage and conviction will always inspire me and I hope to continue to work with his noble thoughts.

Professor Conrad Bertrand Tabi it is with great satisfaction that I extend my sincere thanks to him. He is very careful, and very demanding. From the research initiation phase to the thesis, he instilled in me the spirit of precision. We have faced several challenges together, and he has always been able to give me reason to continue. His generosity and his advice gave me the strength not to sink.

For this thesis, I would like to thank the different members of the jury.

I would like to thank **Pr. NDJAKA Jean Marie Bienvenu**, Head of the Department of Physics. I am very grateful for his administrative contribution and encouragement.

I am grateful to **Pr. WOAFO Paul**, Chairman of the Cameroon Physical Society for his teaching, particularly in numerical methods.

It would be very pleasing to recognize trade and constructive discussions combined with great moments of sharing with all the teachers of the Department of Physics. I have named: **Pr. BOUETOU BOUETOU Thoma**, **Pr. PEMHA ELKANA**, **Pr. Clement TCHAWOUA**, **Pr. YMELE David**, **Pr. PELAP François Berçeau**, **Pr. Germain Hubert BEN-BOLIE**, **Pr. SIEWE SIEWE Martin**, **Pr.Serge Ibraïd FEWO Pr. Germaine DJUDJE**, **Pr. Jacque HONA**, **Pr. NANA Benjo**, and **Dr. MVOGO Alain**, for their daily support and especially for their moral support when i was sometimes tempted to get discouraged by the rebellious criticism of some reviewers.

The fulfillment of my thesis is the work of the good atmosphere in my family. I would like to thank:

My brothers and sisters **MEKOAGNE Epiphanie** and her husband **KENGNE Duclaire**, Mrs **MEDAVE Vanessa**, Mrs **MOTIE TIAM yden**, **KAHEGAM TIAM Oriane** , Mrs **MEGNE POULINOUO Beribelle**, Mr **TCHEGUEM TIAM Franklin**. I thank all of them for their moral and financial supports and for all their prayers for me.

I thank all my uncles, aunts, cousins, nephews and nieces in particular Mr. **TAGNE Samuel** for his constant support. Mr. **OUAFO Richard**, Mr. **FOTIE Roger**, Mr **FOKA Robert**, Mrs. **MOTIE TAFFO Rose**. I do not forget here my friends **TEKAM NEKAM Carlos**, **MEKAHA POULINOUO Christelle**, **TIEMDJO Charlie**, for the constant affection and joy that they have always given me.

I would also like to thank all my Ph.D mates of the laboratory of mechanics, Material and Structure of the University Yaounde I for their contributions. A special thanks to **Dr. DJOKO Martin**, **Dr. DJAZET Alain**, **Dr. Zanga Dieudonné**, **Mme AMBASSA OTSOBO Jenny Alban**, **Mme GANYOU Stephanie**, for playing a very important accompanying role since I started this thesis.

I am also thankful to all my committee members and international reviewers for their

stimulating questions on this work. Thank you to have agreed to discuss and appreciate the results of this thesis.

I greatly thank the **FONGANG** family, for their support after the death of the father of my child (my darling **(FONGANG Emmanuel)**), thank you mom **DABOU Jaqueline** for your support, moral, financial for your little niece

Finally, there are a lot of them and they will certainly recognize themselves, my thanks go to all those who have contributed from near or far for the achievement of this work of mine and whose names are not listed here. I would like to express my gratitude to them.

Abstract

We study theoretically and numerically the modulation instability of plane waves in the complex cubic-quintic at (3+1)-dimension Ginzburg-Landau equation, and we present the evolution of various dissipative optical light bullet characterized by different topological charges in the complex cubic-quintic-septic at (3+1)-dimension Ginzburg-Landau equation, which describes the dynamics of light bullet in nonlinear metamaterials.

We introduce a new equation (cubic-quintic-septic (3+1)-dimensional complex Ginzburg-Landau equation) for the propagation of impulses in materials with negative refractive index, considering the theory of electromagnetic waves from the equations by Maxwell. This new nonlinear model is derived beyond the slowly varying field envelope approximation, which is affected by emerging physical mechanisms. These are linear loss, diffusion, higher-order dispersion effects, cubic, quintic and septic nonlinearities, as well as cubic, quintic and septic self-steepening effects. When studying the modulation instability with the complex cubic-quintic (3+1)-dimensional Ginzburg-Landau equation, the analytical results are confronted with the numerical results and are fully in agreement with the predictions of the gain spectra.

The analysis of the modulation instability of the system was carried out analytically, using the linear stability analysis which allows us to plot curves giving the instability gain, and numerically, using direct simulations of the Fourier space of the proposed nonlinear wave equation, based on Drude's model. Choosing a specific set of parameters allows us to generate a stable propagation of dissipative light bullets.

Keywords: Metamaterials, Complex Ginzburg-Landau equation, Linear stability, Split-Step Fourier Method, Solitons.

Résumé

Nous étudions théoriquement et numériquement l'instabilité de modulation des ondes planes dans les équations de Ginburg-Landau complexe Cubique-quintique à (3+1)-dimention, et nous presentons l'évolution de diverses balles de lumineuses optiques dissipative caracterisées par différentes charges topologiques dans l'équation de Ginzburg-Landau complexe cubique-quintique-septique à (3+1)-dimension, qui décrit la dynamique des balles lumineuses dans les métamatériaux non linéaires.

Nous introduisons une nouvelle équation(équation de Ginzburg-Landau complexe cubique-quintique-septique (3+1)-dimension) pour la propagation des impulsions dans les matériaux à indice de réfraction négatif, en considérant la théorie des ondes électromagnétiques à partir des équations de Maxwell. Ce nouveau modèle non linéaire est dérivée au-delà de l'approximation de l'enveloppe de champ lentement variable, qui est affecté par des mécanismes physique qui apparaissent. Il s'agit des effets de perte linéaire, de diffusion, de dispersion d'ordre superieure, des nonlinéairités cubique, quintique et septique, ainsi que les effets de auto-raidissement cubique, quintique et septique. Lors de l'étude de l'instabilité de modulation avec équation de Ginzburg-Landau complexe cubique-quintique (3+1)-dimension , les résultats analytiques sont confrontés aux résultats numériques et sont entièrement en accord avec les prédictions des spectres de gains.

L'analyse de l'instabilité de modulation du système a été realisé analytiquement, en utilisant l'analyse de la stabilité linéaire qui nous permet de tracer des courbes donnant le gain d'instabilité, et numériquement, en utilisant des simulations directes de l'espace dans Fourier de l'équation d'onde non linéaire proposée, basée sur le modèle de Drude. Le choix d'un ensemble spécifique de paramètres nous permet de générer une propagation stable de balles lumineuses dissipatives .

Mots clés: Métamatériaux, équation de Ginzburg-Landau complexe, stabilité linéaire, Méthode de Fourier à pas divisé, Solitons.

List of abbreviations

Acronym	Meaning
MMs:	Metamaterials
NIM:	Negative index material
SEVA:	Slowy varing envelope approximation
SEWA:	Slowy evolving wave approximation
MI:	Modulation instability
XPM:	Cross-Phase Modulation
SPM:	Self-Phase Modulation
1D:	One-dimensional
2D:	Two-dimensional
3D:	Three-dimensional
STS:	Spatiotemporal Solitons
GVD:	Group Velocity Dispersion
CGL:	Complex Ginzburg-Landau
CQ-CGL:	Cubic-quintic Complex Ginzburg-Landau
BECs:	Bose-Einstein Condensates
NLS:	Nonlinear Schrödinger
SSFM:	Split-Step Fourier Method

Acronym	Meaning
PMD:	Polarization Mode-Dispersion
CW:	Continuous Wave
CV:	Collective Variable
DS:	Dissipative Soliton
PDE:	Partial Differential Equation
FODEs:	First-Order Differential Equations
ODEs:	Ordinary Differential Equations
SVS:	Stabilized Vector Solitons
NDFA:	Normal Dispersion Fiber Amplifier

General Introduction

The search for materials with extraordinary properties has always been one of the obsessions of the man. The science of metamaterials, which appeared at the end of the 20th century, marks a turning point important concept. Indeed, until now, the properties of materials were always governed by the atomic properties of the constituent elements. The innovative principle of metamaterials is to fashion artificial resonators whose properties of electromagnetic fields dominate the response of the atoms and make it possible to generate a radically different optical behavior **[1]**.

New electromagnetic properties could be realized by creating a composite artificial structure consisting of well-arranged functional inclusions of dimensions sub-wavelength. Generally, the size of the unit cells of these artificial structures is much smaller than the wavelength of interest and the electromagnetic response of such structures are expressed in terms of homogenized and effective material parameters **[1]**. These artificial structures, created by man, are called metamaterials. Although there is no universal definition of the term "metamaterial", we prefer the following definition proposed by W. Cai and V. Shalaev **[2]**: "A metamaterial is an artificially structured material which acquires its properties from of the structural unit rather than the constituent materials. A metamaterial has a scale of inhomogeneity that is much smaller than the wavelength of interest, and its electromagnetic response is expressed in terms of the parameters of homogenized materials". One of the most fascinating example of such structures is the so-called negative-index metamaterials (NIM).

Indeed, metamaterials, also called "left-hand materials", are a structuring artificial periodic metallo-dielectric on a sub-wavelength scale, which exhibits electromagnetic properties not accessible in nature, namely permittivity and permeability, both negative. The first theory concerning their electromagnetic properties was introduced by the Russian researcher Veselago,

in 1964 **[3]**. This subject has known a long hibernation until 2000, when a first practical realization was proposed by the American researcher D. Smith **[4]**. Since then, metamaterials have not ceased to arouse the interest of researchers, because they make it possible to envisage new applications and optimizations in the field of microwaves, in particular at the level of the miniaturization of circuits and the introduction of new properties (dual band filter, phase advance line). The application possibilities of metamaterials are found in industrial sectors such as information and communication technologies, space, security, and defense, but also applications in health, energy, and environmental areas are foreseen. Examples of devices that have been made in recent years are sensors, superlenses, masking and light emitting diodes or cavities for low threshold lasers, and these were based on controlling wave propagation and used dynamic, reconfigurable, and tunable materials. Another potential application that has aroused great interest from researchers is the invisibility cloak or "Cloaking" **[5]**. This structure aims to make an object invisible by surrounding it with a network of metamaterials that will divert light (or electromagnetic waves in general) and allow the reconstruction of wave fronts downstream of this object. This approach is of great interest, particularly in the field of defense for stealth applications.

A great deal of research has been exclusively focused on the linear MMs both theoretically and experimentally **[6,7]**. In the linear region, it has been assumed that the electric permittivity and magnetic permeability does not depend on the intensity of incident radiation. Recently, the nonlinear effects in MMs become interesting field of research, particularly among the theoretical physicists. As the linear responses of MMs show various unusual properties which are not found in naturally occurring materials, in the same way, the study of nonlinear MMs may have a path breaking impact in the context of nonlinear optics. Kivshar and his colleagues were the first to explore theoretically the nonlinear properties of metamaterial **[8]**.

Many authors have investigated and proposed nonlinear pulse propagation models in MMs in various contexts. The first significant attempt in deriving a proper model equation to describe nonlinear pulse propagation was made by Scalora et al. **[9]**. They derived a new generalized one-dimensional (1D) nonlinear Schrödinger (NLS) equation without taking nonlinear magnetization into account. This model equation describe the propagation of ultrashort pulses in bulk negative index media, exhibiting frequency-dependent dielectric susceptibility and magnetic

permeability. Following a similar approach, but eliminating the magnetic field at the very start, Wen et al.**[10]** have derived a (3+1)-D evolution equation for MMs. The self-modulation of waves propagating in nonlinear magnetic metamaterials is governed by the 1D NLS equation **[11]**. This self-modulation of the carrier wave leads to a spontaneous energy localization via the generation of localized envelope structures (envelope solitons). The NLS equation has exact soliton solutions that correspond to a balance between nonlinearity and dispersion in the case of temporal solitons or between nonlinearity and diffraction in the case of spatial solitons.

In real media, the dissipation is inevitable. A wide class of dissipative systems, ranging from nonlinear optics, plasma physics, and fluid dynamics to superfluidity, superconductivity, Bose-Einstein condensates, liquid crystals, and strings in field theory can be modeled by the cubic complex Ginzburg-Landau (CGL) equation **[12]**. Such a cubic CGL equation describes a very promising class of self-organized localized electromagnetic (EM) structures, dissipative spatiotemporal solitons **[13]**. Aprerequisite for generation of these solitons is a simultaneous balance of not only diffraction and dispersion with saturating nonlinearity, but also loss with gain **[14]**. A generalized CGL equation modeling dissipative spatiotemporal solitons in NIMs has been derived **[15]** and established that solitons behave as dissipationless due to the cross-compensation of the saturating nonlinearity excess, losses, and gain. A medium in the presence of such dissipationless solitons may be considered as a novel effectively lossless active composite metamaterial. The compensation of the dissipation is of particular interest for materials with resonant character of interactions like NIMs.

Evolution of optical vortex beams characterized by different topological charges (TCs) has been presented numerically based on the cubic-quintic CGL equation **[16]**. New families of spatiotemporal dissipative optical bullets, including self-trapped, necklace-ring, ring-vortex solitons, uniform-ring beams, spherical and rhombic distributions of light bullets, fundamental and cluster solitons have been numerically reported based on**[17]**, the higher-order (3 + 1)-D cubic-quintic-septic complex Ginzburg-Landau equation with higher-order effects such as stimulated Raman scattering, self-steepening and third-, fourth-, fifth- and sixth-order dispersion terms.

It is well-known that a continuous-wave (CW) or quasi-CW radiation propagating in a nonlinear dispersive medium may suffer an instability with respect to weak periodic modulations of the steady state and results in the breakup of the wave into a train of ultrashort pulses **[18]**.

Modulational instability (MI), occuring as a result of an interplay between nonlinearity and dispersion (or diffraction, in the spatial domain), is a fundamental and ubiquitous process that appears in most nonlinear wave systems in nature such as fluid dynamics **[19, 20]**, nonlinear optics **[21, 22]**, and plasma physics **[23]**, just to name a few. In the context of fiber optics, the temporal MI has been experimentally verified for a single pump wave propagating in a standard non birefringence fiber, which can be modeled by the NLS equation, and it was found that the MI only occurs in anomalous group-velocity dispersion (GVD) regime with a positive cubic nonlinear term **[24]**. Recently, Hong **[25]** has investigated the MI of optical waves in a high dispersive cubic-quintic higher-order NLS equation. In the more complicated optical systems with gain and loss terms, described by the cubic-quintic CGL equation , the MI of CWs of the cubic-quintic CGL equation has been investigated. It has been found that the low-amplitude CW solutions are always unstable, which are regions where they are modulationally unstable, on one hand, while for higher-amplitude,CW solutions are always stable, leading to modulationnally stable regime **[26]**.

To enlarge the information capacity, it is necessary to transmit ultrashort optical solitons at high bit rate in the picosecond and femtosecond regimes, and several new effects greatly influence their propagation properties. For example, in the picosecond regimes, the pulse propagation in nonlinear optical communication systems are usually of Kerr type, and the dynamics of light pulses, whose description is based on the slowly varying envelope approximation (SVEA) or quasimonochromatic approximation leads to the NLS or CGL equation with cubic nonlinear terms. The validity of the NLS and CGL equations as reliable models is dependent on the assumption that the spatial width of the soliton is much larger than the carrier wavelength, which is equivalent to the condition that the width of the soliton frequency spectrum is much less than the carrier frequency. In other words, the NLS and CGL equations describe the evolution of an envelope function which is assumed to vary slowly over an optical cycle.

It has been shown that the SVEA breaks down for these ultrashort optical pulses or even for initial pulses that are many optical cycles long **[27, 28]**. Indeed, Rothenberg **[27]** has shown that the 3D NLS equation derived in the SVEA is not adequate for describing the self-focusing of femtosecond pulses in dispersive media and that the breakdown of this approximation occurs for pulses much longer than an optical cycle. Furthermore, Oughstun and Xiao **[28]** have considered

an input pulse envelope propagating in the positive z direction through a linear dielectric, whose frequency dispersion is described by the double resonance Lorentz model with complex index of refraction. The dynamical field evolution shows that at three, five, and seven absorption depths into the dispersive medium, the SVEA remains accurate in its description of the main body of the pulse that is oscillating at (or very near to) the input carrier frequency. However, at 10 absorption depths into the dispersive medium, the accuracy of the SVEA is seen to have completely broken down.

The main objective:

The objective of the present thesis is that, motivated by few-cycle regimes and MI, we focus on the issue of how MI, which is closely related to the existence of optical solitons, may play a key role in the generation of few-cycle pulses and their propagation through MMs. To better understand our objective, we must obtain a qualitative understanding of the physical processes involved in the formation of the spatiotemporal patterns of the propagation of electromagnetic waves in MMs.

Specifics objectives:

In our contribution, we start with the Maxwell's equations describing the response of the nonlinear medium to an electromagnetic wave. Then, we report on the derivation of the (3+1)D cubic-quintic-septique CGL equation, beyond the SVEA, which is further used to discuss theoretically and numerically MI of few-cycle pulses on this equation. We examine plane wave stability by means of both a rigorous analysis of linearized equations for small perturbations and using direct numerical simulations to support our analytical predictions, and we present the evolution of various dissipative optical bullets in MMs characterized by different topological charges namely, the fundamental vortex, necklace and azimuthon that can exhibit stable propagation for very large distances.

The rest of the work is organized as follows.

Chapter 1 is devoted to the literature review on the generalities related metamaterials theory. The following concepts will therefore be addressed: history of metamaterials, type of metamaterials, metamaterials in optical communication systems, dissipative soliton in metamaterials.

The chapter 2 is devoted to the models describing the dynamics in nonlinear metamaterials.

Here, we also present some analytical and numerical methods used for our different studies.

Chapter 3 presents the main results of this thesis. These results concern the modultionnel instability in the dissipative systems:nonlinear MMs, model by the (3+1)D cubic-quintic complex Ginzburg-Landau equation, and the evolution of various dissipative optical bullets in MMs, model by the (3+1)D cubic-quintic-septic complex Ginzburg-Landau equation.

The present thesis ends with a general conclusion. We summarize our results and give some future directions that could be investigated.

Chapter I

Literature review on metamaterials

1.1 Introduction

What are metamaterials? Semantically, the prefix "meta" means "beyond" in Greek; the term metamaterial, therefore, designates a class of material whose properties go in some way beyond those of classical materials. More specifically, this means media whose internal structure interacts with an incident wave (acoustic or electromagnetic), so as to create the so-called "effective" macroscopic properties that are unusual, even unobserved in natural materials. In the case of electromagnetic metamaterial, which is our system in the context of our thesis work, the fundamental electromagnetic parameters describing the wave-matter interaction are the electrical permittivity and the magnetic permeability. Metamaterials make it possible, for example, to achieve, depending on the proposed structures and the target frequency ranges, "extreme" values of permittivity, either unusually large or, on the contrary, close to zero. Similarly, some structures make it possible to obtain non-trivial values of the effective permeability in the frequency ranges, where it is naturally equals to unity, giving rise to an artificial magnetism. A localized structure in such a system, i.e. a "dissipative soliton", well deserves to be an established scientific keyword. The use of soliton in optical communication systems improves the use of metamaterial action, as they carry a large amount of information, such as: footprint, power consumption and cost. Optical systems inevitably have chromatic dispersion/diffraction, losses (signal attenuation) and nonlinearity. In order for the soliton pulses to propagate through this optical system without signal loss or without changing their spectrum and spatial shape, the dispersion/diffraction and the nonlinearity must compensate each other.

For a better understanding of the rest of our work, this chapter will highlight information on the history of metamaterials, the different types of metamaterials, some electromagnetic

properties of metamaterials, dissipative solitons.

1.2 A brief history of metamaterials

Even before the appearance of the term metamaterials, men sought to go beyond the properties of conventional materials. As evidenced by the creation of the cup of Lycurgus in the 4th century, whose glass has inclusions of gold and silver nanoparticles, which cause a change in color of the cup, depending on whether it is observed in transmitted light or thoughtful. We retrace here, in broad outline, the history of the birth and development of the field of metamaterials.

1.2.1 The works of Veselago

A first step towards metamaterials in the contemporary sense of the term is made by Viktor Veselago in 1967 **[3]**, with the publication of a theoretical study on the propagation of an electromagnetic wave in a material medium according to the values taken by the relative dielectric permittivity and magnetic permeability of the medium. Veselago notices that the tried formed by the wave vector, the electric field and the magnetic field is indirect, while in the classical case this same triedfghjklmùd is known to be direct. Furthermore, Veselago observes that, at the same time, the tried formed by the Poynting vector, the electric field and the magnetic field remains direct, which means that for these media, the wave vector and the vector of Poynting point in opposite directions-an unprecedented situation a priori. Taking into accouunt the orientation of the wave vector, giving the direction of propagation of the phase and the orientation of the Poynting vector, that of the propagation of energy, Veselago concludes that in this type of material, the phase and the energy propagate in opposite directions. From Snell's laws of refraction and relations of passages between two media, he also shows that the index of such a medium is negative, in the sense that, during the passage from a medium with a positive index to negative (or vice-versa), any ray is refracted on the same side of the normal to the plane of incidence (let's recall that in a classic dioptre, the ray "crosses" the normal to the refraction). However, as Veselago points out in the final part of his theoretical publication, the absence of materials with negative permeability made the experimental demonstration of his results impossible at that time and the subject remained a dead letter for many years.

1.2.2 Experimental confirmation

For the subject to really take off, it was necessary to wait until the end of the 1990s, with J. Pendry and his team carrying out work on networks of wires metallic **[29, 30]** and on resonators in the form of split rings (split-ring resonators or SRR) **[31]**. These two types of media are made up of resonators whose characteristic sizes are much smaller than the incident wavelength, and allow respectively to obtain permittivity and negative permeability, in the microwave range. From then on, all the tools are gathered for the experimental verification of Veselago's work, and it was the group of D. Smith who manufactured in 2001 the first material with simultaneous permeability and negative permittivity in the microwave range**[32]**. These researchers showed that for a material of which only one of the parameters is negative, the waves cannot propagate (as expected), but that the propagation is well restored in a medium where the two parameters are negative (as predicted by Veselago)**[4]**. In a second publication**[32]**, they then confirmed, thanks to an assembly involving a metamaterial cut in the shape of a prism, that there is indeed a negative refractive index with this type of material.

1.2.3 Possibility of perfect imaging

The existence, then proven, of materials with a negative index was certainly sensational, but without potential applications. One can suppose that the subject would undoubtedly have been condemned to oblivion progressive without the publication of J. Pendry entitled "negative refraction make a perfect Lens" published in 2000 **[33]**. Pendry took Veselago's work a little further, this time examining the transmission and reflection of a plate with a parallel face of index $n = -1$. He showed that this type of structure not only focuses the far field (like a conventional Lens), but also the evanescent part field (see Figure 1.2). A Lens of this kind, which Pendry calls "super-Lens", therefore offers possibilities of perfect imaging, potentially making it possible to cross the diffraction limit of usual Lenses. Note, however, that the diffraction limit was no longer an insurmountable limit since near-field imaging techniques (SNOM) already existed. However, Pendry's discovery allowed to imagine making an image, almost instantaneously and in its entirety, of a sample, without needing to scan it point by point (a process that can take some time) like we did it with a SNOM. As a result, this brilliant idea, which caused a

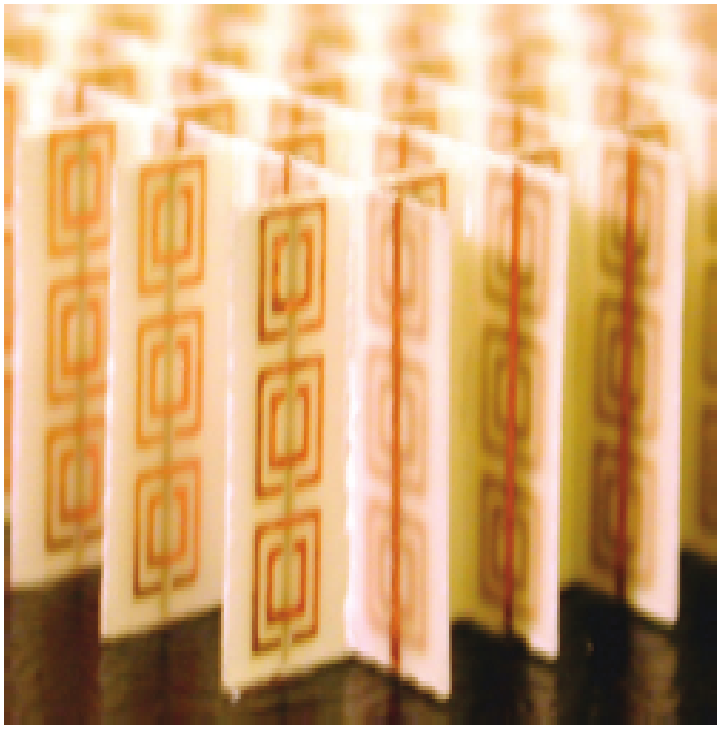

Figure 1.1: The first negative-index (two-dimensional) metamaterial in the microwave range. It consists of SRRs and copper wires deposited on a fiber glass substrate. The unit cell has a size of 5mm and the metamaterial is designed to operate in a range of wavelengths around 3cm **[32]** .

stir and sparked heated debate, really acts as a starting point for the metamaterials branch.

From the discovery of Pendry, many research teams were interested in the physics of complex electromagnetic media and its applications for imaging and telecommunications. The field of metamaterials then widened greatly, new applications appeared (the most spectacular being certainly "invisibility") and experimental verifications were carried out in each part of the electromagnetic spectrum. In the following section, we rewiev the different types of metamaterials.

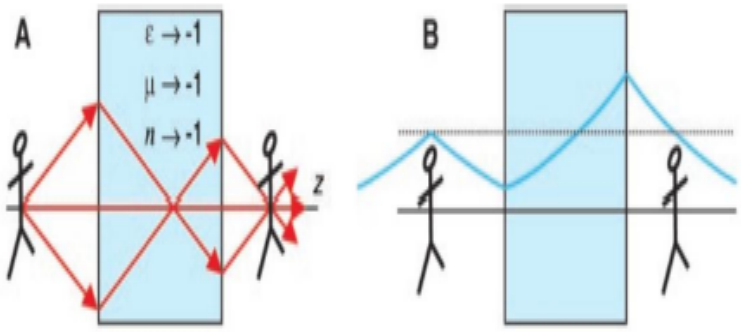

Figure 1.2: Diagram taken from **[34]**, illustrating the principle of a super-Lens. The far field (A) as well as that of the evanescent field (B) coming from the object are focused at the same image point, thus giving, in the principle, an image of ideal resolution.

1.3 Different types of metamaterials

1.3.1 Metamaterials with negative electric permittivity

At the time of Veselago, we already knew about materials with negative permittivity in a given frequency range such as gaseous plasmas and metals. To obtain a negative permittivity in the microwave range, one can use "wire medium" as proposed by Brown in 1953 **[35]** and Rotman **[36]**. This idea was then taken up by Pendry at the end of the 90s and then used for the manufacture of the first metamaterial. It is now known how to manufacture structures giving a negative permittivity for almost the entire electromagnetic spectrum, from such wire media or from plasmonic structures. The metal thin-wire structure exhibits negative permittivity under certain conditions (Figure 1.3).

Indeed, when the excitation of the electric field E is parallel to the axis of the wires (E||z), this induces a current along these wires and generates equivalent electric dipole moments. The permittivity is given as a function of the plasma frequency ω_{pe} and the excitation frequency ω:

$$\epsilon(\omega) = 1 - \frac{\omega_{pe}^2}{\omega^2}, \tag{1.1}$$

According to relation 1.1, the plasma permittivity is negative for frequencies below the plasma frequency. Therefore, to have a negative permittivity, the electric field must be parallel to the z axis and the frequency of the plasma must be higher than the frequency of the excitation source.

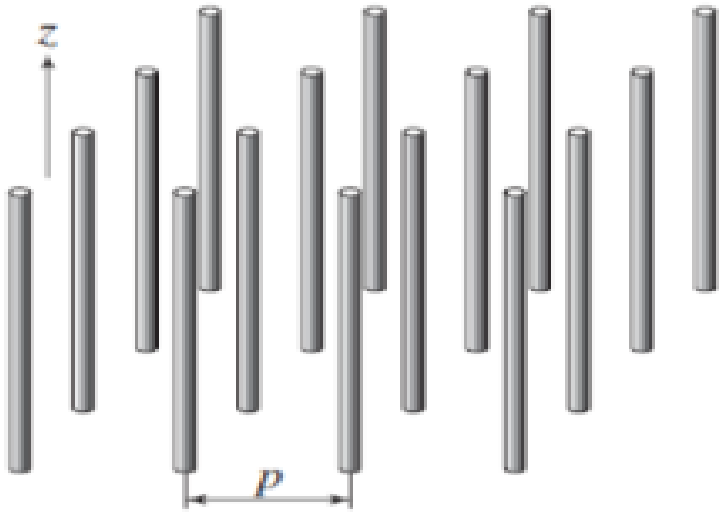

Figure 1.3: Fine wire structure presenting ϵ negative/μ positive, when $E//z$ **[30]**.

1.3.2 Metamaterials with negative magnetic permeability

Veselago had already pointed out in his publication the fact that no material has naturally negative permeability at high frequency. Hardy and Whitehead **[37]** proposed in 1981 metal structures in the form of a split ring operating in the microwave and whose induced currents give rise to a strong magnetic response. Pendry took over and improved these structures, to show in 1999 that they could give rise to negative permeability in the microwave range **[30]**. With the emergence of metamaterials and means miniaturization by lithography, several groups extended these "split ring resonator" (SRR) structures to make them work in the near infrared **[38-40]**. The SRR exhibits negative permeability under certain conditions (Figure 1.4).

When a magnetic excitation field H is parallel to the plane of the rings (H //y), it generates a magnetic dipole moment. The permeability is given by:

$$\mu(\omega) = 1 - \frac{F\omega^2}{\omega^2 - \omega_{0m}^2 + j\omega\zeta}, \tag{1.2}$$

where $F = \pi(\frac{a}{p})^2$, with a is the radius of the small ring), ω_{0m} is the magnetic resonance frequency tuned to the GHz range, ζ is the attenuation factor due to metal losses.

This structure is anisotropic. In order to solve the anisotropy problem of the SRR, a Swiss team **[41]** introduced a two-dimensional pattern called Crossed SRR "CSRR" (Crossed Split Ring Resonator) (Figure 1.5) consisting of two SRRs of the same dimension. This pattern

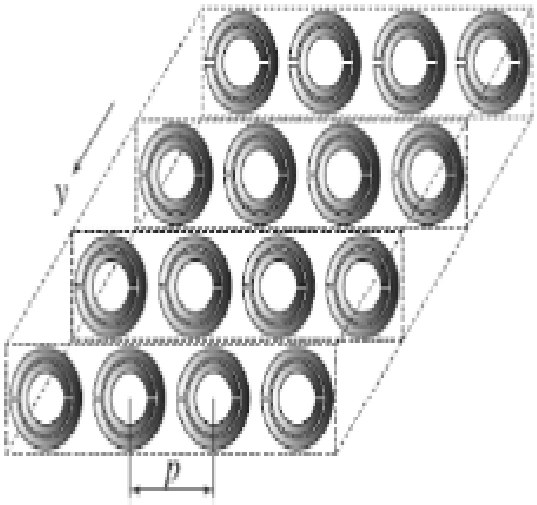

Figure 1.4: SRR structure presenting ϵ positive/μ negative when $H//z$ **[31]**.

increases hence the isotropy in two directions of space.

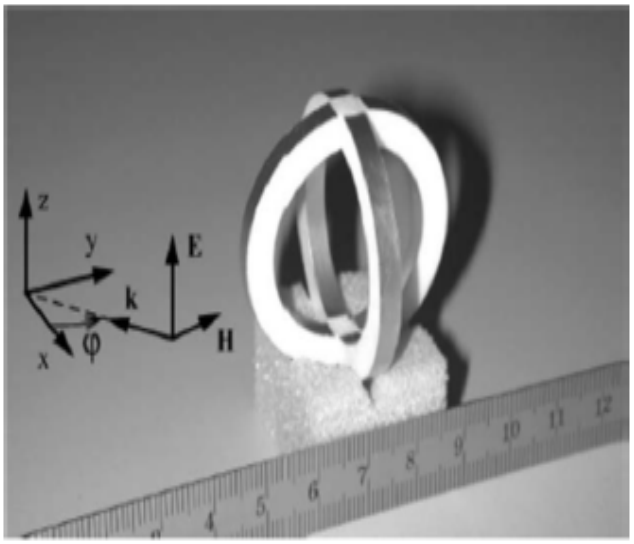

Figure 1.5: Two-dimensional SRR pattern proposed by Balmaz and Martin **[41]**.

The same authors also speak of three-dimensional isotropy, see (Figure 1.6), where three SRRs are placed perpendicular to each other. In the first case Figure 1.6 (a), where the dimensions of the three SRRs are identical, they unfortunately show that this type of pattern does not constitute, in any case, a three-dimensional isotropic pattern. On the other hand, it is possible to obtain a 3-D isotropic structure with three SRRs of different dimensions Fig 1.6(b)**[42]**

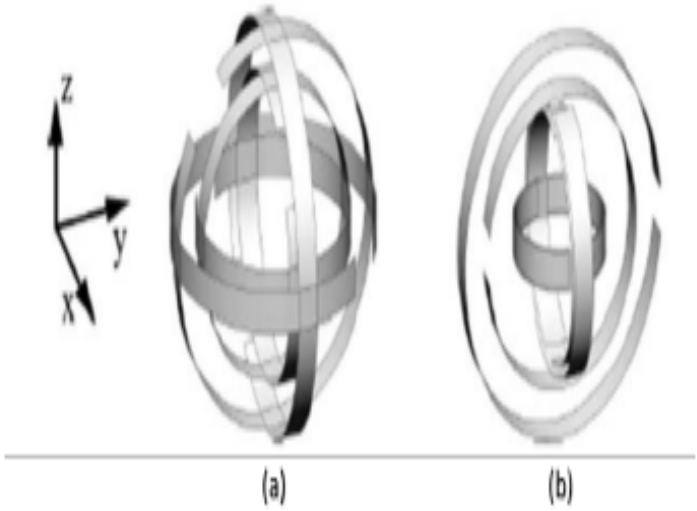

Figure 1.6: Three-dimensional pattern proposed by Balmaz and Martin **[41]**. (a): Structure composed of three identical SRRs perpendicular to each other. (b): Structure composed of three SRRs of different dimensions perpendicular to each other.

Figure 1.7 shows the equivalent circuit of a split ring resonator. In the double ring configuration, the capacitive and inductive couplings between the large and the small ring are modeled by a coupling capacitance C_m. In Figure 1.7(b), the ring is equivalent to a resonator RLC circuit, with a resonant frequency $\omega_0 = \frac{1}{\sqrt{LC}}$. The double SRR is equivalent to the single SRR if the mutual coupling is weak **[43]** .

1.3.3 Metamaterials with negative electic permittivity and negative magnetic permeability

In general, the electromagnetic response of any material to a wave incident electromagnetic radiation is determined by its two intrinsic parameters ϵ_r and μ_r. So, depending on the signs of ϵ_r and μ_r, four combinations are possible. Figure 1.8 represents the different types of materials according to these combinations.

The case where $\epsilon_r > 0$ and $\mu_r > 0$ (right hand) represents the case of materials classic, like dielectrics. The case where $\epsilon_r < 0$ and $\mu_r < 0$ (left hand) represents the case metamaterials. Returning to the case that interests us (dial 4), as noted before, the metamaterials also called left-hand materials or double-negative materials do not exist in nature.

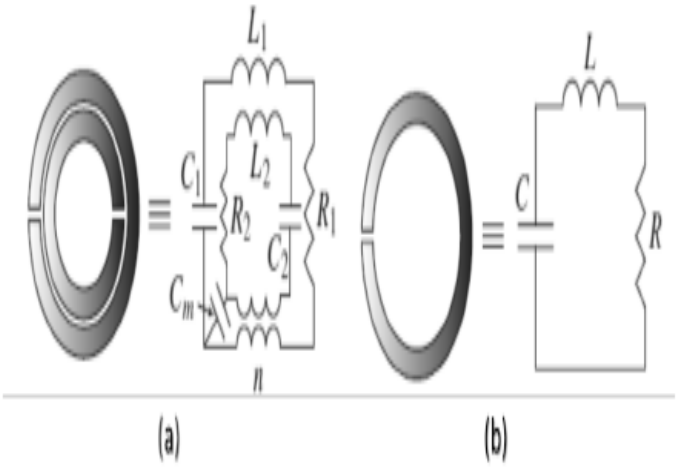

Figure 1.7: SRR equivalent circuit model. (a): Configuration of a dual SRR. (b): Simple configuration of an SRR **[43]**.

The original idea to obtain negative index metamaterials was to superimpose, at the same frequency, the effect of negative permittivity and negative permeability. This type of metamaterial forms our system in our thesis work. In **[4]**, Smith et al. combined Pendry's thin wires and "SRRs" structure into a compound structure seen in Figure 1.9 (a), which represented the first experimental prototype of the left-hand metamaterial.

The structure seen in Figure 1.9(a) is a one-dimensional left-handed material, since only one direction is allowed for the doublet (E,H) to have negative permittivity and permeability. The structure seen in Figure 1.9(b) is a bidirectional left-handed material because, although E must be directed along the z-axis of the wires, two directions are possible for H.

In the following section, we recall the basics of electromagnetism to better understand this thesis. We begin by recalling Maxwell's equations and their consequences for the propagation of electromagnetic waves in doubly negative metamaterials.

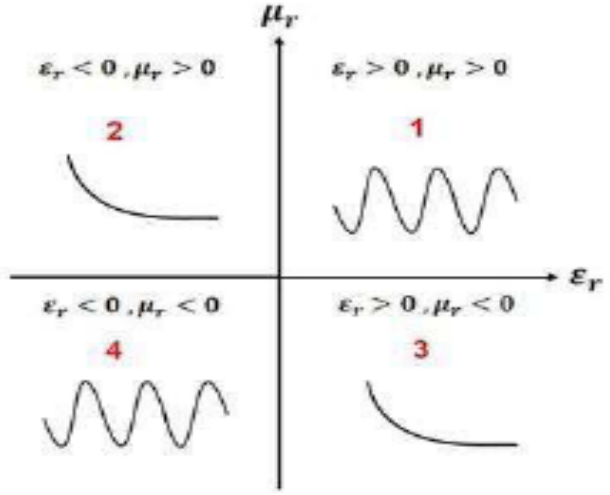

Figure 1.8: Propagation of a plane wave through a medium according to the sign of these constitutive parameters (permittivity and permeability)**[44]**.

1.4 Electromagnetic properties of metamaterials and Maxwell's equations

The description of the electromagnetic properties of a material by the macroscopic quantities ϵ_r and μ_r supposes that this material is homogeneous, which is a priori contradictory with a composite structure. However, the notion of homogeneity depends on the scale of measurement with a simple criterion: a (meta)material will be considered homogeneous for the propagation of a wave if the size of its resonators and the distances which separate them are very small compared to the wavelength in the material (which can be significantly different from its value in vacuum).

1.4.1 Maxwell's equations

Maxwell's equations summarize several important findings in electromagnetism. They describe, in a mathematical way, how are bound and how interact electric charges, electrical currents,

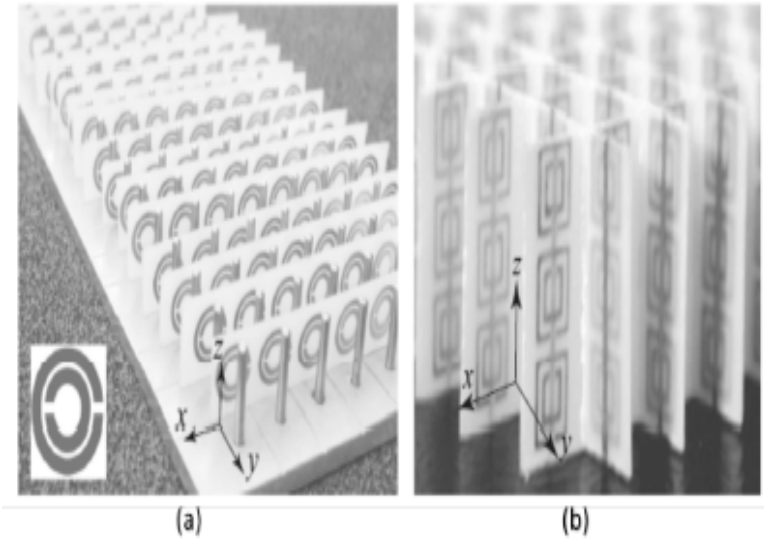

Figure 1.9: First left-hand experimental structure, consisting of thin wires (TWs) and SRRs introduced by the team from the University of California, San Diego. (a): One-dimensional left-hand structure **[4]**. (b): Two-dimensional left hand structure**[4]**.

electric fields and magnetic fields. For simply statement, they describe the electric, magnetic and luminous phenomena quantitatively. These equations are very significant in physics.

Maxwell-Gauss equation: This equation can be expressed as follows and shows that the divergence of the electric field **E** is proportional to the electric charge distribution ρ:

$$\nabla.\mathbf{E} = \frac{\rho}{\epsilon_0}. \tag{1.3}$$

A particle or an electrically charged body, constitutes a concentration of electric charges of the same sign. This means that the electrical field is diverging since the source of electric charges is proportional to the distribution of these charges.

Maxwell- Flux equation: The divergence of the magnetic field **B** is nought and is given as follows:

$$\nabla.\mathbf{B} = 0. \tag{1.4}$$

There is no divergence of the magnetic field, so the magnetic field lines do not point towards infinity. This law reflects the simple fact that there is no magnetic monopole. A magnet monopole does not exist as there are electric monopoles such as electron and proton. If we break a magnet,

we get several magnets with north and south pole. Mathematically, the law can also be read as the lines of outgoing magnetic field of one of the poles of a magnet which return in the other pole. This formulation explains better the fact that the sum of all lines of fields is equal to nought. What leaves one side returns to the other and final one does not lose nor creates thing.

Maxwell-Faraday equation: The curl of electric field **E** is proportional to the variation of the magnetic field **B** over time:

$$\nabla \times \mathbf{E} = -\frac{\partial \mathbf{B}}{\partial t}. \tag{1.5}$$

If we take a varying magnetic field in a conductor, then, there appears a rotating electric field around the magnet. In the Maxwell-Faraday equation, the curl of electric field is proportional to the variation of magnetic field. Indeed, it is the variation of the magnetic field that generates an electric field and not the magnetic field alone. If we place a magnet in a coil, nothing happens. On the other hand, if you move the magnet, an electric field is created around, which itself will generate an electric current in the wire.

Maxwell-Ampere equation: The curl of magnetic field **B** is the sum of his time dependence variation of electric field **E** and electric current **J**:

$$\nabla \times \mathbf{B} = \mu \mathbf{J} + \mu\epsilon \frac{\partial \mathbf{E}}{\partial t}. \tag{1.6}$$

This equation shows that the magnetic field is produced by the variation of electric field during the time. The term $\mu\mathbf{J}$ shows also that the magnetic field as well depends on electric current in the case of conductor. There are no free charges, and no free currents flow, in the framework.

These relations allow us to have the wave equation and the refractive index $n^2 = \mu\epsilon$, with the parameters μ and ϵ, which are usually complex. This expression is well defined when the two real parts of μ and ϵ are positive, or when one of the two is negative (as is the case for classical materials). But when both parties are negative simultaneously, we must carefully consider the definition of the square root complex, and in particular, to make an adequate choice of the branch cut of the root function in the complex plane.

Today, the artificial structures exhibiting electromagnetic responses at light frequencies, known as optical metamaterials, are considered to be one of the most fascinating and fruitful

area of MMs research. It is well understood in elementary physics that if either the permittivity ϵ or the permeability μ is negative, while the other one is positive, then the refractive index is purely imaginary resulting in no propagating waves. If we assume that materials with both $\epsilon < 0$ and $\mu < 0$ exists, then one can show that propagating waves are possible and one must write $n = -\sqrt{\epsilon\mu}$ due to causality condition. It may be explained as follows. Let us consider a passive medium with $\epsilon = -\epsilon_1 + i\epsilon_2$ and $\mu = -\mu_1 + i\mu_2$, where $\epsilon_2 \ll \epsilon_1$ and $\mu_2 \ll \mu_1$. Then, we have $n = \pm\sqrt{\epsilon\mu} = \pm\sqrt{(-\epsilon_1 + i\epsilon_2)(-\mu_1 + i\mu_2)} \approx \pm\sqrt{\epsilon_1\mu_1}[1 - i\frac{\epsilon_1\mu_2+\epsilon_2\mu_1}{2\epsilon_1\mu_1}]$.

Causality requires that the imaginary part of the refractive index must be positive for any passive medium, and hence, we must choose the negative sign, when the real parts of both ϵ and μ are negative. One can immediately see some of the consequences of negative refractive index and of the fact that $\epsilon, \mu < 0$.

Let us consider a plane electromagnetic wave propagating through a medium, where the electric field is written as: $\overrightarrow{E} = \overrightarrow{E_0}e^{i(\overrightarrow{k}.\overrightarrow{r}-\omega t)}$, where $\overrightarrow{E_0}$, $\overrightarrow{k}$ and ω are electric field amplitude, wave vector and angular frequency of the wave respectively. Maxwell's curl equations $\nabla \times \mathbf{E} = -\frac{\partial \mathbf{B}}{\partial t}$, $\nabla \times \mathbf{H} = \frac{\partial \mathbf{D}}{\partial t}$ take the following form in an isotropic medium: $\mathbf{k} \times \mathbf{E} = \omega\mu(\omega)\mathbf{H}$, $\mathbf{k} \times \mathbf{H} = -\omega\epsilon(\omega)\mathbf{E}$. For a common material, $\epsilon(\omega), \mu(\omega) > 0$ and so, the vectors $\mathbf{E}$, $\mathbf{H}$ and $\mathbf{k}$ form a right-handed coordinate system. Also, the wave vector $\mathbf{k}$ is parallel to the Poynting vector $\mathbf{s} = \mathbf{E} \times \mathbf{H}$. On the other hand, for a negative index material, for which $\epsilon(\omega), \mu(\omega) < 0$, the vectors $\mathbf{E}$, $\mathbf{H}$ and $\mathbf{k}$ form a left-handed coordinate system.

This is the reason why NIMs are known as left-handed materials also. It is interesting to note that in NIM, the wave vector is directed opposite to the Poynting vector. This physically means that in MM, the energy propagates opposite to the wave vector direction and the phase is advanced in the propagation direction.

We will thus give some consequences of a doubly negative medium.

1.4.2 Inversion of the Snell-Descartes law

The refraction of light at the interface of a positive medium and a negative medium has been discussed by Veselago. Consider the plane incident electromagnetic wave, on a positive medium, with a wave vector . It is clear that the field continuity and Maxwell's equations require the transmitted wave vector to be, based on the choice of wave vector. Noting that the Poynting

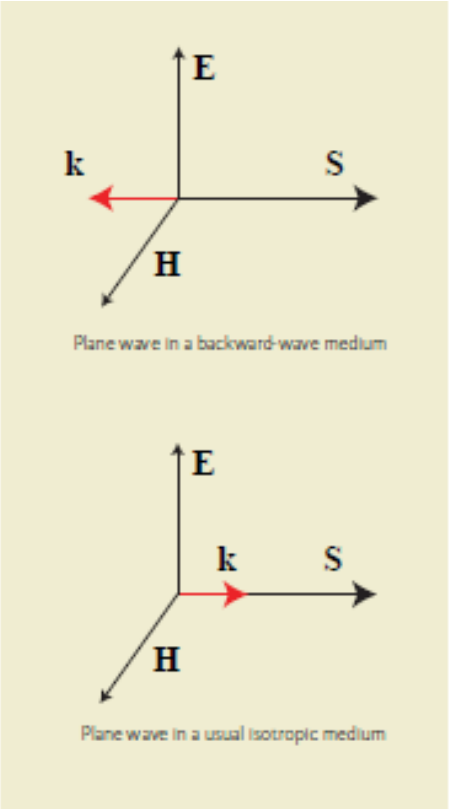

Figure 1.10: Orientation of **E**, **H**, **k** and **s** (a): Right handed medium (RHM). (b): Left handed medium (LHM).

vector is oriented exactly with respect to the phase vector, in a negative refractive index material. We realize that the ray representing the energy corresponding to the refracted wave should now be on the other side of normal. This negative angle can also be intuitively implied in the Snell-Descartes law:

$$n_1 sin\theta_1 = n_2 sin\theta_2, \tag{1.7}$$

where $n_2 < 0$ which implies $\theta_1 < 0$.

The modification of the Snell-Descartes law is the opposite of a fundamental concept in the optical system of isotropic media, depending on how dense the medium is, the wave can bend near the normal, but not never cross. In this case, the refracted beam emerges on the other side of the normal. However, the angle of the reflected beam remains unchanged. A consequence of this gives us for a convex object to make a plane wave diverge, while the concave object makes the plane wave converge.

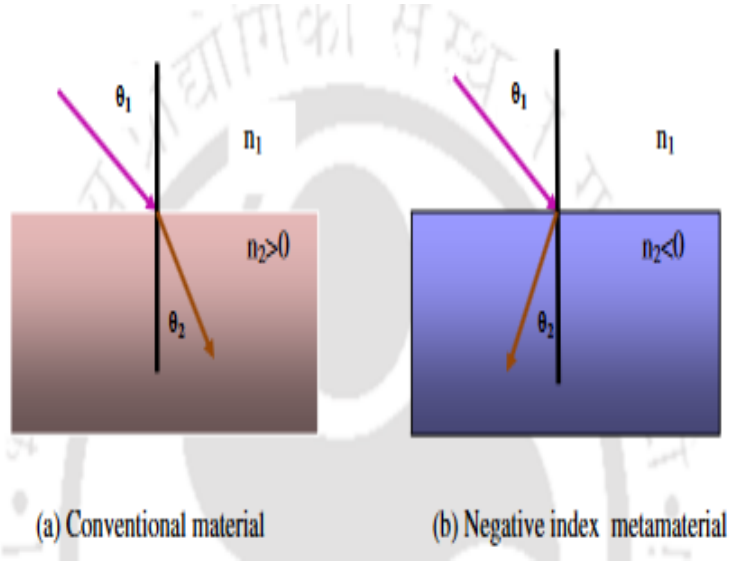

Figure 1.11: Ray diagram of Snell's law (a): conventional material. (b): negative index metamaterial.

Apart from the above two phenomena, many interesting phenomena such as reversal of the Doppler effect **[45, 46]**, reversal of Cerenkov radiation **[47]**, reversal of Goos-Hanchen shift **[48]**, etc have been realized in negative index metamaterials

1.4.3 The reverse Doppler effect

The Doppler effect is a well-known phenomenon. It describes the frequency shift a wave experiences whether it is emitted from a moving source or reflected away from a moving boundary. It has well-established applications in astrophotonic, biological diagnostic, weather and air craft radar systems, velocimetry and vibrometry. Consider a source emitting radiation at a frequency ω, in a material with a negative refractive index, having a speed v, with respect to the medium. The frequency measured in the material reinforcement is:

$$\omega^{'} = \gamma(\omega + kv). \tag{1.8}$$

Here $\gamma = (1 - \frac{v^2}{c^2})^{\frac{-1}{2}}$ is the relativistic factor. note that $k = \frac{n\omega}{c}$, for emission along the direction of source motion in the left material. The frequency measured by a detector would be smaller when the source moves towards it. This is the opposite of an increase in frequency, which we will get in a normal setting. The wave vector being opposite, this is what is responsible

for the reversed Doppler effect. The counter intuitive inverse Doppler effect was theoretically predicted in 1968 by Veselago in a new type of novel artificially structured materials called negative refractive index metamaterials (NIM) or simply known as metamaterials (MM) making nonlinear optics research a very useful and exciting activity **[1]**. However, because of the fremendous challenges of frequency shift measurements inside such materials, most investigations of the inverse Doppler effect have been limited to theorecal predictions and numerical simulations. Study of solitary waves in such novel nonlinear optical systems is extremely challenging and fruitful.

1.5 Dissipative soliton in physical systems and some derivative equations beyond the slowy varying envelope approximations

1.5.1 Dissipative solitons

The term 'soliton' was introduced in 1965 **[49]**, but the scientific research of solitons had started way back in 1834 when John Scott Russell observed a large solitary wave propagating at a constant speed without changing its shape over a long distance in a canal near Edinburgh, (see fig.1.12) **[50]**. In the days of Scott Russell, there was much debate from the leading scientific scholars of the day regarding the very existence of this kind of solitary waves. In 1845, Airy's nonlinear shallow-water wave theory predicted that a wave with elevation of finite amplitude cannot propagate without change of its form i.e. solitary waves could not exist **[51]**. Later on in 1849, Stokes showed that it is possible to have solitary waves with finite amplitude and permanent shape in deep water and they are periodic wave trains **[52]**. Then, it was followed by water tank experiments by H. Brazin **[53]** and the theoretical developments by Joseph Boussinesq in 1871 and Lord Rayleigh in 1876 independently**[54, 55]**. In 1895, Korteweg and de Vries derived a mathematical model equation, popularly known as the KdV equation, which describes the unidirectional propagation of shallow water waves **[56]**. The KdV equation successfully explained the 1834 observations of John Scott Russell. Though the existence of solitary waves were proved beyond doubt, not much progress have been made until the 1960s,

when N. Zabusky and M. Kruskal numerically re-investigated the KdV equation and discovered the elastic collision between KdV solitary waves **[49]**. It is worth noting that Zabusky and Kruskal were motivated to study the KdV equation numerically by the so-called Fermi, Pasta and Ulam (FPU) problem **[57]**. In 1967, Gardner et al. **[58]** obtained the analytical solution of the KdV equation for the localized solitary waves by using the idea of Inverse Scattering method, and their results agreed well with the experimental results obtained by John Scott Russell . This pioneering work triggered unprecedented burst of research activities on nonlinear waves and which is continuing till today. One year later, Lax generalized their results **[59]** and in 1972, Zakharov and Shabat exactly solved the nonlinear evolution equation known as nonlinear Schrödinger equation (NLS) for weakly nonlinear deep water waves by the same method and they termed the solutions as envelope soliton **[60]**. In the context of nonlinear optics, Hasegawa and Tappert in 1973 showed theoretically the existence of optical solitons inside an optical fiber **[61]**, where the propagation of light is modeled by the NLS equation and it was experimentally observed by Mollenauer et al. in 1980 **[62]**. Since then, optical solitons have found practical applications in long distance communicational systems, producing short pulse lasers, pulse compression technique, electronic devices like optical switching and optical logic gates, etc **[63]**.

In the context of nonlinear optics, solitons are classified as being either **temporal**, **spatial**, or **spatiotemporal** depending on whether the confinement of light occurs in time or space during wave propagation **[64]**. It is worthy to mention that the **space-time** coupling occurring when a pulsed optical beam propagates through a nonlinear medium leads to unique nonlinear effects.

• **Temporal soliton** represent optical pulses that maintain their shape during propagation. Their existence was predicted in 1973 in the context of optical fibers **[61]**. Since then, fiber solitons have been studied extensively and have even found applications in the field of fiber-optic communications **[65, 66]**.

A temporal soliton is controlled by dispersion and nonlinearity. Strictly speaking, such a soliton emerges when the chirping induced by the dispersion and the nonlinearity exactly cancels each other out to give a constant phase across the pulse **[18]**. The manner in which attention can be directed only towards nonlinearity and dispersion depends upon the waveguide structure

Figure 1.12: Recreation of a solitary wave on the Scott Russell Aqueduct on the Union Canal. Photograph courtesy of Heriot-Watt University **[50]**.

that is supporting the solitons. For example, in an optical fibre, diffraction is eliminated in all directions perpendicular to the propagation axis. Here, a planar waveguide is used. The temporal soliton propagation in double-negative metamaterials has been discussed with an emphasis upon short pulses that exhibit self-steepening controlled by the frequency dependence of the relative permittivity and permeability **[67]**.

Let us consider the generalized NLS equation describing the evolution of femtosecond optical field $\psi(z;t)$ in nonlinear metamaterials **[68, 69]**:

$$i\frac{\partial\psi}{\partial z}+\frac{k_2}{2}\frac{\partial^2\psi}{\partial t^2}+p_3|\psi|^2\psi-p_5|\psi|^4\psi-is_1\frac{\partial(|\psi|^2\psi)}{\partial t}=0 \tag{1.9}$$

where $t=cT$ and $z=Z/\lambda_p$ are the respective normalized time and propagation distance, with λ_p being the plasma wavelength. Also, k_2 stands for the GVD coefficient, s_1 represents the self-steepening coefficient, while p_3 and p_5 represent cubic and pseudo-quintic nonlinear coefficients, respectively.

This equation contains several particular cases such as the standard NLS equation, who is the basis of many researches in the field of telecoms ($p_5=s_1=0$) **[70]**, the modified NLS equation($p_5=0$) **[71]**, the Kaup-Newell equation ($p_3=p_5=0$) **[72]**], the cubic- quintic NLS

equation ($s_1 = 0$)**[73]**, and the pure quintic NLS equation ($p_3 = s_1 = 0$) **[74]**. Each particular case is important to describe nonlinear wave dynamics in specific physical systems.

Bright and dark solitons, as well as combined solitary waves and periodic waves have been analytically or numerically studied from different viewpoints **[77,78]**. In order to observe solitons in experiments, left-handed nonlinear transmission lines (NLTL), employed as nonlinear MMs, have been used to investigate the generation of solitons **[79-82]**. The trains of both bright and dark envelope solitons were observed in the left-handed NLTL MMs **[79-81]** and stable generation of soliton pulses was experimentally demonstrated in an active NLTL MM composed of a left-handed NLTL inserted into a ring resonator **[79]**, in which the approach can be employed for the other types of active MMs. In addition, dark solitons in a practical left-handed NLTL MMs with series nonlinear capacitance are demonstrated by circuit analysis, which verified analytically that the left-handed NLTL could support dark solitons by tailoring the circuit parameters **[80]**. These theoretical and experimental studies show that it is practical and significant to search for new and possible solitons in MMs.

• **Spatial soliton** represent self-guided beams that remain confined in the transverse directions orthogonal to the direction of propagation. In similar to the temporal soliton, they evolve from a nonlinear change in the refractive index of an optical material induced by the light intensity phenomenon known as the optical Kerr effect in the field of nonlinear optics **[81, 82, 83]**. The intensity dependence of the refractive index leads to spatial self-focusing (or self-defocusing), which is a major nonlinear effects that is responsible for the formation of optical solitons. A spatial soliton is formed when the self-focusing of an optical beam balances natural diffraction-induced spreading (see Fig. 1.13).

Self-focusing and self-defocusing of continuous-wave (CW) optical beams in a bulk nonlinear medium have been studied extensively **[84]**. Self-trapping was not linked to the concept of spatial solitons immediately because of its unstable nature. During the 1980s, stable spatial solitons were observed using nonlinear media in which diffraction were limited to only one transverse dimension **[85]**. The formation of spatial solitons is based on the geometry of the waveguide and on the photo-induced phase shift **[86]**. Concerning the geometry of the induced waveguide, we know that a beam of limiting width obeys the laws of diffraction characterized by the Rayleigh length:

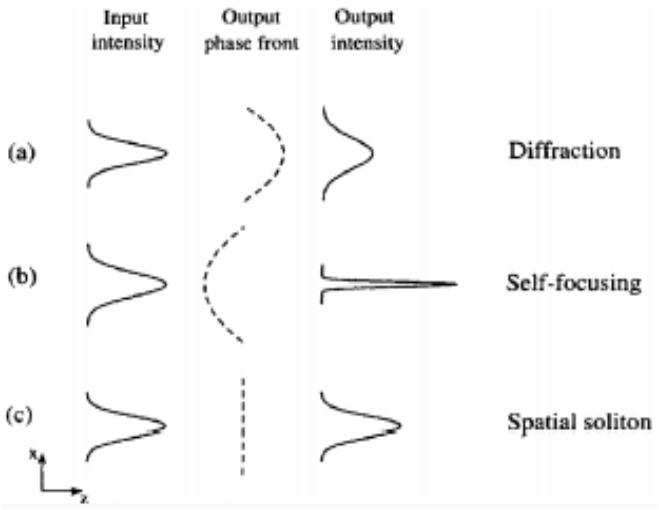

Figure 1.13: Schematic illustration of the Lens analogy for spatial solitons. Diffraction acts as a concave Lens, while the nonlinear medium acts as a convex Lens. A soliton forms when the two Lenses balance each other such that the phase front remains plane **[86]**.

$$L_D = \frac{r}{\theta_D} = \frac{\pi n_0 r^2}{\lambda}, \tag{1.10}$$

where r is the mode radius ("waist"), n_0 the linear refractive index and λ the optical wavelength. The length of Rayleigh L_D is the propagation distance after which the size of the beam has increased by a factor $\sqrt{2}$ (its area doubled). In the presence of a positive nonlinearity medium ($\gamma > 0$), the beam induces an increase in index Δn, proportional to the intensity. The critical angle of total reflection between the two media, defined by $\theta_c = \sqrt{2\Delta n/n_0}$, allows to determine the characteristic length of nonlinearity (auto-focusing) in the approximation of small angles **[86]**,

$$L_{NL} = \frac{r}{\theta_c} = \frac{r}{\sqrt{2\Delta n/n_0}}. \tag{1.11}$$

The spatial soliton corresponds to a balance between diffraction and self-focusing. In this case, the two widths are equalized, so that $L_{NL} = L_D$ leads to $\theta_c = \theta_D$.

As indicated by Zakharov and Shabat **[87]**, a continuous wave with (1+1)D with a *sech* profile and a prescribed relation between its width and its power can propagate as fundamental spatial soliton in a homogeneous Kerr medium, with exact balance between the Kerr effect and the diffraction. However, in the case with two transverse dimensions (2+1)D, the situation is

quite different, marked by collapse; there is therefore no spatial Kerr soliton at (2+1)D. For an understanding of the evolution of the optical field in the optical system and consequently the resulting phenomena, it is necessary to consider the theory of electromagnetic wave propagation in dispersive nonlinear media. Like all electromagnetic phenomena, the propagation of optical fields in optical fibers is governed by Maxwell's equations. From the Maxwell's equations, the evolution of optical field inside the optical system, where the input electric field is assumed to propagate in the $+Z$-direction and is polarized in the X-direction is described by the NLS equation written as

$$i\frac{\partial\psi}{\partial z} + \eta\Delta\psi + \kappa|\psi|^2\psi = 0, \tag{1.12}$$

where η is the dispersion coefficient, κ in the nonlinear coefficient, $\psi(z, X)$ is the wave envelope, $X = x_1, ..., x_d$, $\Delta = \sum_{l=1}^{d} \frac{\partial^2}{\partial x_l^2}$, and $d = 1$ or 2.

There is self-confinement of impulsions when $\kappa > 0$, and the opposite phenomenon when $\kappa < 0$. When $\kappa > 0$, Eq. (1.28) admits solutions which become singular after a finite time when $d = 2$ (critical case), or $d > 2$ (super-critical case). For $d = 1$, Eq. (1.28) is integrable and gives soliton solutions which result from the exact balance between diffraction and nonlinearity. For $d = 2$, in order to avoid the singularity in the wave function and thus, limit the risk of collapse of the pulses, it has been shown that the presence of a damping due to inhomogeneities in the structure of the fields and in the particle distribution function **[88]**, either by saturation of nonlinearity **[89]**, partial coherence **[90]**, or non-paraxiality of small beams **[89]** can be considered.

Therefore, in (2+1)D systems, the diffraction is not strong enough to overcome self-phase modulation. It then becomes difficult to find spatial solitons with (2+1)D stable over long distances **[91, 92]**. The disturbance effects which can modify or stop the "collapse" are dissipation, normal dispersion and the saturation of nonlinearity **[93]**. The most used alternative to obtain the formation of space solitons with more than one dimension is to use dissipative media, where the presence of gains and nonlinear losses allows to have more stable solitons, and thus, avoid the wave collapse.

• One of the major goals in the study of optical solitons is the possibility to generate pulses that are localized in the transverse dimensions of space, as well as in time. Such solitons of the (3 + 1)D NLS equation are called **spatiotemporal solitons** or "light bullets", a term coined

by Silberberg **[94]** which stresses their particle-like nature. In contrast to the extensive studies of spatial and temporal (1+1)D and spatial (2+1)D solitons, experimental progress toward the production of (3 + 1)D solitons has been slow. One of the reason for that is that the conditions for formation of stable spatiotemporal solitons were not identified theoretically yet. Indeed, evidence for spatiotemporal solitons in one spatial dimension has been given by Wise group in quadratic media **[95, 96]** and Barad group in cubic media **[97]**. However, even in these cases, the beam splits in space and in time after propagating a few characteristic lengths. To date, true (3+1)D spatiotemporal solitons have not been observed. For a discussion of the current status of the problem, see **[98]**.

In recent times, investigation on the nonlinear pulse propagation in NIMs is being actively pursued. The nonlinear partial differential equation governing the propagation of light pulse in the NIM has been derived and is found to admit envelope solitary wave solutions **[99]**. A generalized nonlinear Schrödinger equation for dispersive dielectric susceptibility and permeability has been derived to describe the propagation of electromagnetic pulse in the NIM and it has been found that the linear properties of the medium can be tuned to modify its linear as well as nonlinear effective properties, which lead to a new form of dynamical behavior **[9]**. The role of second-order nonlinear dispersion in the stable propagation of Gaussian pulse in the NIM in focusing or defocusing cases with normal or anomalous regimes has been analyzed **[100]**. The evolution equations for the envelopes of beams and spatiotemporal pulses in nonlinear dispersive NIM have been derived and stability of solitary wave solutions has been analyzed using numerical methods based on fast Fourier-Bessel transforms **[101]**. By adopting the methods of quantum statistics and a kinetic equation for the pulses, the partial coherence in NIMs has been discussed **[102]**. The Raman soliton self-frequency shift in the nonlinear NIMs can be controlled by nonlinear electric polarization **[103]**. The existence of gray solitary waves and the conditions for their formation in NIMs have also been studied **[104]**. The propagation of ultrashort electromagnetic pulse in metamaterials with cubic electric and magnetic nonlinearities have been investigated and it has been predicted that spatiotemporal electromagnetic solitons may exist in the negative index regime of the metamaterials with defocusing nonlinearity and normal group velocity dispersion**[105]**. The self-focusing of ultrashort pulses in NIMs can be controlled by tailoring dispersive magnetic permeability **[106]**. In contrast to ordinary

positive index materials, in the case of NIMs dark solitons may exist for the case of normal second-order dispersion, anomalous third-order dispersion, self-focusing Kerr nonlinearity, and non-Kerr nonlinearities**[107]**.

•Dissipative nonlinear systems suggest an interesting alternative. The additional balance between gain and loss in dissipative systems provides the necessary for the generation of stable dissipative solitons. Rosanov has shown that dissipative optical systems can admit solitons in one, two, and three dimensions **[108]**. These formations are stable during propagation, provided the system parameters are chosen in specific regions. Hence, the term "dissipative soliton" is used as the one that covers the majority of relevant phenomena in optics, biology and medicine. As a fuller explanation, it means "soliton in a dissipative system", where "dissipative system" is to be understood in Prigogine's sense as a sub-system with an external pump of energy, rather than a system with losses only. An optical laser is one of the examples of such subsystem in optics**[109]**. There is a significant difference between solitons in Hamiltonian systems and in dissipative ones. In Hamiltonian systems, soliton solutions appear as a result of a balance between diffraction (or dispersion) and nonlinearity. Diffraction spreads the beam, while nonlinearity focuses it and makes it narrower. In addition to the balance between diffraction/diffusion and nonlinearity, in systems with gain and loss, in order to have stationary solutions, gain and loss must be balanced in the first place. The two balances result in solutions which are fixed. The shape, amplitude and the width are all fixed and depend on the parameters of the equation.

On the other hand, a dissipative soliton is a stable localized structure formed by the double balance between nonlinearity and dispersion and between gain and loss which change the pulse energy. It can be observed in a variety of fields such as optics, cosmology, biology, condensed matter physics and medicine**[110]**. In fiber-laser, cavities with third order dispersion (TOD) can form stable and oscillatory bound states of dissipative soliton **[111]**. Stability of discrete dissipative localized modes in metamaterials composed of weakly coupled SRRs have been studied **[112]**. Knotted solitons, which are stable self localized dissipative structures in the form of closed knotted chains has been identified in magnetic metamaterials **[113]**. The delicate balance between input power and intrinsic losses results in the formation of stable dissipative breather in a superconducting quantum interface device metamaterials**[114]**.

In the present context of this work about dissipative solitons, gain and loss are important,

and this statement requires a further comment. The problem of instabilities, leading to the collapse, and which depends on the number of space dimensions and strength of nonlinearity has attracted the attention. The most straightforward modification of the model, which opens the way to the stable solitary pulse, is the introduction of the cubic-quintic (CQ) nonlinearity, with linear gain and cubic loss in the cubic CGL equation **[110]**. Dynamics of dissipative solitons can then be described by a (D+1)-dimensional CQ-CGL equation**[14]**:

$$i\frac{\partial E}{\partial z} + \Delta E + |E|^2 E - \nu|E|^4 E = \mathbf{Q}, \tag{1.13}$$

with

$$\mathbf{Q} = i\left[\delta E + \mu|E|^4 E + \varepsilon|E|^2\psi + \beta\Delta E\right]. \tag{1.14}$$

The left-hand-side of Eq. (1.13) contains the conservative terms. E is the normalized complex envelope of the optical field, and $\Delta = r^{1-D}\frac{\partial}{\partial r}\left(r^{1-D}\frac{\partial E}{\partial r}\right)$ is the D-dimensional Laplacian describing beam diffraction and/or anomalous group velocity dispersion. Therefore, cubic and quintic nonlinearities have to be in opposite signs; i.e., parameter ν is negative. Dissipative terms are denoted by $\mathbf{Q}$ given in Eq. (1.14). Depending on the sign of the parameter δ, the first term is either linear gain or loss. $\beta > 0$ accounts for diffusive coefficient. The cubic and quintic gain-loss parameters are, respectively, ε and μ. In addition to the balance between diffraction and/or dispersion and nonlinearity, the balance between loss and gain is a prerequisite for the generation of dissipative solitons.

In optical transmission systems, the CGL equation has been the subject of considerable studies, and it has been found that, the diffusivity in the transverse plane is a necessary ingredient to get stable dissipative structures even in the lack of bandwidth limited gain. The notion of the dissipative soliton has emerged from a three-part foundation. To be specific, these parts are classical soliton theory, nonlinear dynamics (with its theory of bifurcations) and Prigogine concept of self-organization. These underlying ideas set us up for a comprehensive understanding of the new notion and allow us to explain the basic properties of solitons in dissipative systems. Complications which arise from the fact that the dynamical systems usually have an infinite number of degrees of freedom can be overcome by using reductions to low-dimensional systems. However, these reductions always need to be done carefully by comparing the conclusions with the results of particular numerical simulations of the original equation.

1.5.2 Some derivative equations beyond the slowy varing envelope approximations

Physical, engineering, chemical and biological sciences are continuously generating problems of either theoretical or practical interest. The necessary investigations of these problems involve models that, very often, are mathematically expressed as ordinary or partial differential equations, which in most of the cases, are nonlinear. In this respect, it is of great importance for the refinement of the designed models in view of the best understanding of the original problems or phenomena and, hence, their optimal exploitation or eventually their control.

Many authors have used the concept of nonparaxial beams of various orders leading to a hierarchy of differential equations that can be used to determine the paraxial beam and the various orders of nonparaxial beams successively **[115, 116, 117]**. Thus, nonparaxial corrections for the fundamental Gaussian beam have been expressed on the basis of wave functions by using the transition operators **[118, 119, 120]**. However, the wave functions do not have a radial dependence that reflects correctly the cylindrical symmetry of the total field. Later, it has been shown that the representation of the fields in term of modal functions constructed from the Laguerre-Gauss modes was able to explain in physical terms the sequential development of the various orders of nonparaxial corrections **[121]**. The electrodynamics of the fundamental electromagnetic Gaussian beam has been constructed beyond the paraxial approximation by the use of a single component of the electric vector potential oriented normal to the propagation direction. It has been shown that the paraxial beam is governed by the homogeneous paraxial wave equation and the nonparaxial beams are governed by the inhomogeneous paraxial wave equations. Most importantly, the governing equations for paraxial and nonparaxial beams are first-order differential equations in z, requiring only one condition for obtaining a unique solution **[122]**.

→ **The slowly varying envelope and paraxial approximations: the beam radius is sufficiently large compared with the wavelength**

It is well-known that the nonlinear Schrödinger (NLS) equation is one of the most important models in mathematical physics. This model appears in many fields of physics and applied mathematics, for example condensed matter physics, plasma physics, nonlinear optics, fluid

mechanics and phase transitions, to cite only a few. In particular, the propagation of one-dimensional (1D) optical pulses, in the regime of slowly varying envelope amplitude, and in the paraxial approximation, is usually described by a (1+1) D NLS equation with a focusing cubic nonlinearity, that includes both dispersion and nonlinearity. For the case of instantaneous response, it is written in the form **[18]**

$$i\frac{\partial E(z,t)}{\partial z}+\beta_2\frac{\partial^2 E(z,t)}{\partial t^2}+\gamma|E(z,t)|^2E(z,t)=0, \tag{1.15}$$

where $E(z,t)$ is the complex envelope amplitude of the pulse assumed to vary slowly with respect to both z and t. Here, z represents the distance along the medium and t is the time measured in the frame of reference of the pulse , respectively. β_2 is the group velocity dispersion parameter and γ is the nonlinear parameter that is proportional to the nonlinear refraction index n_2. Physically speaking, the slowly varying envelope approximation (SVEA) in space is valid when the beam is wider than just a few wavelengths: $\frac{\partial^2 E(z,t)}{\partial z^2}\ll k_0\frac{\partial E(z,t)}{\partial z}$, where k_0 is the wavenumber. For this reason, we select a ray which travels close to the optical axis. This is the so-called paraxial approximation of small angles. The process of formation of solitary waves can be triggered by small perturbations superposed to a continuous radiation that evolves in time into a train of ultrashort solitary pulses. A linear stability analysis around the steady-state solution of the NLS equation shows that harmonic perturbations grow exponentially within a given frequency range, a process usually termed as MI. The dynamics of MI is governed by the NLS equation, which admits soliton or solitary wave through a conservative interaction between anomalous GVD and self-focusing Kerr nonlinearity. It is well-known that the NLS equation is derived from the scalar nonlinear Helmholtz (NLH) equation, using the paraxial approximation, which is valid when the beam radius is sufficiently large compared with the wavelength.

In higher dimensions, the paraxial 4D NLS equation, which, in optics, governs the evolution of the electric field envelope,$E(x,y,z,t)$, of a beam propagating in the $+z$ direction through a Kerr medium, can be written as **[94]**:

$$i\frac{\partial E(x,y,z,t)}{\partial z}+\alpha(\frac{\partial^2 E(x,y,z,t)}{\partial x^2}+\frac{\partial^2 E(x,y,z,t)}{\partial y^2})+\beta_2\frac{\partial^2 E(x,y,z,t)}{\partial t^2}+\gamma|E(x,y,z,t)|^2E(x,y,z,t)=0, \tag{1.16}$$

where α defines the scale of the transverse plane. If diffraction ? is fixed to be positive, we

have the following four cases: anomalous dispersion ($\beta_2 > 0$) , normal dispersion ($\beta_2 < 0$), self-focusing media ($\gamma > 0$) , self-defocusing media ($\gamma < 0$) . The self-focusing effects of an optical beam beyond the slowly varying envelope and nonparaxial approximations, in cases of rapid evolution of the field envelope at large angles of propagation, or when the beam waist and the diffraction length become comparable, or when the spectral width of a pulse is much smaller than the pulse central frequency have been investigated in two principal directions. In the first direction, some nonlinear nonparaxial wave equations have been derived including the $\frac{\partial^2 E}{\partial z^2}$ term. In the second direction, other nonlinear nonparaxial wave equations have been derived by dropping the $\frac{\partial^2 E}{\partial z^2}$ term and $\frac{\partial^2 E}{\partial z \partial t}$, respectively.

→ **The slowly varying envelope and nonparaxial approximations: the beam radius is sufficiently large compared with the wavelength**

The formalism of coupled-mode theory applied to the continuum of transverse radiation modes, which automatically includes nonparaxial contributions up to the second order and vectorial effects, has been used by Crosignani, Porto, and Yariv **[123]**, to derive the following nonlinear nonparaxial evolution equation:

$$\frac{\partial u}{\partial Z} + i\frac{1}{2}\left(\frac{\partial^2 u}{\partial X^2} + \frac{\partial^2 u}{\partial Y^2}\right) - i\frac{1}{8}\left(\frac{\partial^4 u}{\partial X^4} + \frac{\partial^4 u}{\partial Y^4}\right) + i|u|^2 u = -i\frac{1}{2}\left(\frac{\partial^2}{\partial x^2} + \frac{\partial^2}{\partial y^2}\right)(|u|^2 u) - i\frac{1}{3}\left|\frac{\partial u}{\partial X}\right|^2 u - i\frac{1}{3}\left(|u|^2 \frac{\partial^2 u}{\partial X^2} - u^2 \frac{\partial^2 u^*}{\partial X^2}\right). \tag{1.17}$$

Equation (1.17) generalizes the standard NLS equation that describes paraxial propagation by the addition of nonparaxial terms up to the second-order in the ratio λ/w between the wavelength and the typical dimension of the beam, and which is inherently first order in $\partial/\partial Z$ and no approximation is required for neglecting the term in $\partial^2/\partial Z^2$, without any slowly varying approximation hypothesis. This is contrasted with derivations that start with the Helmholtz equation.

The first type of nonparaxiality arises from the rapid evolution of the field envelope at a large angle to the longitudinal axis. The scalar nonlinear Helmholtz equation well describe this nonparaxiality and overcome the limitations of the NLS equation. The nonparaxial nonlinear Helmholtz equation is **[124]**:

$$\frac{\partial^2 E(z,x)}{\partial z^2} + \frac{\partial^2 E(z,x)}{\partial x^2} + k_0^2(1 + (\frac{2n_2}{n_0})|E(z,x)|^2)E(z,x) = 0. \tag{1.18}$$

The first term in Eq. (1.18) represents the nonparaxiality. Here, where E is the electric field envelope, z the propagation axis and x the transverse axis, k_0 is the linear wave number, n_0 is the linear index of refraction and n_2 is the Kerr coefficient. The subscripts z and x denote the partial derivatives with respect to z and x, respectively. Using the standard approach to derive the NLS equation, the field E is represented as $E = Aexp(ik_0z)$, where A is assumed to be slowly varying, the nonparaxial nonlinear Helmholtz equation can be written as **[124, 125, 126]**:

$$d\frac{\partial^2 A}{\partial z^2} + i\frac{\partial A}{\partial z} + \frac{\partial^2 A}{\partial x^2} + q|E(z,x)|^2E(z,x) = 0, \tag{1.19}$$

where d is the non-paraxiality parameter. The parameters p and q are related to dispersion and self-phase modulation, respectively. An exact nonparaxial soliton solution from which the paraxial soliton is recovered in the appropriate limit has been proposed by Chamorro-Posada, McDonald and New **[127]**, and the physical and mathematical geometry of the nonparaxial soliton have been explored through the consideration of dispersion relations, rotational transformations and approximate solutions.

The 2D generalization of equation (1.16) to include nonparaxial effects leads to the consideration of the following evolution equation:

$$\frac{\Theta^2}{4}\frac{\partial^2 E(x,y,z,t)}{\partial z^2} + i\frac{\partial E(x,y,z,t)}{\partial z} + \alpha(\frac{\partial^2 E(x,y,z,t)}{\partial x^2} + \frac{\partial^2 E(x,y,z,t)}{\partial y^2}) + \beta_2\frac{\partial^2 E(x,y,z,t)}{\partial t^2} + \gamma|E(x,y,z,t)|^2E(x,y,z,t) = 0, \tag{1.20}$$

where Θ is a parameter equivalent to the divergence angle for a Gaussian beam in linear propagation and naturally reflects the role of the transverse size of the beam and the tendency for light to travel off-axis in nonlinear propagation.

The nonlinear effects of beam size stabilization due to nonparaxiality on the self-focusing of Gaussian and ring-shaped optical beams have been studied for the first time by Feit and Fleck **[128]**, where a nonparaxial algorithm for the Helmholtz equation to some self-focusing situations of experimental interest has been applied. Furthermore, the following nonparaxial scalar model has been derived by Akhmediev, Ankiewicz, and Soto Crespo **[129]**:

$$\frac{\partial^2 \psi}{\partial z^2} + \frac{\partial^2 \psi}{\partial x^2} + \frac{\partial^2 \psi}{\partial y^2} + \epsilon_1(x)\psi + \alpha(x)|\psi|^2\psi = 0, \tag{1.21}$$

where ϵ_1 is the linear part of the transverse profile of the dielectric permittivity of the layered medium and $\alpha(x)$ is the transverse profile of the nonlinear susceptibility. It has been shown that the standard approximation, which uses the parabolic equation (NLS equation) in the analysis of nonlinear self-focusing and self-guiding, should be completed with an additional term that takes into account the variation of the propagation constant along the propagation direction.

Spatial solitary waves carried by a TE mode in planar optical waveguides, with Kerr-type of nonlinearity, have been investigated theoretically and numerically by Boardman, Marinov, Pushkarov and Shivarova, based on the following modified (1+1) modified NLS equation **[130]**:

$$i\frac{\partial E}{\partial z}+\frac{\partial^2 E}{\partial x^2}+|E|^2E+\frac{\partial^2 E}{\partial z^2}+4E(|\frac{\partial E}{\partial x}|^2+\frac{1}{3}\frac{\partial^2|E|^2}{\partial x^2})+4\frac{\partial}{x}(E\frac{\partial|E|^2}{\partial x})=0, \tag{1.22}$$

where the first three terms give the NLS equation in its usual form. The next one is the nonparaxial correction, and the last terms can be considered as nonlinearity induced diffraction. New solitary solutions have been found analytically and numerically, where the influence of each of the effects associated with the different terms in the nonlinear wave equation has been clarified.

→ **Beyond the slowly varying envelope and nonparaxial approximations: The beam waist and the diffraction length become comparable, or when the spectral width of a pulse is much smaller than the pulse central frequency. Derivation of the nonlinear nonparaxial wave equation dropping the $\partial^2 A/\partial Z^2$ term**

In contrast to the first type, the second type is the high intensity light beams. This second type of nonparaxiality results from the evolution of ultra-narrow beams in nonlinear media. A difficulty in describing the nonparaxial propagation of an electromagnetic field by means of a parabolic wave equation arises whenever the beam waist and the diffraction length become comparable, or when the spectral width of a pulse is much smaller than the pulse central frequency. However, as one increases the intensity of the incident light to produce shorter (femtosecond) pulses, non-Kerr nonlinearity effects become important and the dynamics of pulses should be described by the NLS family of equations with higher-order nonlinear terms.

Indeed, in the second direction, for example, a vector nonparaxial theory for a very narrow beam has been developed from the vector Maxwell equations by means of the order-of-magnitude analysis method by Chi and Guo as follows **[131]**:

$$i\frac{\partial u}{\partial \zeta}+\frac{1}{2}(\frac{\partial^2 u}{\partial \xi^2}+\frac{\partial^2 u}{\partial \eta^2})+|u|^2u+\sigma^2(\frac{1}{2}\frac{\partial^2 u}{\partial \zeta^2}+\frac{\partial^2}{\partial \xi^2}[|u|^2u+\frac{2}{3}|\frac{\partial u}{\partial \xi}|^2u-\frac{1}{3}(\frac{\partial u}{\partial \xi})^2u^*])=0. \quad (1.23)$$

In order to use the split-step Fourier method to solve the wave equation numerically, the $\frac{\partial^2 u}{\partial \zeta^2}$ term must be replaced by the transverse derivative. Partial derivative of the above equation with respect to ζ gives the expression $\frac{\partial^2 u}{\partial \zeta^2}$. Introducing this partial derivative in the above equation leads to:

$$\begin{aligned}\frac{\partial u}{\partial \zeta}&=i\frac{1}{2}(\frac{\partial^2 u}{\partial \xi^2}+\frac{\partial^2 u}{\partial \eta^2})+|u|^2u-i\frac{\sigma^2}{8}(\frac{\partial^4 u}{\partial \xi^4}+\frac{\partial^4 u}{\partial \eta^4})-i\sigma^2(\frac{1}{2}|u|^4u+|u|^2(\frac{\partial^2 u}{\partial \xi^2}+\frac{\partial^2 u}{\partial \eta^2})+|\frac{\partial u}{\partial \eta}|^2u\\&-\frac{11}{3}|\frac{\partial u}{\partial \xi}|^2u+\frac{1}{2}u^*[(\frac{\partial u}{\partial \eta})^2-\frac{7}{3}(\frac{\partial u}{\partial \xi})^2]-u^2\frac{\partial^2 u^*}{\partial \xi^2}).\end{aligned} \quad (1.24)$$

Marinov, Pushkarov and Shivarova **[132]** have derived the following nonlinear nonparaxial wave equation:

$$i\frac{\partial u}{\partial z}+\frac{\partial^2 u}{\partial x^2}+\frac{\partial^2 u}{\partial z^2}+|u|^2u+4|\frac{\partial u}{\partial x}|^2u-\frac{4}{3}\frac{\partial |u|^2}{\partial x}\frac{\partial u}{\partial x}+\frac{16}{3}\frac{\partial}{\partial x}(u\frac{\partial |u|^2}{\partial x})=0. \quad (1.25)$$

Partial derivative of the above equation with respect to z gives the expression $\frac{\partial^2 u}{\partial z^2}$, that is,

$$\frac{\partial^2 u}{\partial z^2}=-\frac{\partial^4 u}{\partial x^4}-\frac{\partial^2 |u|^2}{\partial x^2}+u^2\frac{\partial^2 u^*}{\partial x^2}-2|u|^2\frac{\partial^2 u}{\partial x^2}-|u|^4u. \quad (1.26)$$

After replacing this equation in the nonparaxial wave equation, we obtain:

$$\begin{aligned}&i\frac{\partial u}{\partial z}+\frac{\partial^2 u}{\partial x^2}-\frac{\partial^4 u}{\partial x^4}-\frac{\partial^2 |u|^2}{\partial x^2}+u^2\frac{\partial^2 u^*}{\partial x^2}-2|u|^2\frac{\partial^2 u}{\partial x^2}-|u|^4u+|u|^2u+4|\frac{\partial u}{\partial x}|^2u-\frac{4}{3}\frac{\partial |u|^2}{\partial x}\frac{\partial u}{\partial x}\\&+\frac{16}{3}\frac{\partial}{\partial x}(u\frac{\partial |u|^2}{\partial x})=0.\end{aligned} \quad (1.27)$$

This NLS equation containing nonparaxial correction terms has been solved numerically by employing a fully explicit , noniterative difference scheme **[132]**. Boardman, Marinov, Pushkarov and Shivarova **[133]** have derived the following nonlinear nonparaxial wave equation:

$$\begin{aligned}&i\frac{\partial u}{\partial z}+\frac{\partial^2 u}{\partial x^2}+|u|^2u+\frac{\partial^2 u}{\partial z^2}+\frac{8}{3}|\frac{\partial u}{\partial x}|^2u-\frac{\partial^4 u}{\partial x^4}-\frac{4}{3}(\frac{\partial u}{\partial x})^2u^*+k\frac{\partial^2(|u|^2u)}{\partial x^2}+\frac{k}{3}\frac{\partial}{\partial x}(u^2\frac{\partial u^*}{\partial x})\\&-\frac{2k}{3}\frac{\partial}{\partial x}(|u|^2\frac{\partial u}{\partial x})=0.\end{aligned} \quad (1.28)$$

This equation contains all the first-order correction terms to the NLS equation and accounts for a complete nonparaxial vector model of (1+1)D beam propagation in a Kerr media. By

considering the correction terms as a perturbation, an iterative procedure for solving the above equation analytically has been developed. It has been shown that the differences between the obtained analytical and numerical new solitary wave solutions in a nonparaxial vector approach and the exact solution of the scalar approach are rather small **[133]**.

Syrchin, Zheltikov and Scalora **[131]** have derived the following nonlinear nonparaxial wave equation:

$$i\frac{\partial u}{\partial \xi} = -\mu_z \frac{\partial^2 u}{\partial \xi^2} + \mu_\tau \{ \frac{\partial^2 u}{\partial \xi \partial \tau} - 4i\frac{\partial |u|^2 u}{\partial \tau}\} - |u|^2 u - \frac{|\varepsilon_0|^2 \chi^{(5)}}{\chi^3}|u|^4 u. \tag{1.29}$$

This nonlinear nonparaxial wave equation includes second-order longitudinal spatial $\frac{\partial^2 u}{\partial \xi^2}$, and second-order spatiotemporal $\frac{\partial^2 u}{\partial \xi \partial \tau}$ derivatives. Next, we replace these higher-order spatial and spatiotemporal derivatives by applying successive differentiations with respect to ξ and τ to the above equation. So, differentiating the nonparaxial wave equation with respect to ξ, and neglecting the terms of the order of μ_z^2,μ_τ^2,$\mu_z\mu_\tau$, and $\mu\chi^{(5)}$, we find:

$$\frac{\partial^2 u}{\partial \xi^2} = i\mu_z^2 \frac{\partial^3 u}{\partial \xi^3} + 2i|u|u\frac{|u|}{\partial \xi} + i|u|^2 \frac{\partial u}{\partial \xi} + 0(\mu_\tau) = -|u|^4 u + 0(\mu_\tau) + 0(\mu_z). \tag{1.30}$$

Then, differentiating the nonlinear nonparaxial wave equation with respect to τ, we find:

$$\frac{\partial^2 u}{\partial \xi \partial \tau} = \frac{\partial}{\partial \tau}[i|u|^2 u + 0(\mu_\tau) + 0(\mu_z)]. \tag{1.31}$$

After substitution, we find:

$$i\frac{\partial u}{\partial \xi} = \mu_z |u|^4 u - -\frac{|\varepsilon_0|^2 \chi^{(5)}}{\chi^3}|u|^4 u - \{1 + 3i\mu_\tau \frac{\partial}{\partial \tau}\}|u|^2 u. \tag{1.32}$$

This equation includes the first-order non-slowly varying amplitude approximation and the contribution of the fifth-order nonlinearity. An iterative procedure allowing an analytical integration of the first-order non-slowly varying amplitude approximation for self-phase-modulational equation for the amplitude and the phase for the cubic optical nonlinearity and very short pulses has been developed **[131]**.

Scalora et al. **[134]** have derived the following nonlinear nonparaxial wave equation:

$$i\frac{\partial u}{\partial z} = \frac{i}{2\beta n}\frac{1}{(}V_g^2 - \alpha\gamma - \beta(\frac{\epsilon\gamma' + \mu\alpha'}{2}))\frac{\partial^2 u}{\partial t^2} + \frac{i}{2\beta n}(\frac{\partial^2 u}{\partial z^2} - \frac{2}{V_g}\frac{\partial^2 u}{\partial z \partial t}) + \frac{i\beta\mu\chi^{(3)}}{2n}|u|^2 u - (\frac{\gamma\chi^{(3)} + \mu\chi^{(3)}}{2n})\frac{\partial}{\partial t}(|u|^2 u). \tag{1.33}$$

This nonlinear nonparaxial wave equation includes second-order longitudinal spatial $\frac{\partial^2 u}{\partial z^2}$, and second-order spatiotemporal $\frac{\partial^2 u}{\partial z \partial t}$ derivatives. Next, we replace these higher-order spatial and

spatiotemporal derivatives by applying successive differentiations with respect to z and t to the above equation. So, differentiating the nonlinear nonparaxial wave equation with respect to z and t and neglecting higher-order derivatives, we have:

$$\frac{\partial^2 u}{\partial z^2} \approx \frac{i\beta\chi^{(3)}}{2n}\frac{\partial}{\partial z}(|u|^2 u). \tag{1.34}$$

$$\frac{\partial^2 u}{\partial z \partial t} \approx \frac{i\beta\chi^{(3)}}{2n}\frac{\partial}{\partial t}(|u|^2 u). \tag{1.35}$$

After substitution, we find:

$$\frac{\partial u}{\partial z} = \frac{ik''}{2}\frac{\partial^2 u}{\partial t^2} + \frac{i\beta\chi^{(3)}}{2n}[1 - \frac{\mu\chi^{(3)}}{4n^2}|u|^2]|u|^2 u + \chi^{(3)}\{\frac{\mu}{2V_g n^2} - (\frac{\gamma+\mu}{2n})\}\frac{\partial}{\partial t}(|u|^2 u). \tag{1.36}$$

This generalized NLS equation, that can be solved numerically, includes the first-order non-slowly varying amplitude approximation corrections **[9]**.

→ **Slowly Evolving Wave Approximation (SEWA): The pulse duration is comparable to the carrier oscillation cycle**

A generic nonlinear envelope equation, first-order in the propagation coordinate ξ, which provides a powerful means of describing light pulse propagation in dispersive nonlinear media, has been derived by Brabec and Krausz **[135]** as follows:

$$\frac{\partial u}{\partial \xi} = -\frac{\alpha}{2}u + i\widehat{D}u + \frac{i}{2\beta_0}(1 + \frac{i}{\omega_0}\frac{\partial}{\partial \tau})^{-1}(\frac{\partial^2 u}{\partial x^2} + i\frac{2\pi\beta_0}{n_0^2}(1 + \frac{i}{\omega_0}\frac{\partial}{\partial \tau})|u|^2 u. \tag{1.37}$$

$$\widehat{D} = -\frac{\alpha_1}{2}\frac{\partial}{\partial \tau} + \Sigma_{m=2}^{\infty}(\frac{\beta_m + i\frac{\alpha_m}{2}}{m!})(i\frac{\partial}{\partial \tau})^m. \tag{1.38}$$

In this derivation, backward propagating waves have been neglected. The following single mathematical requirement has been provided:

$$|\frac{\partial u}{\partial \xi}| \ll \beta_0 |u|, \tag{1.39}$$

which has been referred to as the slowly-evolving-wave approximatiom (SEWA). In particular, the concept of the SEWA indicates that

$$|\frac{\beta_0 - \omega_0\beta_1}{\beta_0}| \ll 1, \tag{1.40}$$

that is, the difference between phase and group velocities of the waves involved in the interaction is small compared to the phase (or group) velocity of the fundamental pulse, which is fulfilled

in which all waves propagate in the same direction. In other words, this condition is violated in processes such as Brillouin scattering, where the pulses propagate in opposite directions, and can be addressed using nonlinear envelope equation only in the frame of the SVEA, that is, for pulse durations much longer than the optical cycle **[135]**. The SEWA requires more from the propagation medium than the SVEA: not only the envelope but also the relative carrier phase must not significantly vary as the pulse covers a distance equal to the wavelength, where the characteristic propagation length meets the condition $\beta_0 L_{char} \gg 1$

1.6 Conclusion

In this chapter, we have pointed out some generalities about metamaterials, solitons, dissipative solitons and vortex solitons in nonlinear metamaterial that we will use in this thesis. It follows that the CGL model is promising equation to study the solitons of all optical device.

The propagation of such ultrashort and intense pulses is then affected by additional physical mechanisms like self-steepening and septic nonlinearities, where especially higher-order effects such as fourth, fifth and sixth-order dispersion terms become important. These aspects of the problem will be investigated throughout this work. In the next chapter, we will present the methodology of investigations used to obtain our results.

Chapter II

Models and methodology of investigations

2.1 Introduction

In dissipative systems, research in physics devotes much attention to nonlinear phenomena. Investigations of the propagation of wave in the nonlinear media concern experimental observations and theoretical descriptions. Concerning theoretical descriptions, it appears as an important part of investigations that often come after an experimental observation and, when theoretical explanation is well carried out to generate nonlinear evolution system to model the phenomenon observed. It is then possible to predict theoretically the behavior of the wave in the medium of interest, under some new hypothesis, before returning in laboratories to verify if the theoretical hypothesis are confirmed experimentally. Such an inter-dependence between experiment and theoretical investigation make it clear the importance of both in looking for more innovative technological devices. As far as we are concerned throughout this thesis with MI and the propagation of spatiotemporal wave in metamaterials, theoretical investigations have been carried out beyond the SVEA within the framework of some treatable methods, in particular linear stability analysis.

Very recently, many authors have investigated and proposed nonlinear ultrashort pulse propagation models in NIMs in various contexts **[13,135]**. Scalora et al.**[9]** first derived a new generalized nonlinear Schrodinger (NLS) equation, to describe the propagation of ultrashort pulses in bulk negative index media exhibiting frequency dependent dielectric susceptibility and magnetic permeability. Going beyond the usual SVEA, they investigated the propagation of pulses for at least a few tens of optical cycles in MMs. They did not consider magnetic nonlinearity in

their approach. Wen et al. have derived a (3+1) dimensional evolution equation for NIM with a Kerr nonlinear polarization by following the same procedure as applied to the case of ordinary materials **[10]**.

The CGL equation may be viewed as a dissipative extension of the NLS equation. Accordingly, it can describe a broad range of behaviors suggested by the NLS equation dynamics, ranging from chaos and pattern formation to spatiotemporal dissipative optical solitons. The CGL equation with the cubic-quintic nonlinearity makes it possible to find stable localized solutions in both the 2D and 3D geometries.

The higher-order (3+1)D CQS-CGL equation, taking into account diffraction, diffusion, higher-order dispersion terms up to six with higher-order effects such as self-steepening effects, as mentioned in the general introduction, is the most advanced model in the CGLs-type family equation that no one else has studied yet for the modeling of the dissipative solitons in nonlinear metamatreials. This model equation has been derived for the first time in this thesis.

Our main objective is to investigate new types of dissipative and nonlinear dynamics and thus, contribute to the understanding of 3D dissipative optical solitons. In order to accomplish our aims, we employ some analytical and numerical methods, which lead to describe the beam m behavior correctly beyond the SVEA. The numerical methods are used to consolidate the analytical results. In the first part of this chapter, we derive the (3+1)D CQ-CGL and the higher-order (3+1)D CQS-CGL equations in the physical context of nonlinear metamaterial beyond the SVEA. In the second part, we give general information about our analytical methods and the third part is devoted to the presentation of numerical methods. A concise conclusion finally ends the chapter.

2.2 Governing equation and derivation of the (3+1)D cubic-quintic and cubic-quintic-septic complex Ginzburg-Landau beyond the SVEA

Let us now proceed in deriving at (3+1-dimension cubic-quintic and cubic-quintic-septic CGL equation beyond the SVEA with competing effects ch as dispersion, diffraction, gain, loss, cubic-

quintic-septic nonlinearities, and cubic, quintic and septic self-steepening terms, for dissipative light bullets in nonlinear metamaterials.

2.2.1 Derivation of the (3+1)D cubic-quintic complex Ginzburg-Landau beyond the SVEA

The field of nonlinear optics is complex and encompasses myriads of interesting effects and practical applications. In spite of its richness, most of the effects can be described accurately with just a few equations. This introduction to nonlinear optics is therefore limited to a simple analysis of Maxwell's equations, which govern the propagation of light. The well-known theory of electromagnetic wave propagation in dispersive nonlinear media is considered in order to understand the nonlinear phenomena in metamaterials. In dielectric media, the equations are given by,

$$\nabla \times \mathbf{E} = -\frac{\partial \mathbf{B}}{\partial t}, \;\; \nabla \times \mathbf{H} = \frac{\partial \mathbf{D}}{\partial t}, \;\; \nabla.\mathbf{D} = 0, \;\; \text{and} \;\; \nabla.\mathbf{B} = 0, \tag{2.1}$$

in which there are no free charges, and no fee currents flow. the quantities $\mathbf{E}$ and $\mathbf{H}$ are the electric and magnetic field vectors, respectively. The quantities $\mathbf{D}$ and $\mathbf{B}$ are the electric and magnetic flux densities, respectively. The induced polarization $\mathbf{P}$ and magnetization $\mathbf{M}$ may be made explicit in Maxwell's equations via the constitutive relations

$$\mathbf{D} = \varepsilon_0 \varepsilon \mathbf{E} + \mathbf{P}_{nl}, \;\; \text{and} \;\; \mathbf{B} = \mu_0 \mu \mathbf{H} + \mathbf{M}_{nl}, \tag{2.2}$$

where ε_0 and μ_0 are the respective vaccum electric permittivity and magnetic permeability. ε and μ are dispersive complex permittivity and permeability of a dissipative medium. $\mathbf{P}_{nl}$ is a nonlinear polarization, and $\mathbf{M}_{nl}$ is a nonlinear magnetization. $\mathbf{E}$, $\mathbf{D}$, $\mathbf{B}$, $\mathbf{H}$ are slowly varying functions in space and time. The quasi-monochromatic representation is used for the functions, namely $\mathbf{A}(\mathbf{r}, t) = \mathbf{A} \exp(i\mathbf{kr} - i\omega t)$, where ω is the carrier frequency and $\mathbf{k} = \mathbf{k}_r + i\mathbf{k}_i$ is a complex vector. $\mathbf{k}$ is determined by the linear dispersion relation $\mathbf{k}^2 c^2 = \omega^2 \epsilon(\omega)\mu(\omega)$. The first derivatives of Eqs.(2.2) with respect to time t are

$$\frac{\partial \mathbf{D}}{\partial t} = \varepsilon_0(-i\omega\varepsilon\mathbf{E} - i\omega\varepsilon_{nl}\mathbf{E})e^{-i\omega t} \;\; \text{and} \;\; \frac{\partial \mathbf{B}}{\partial t} = \mu_0(-i\omega\mu\mathbf{H} - i\omega\mu_{nl}\mathbf{H})e^{-i\omega t}. \tag{2.3}$$

We expand the dielectric permittivity $\varepsilon(\omega)$ and magnetic permeability $\mu(\omega)$, in Taylor series around the central frequency ω_0, as follows:

$$\omega\varepsilon(\omega) = \Sigma_{n=0}^{\infty}\left[\frac{\alpha_n}{n!}(\omega-\omega_0)^n\right], \;\; \omega\mu(\omega) = \Sigma_{m=0}^{\infty}\left[\frac{\beta_m}{m!}(\omega-\omega_0)^m\right], \tag{2.4}$$

where $\alpha_n = \frac{\partial^n[\omega\varepsilon(\omega)]}{\partial\omega^n}|_{\omega=\omega_0}$ and $\beta_m = \frac{\partial^m[\omega\mu(\omega)]}{\partial\omega^m}|_{\omega=\omega_0}$.

Substituting Eqs.(2.4) into Eqs.(2.3) yields

$$\begin{aligned}
\frac{\partial\overrightarrow{D}}{\partial t} &\approx \varepsilon_0\left(-i\omega_0\varepsilon\overrightarrow{E} + \alpha_1\frac{\partial\overrightarrow{E}}{\partial t} + i\frac{\alpha_2}{2}\frac{\partial^2\overrightarrow{E}}{\partial t^2} + \frac{\partial(\varepsilon_{nl}\overrightarrow{E})}{\partial t} - i\omega_0\varepsilon_{nl}\overrightarrow{E}\right)e^{-i\omega t},\\
\frac{\partial\overrightarrow{B}}{\partial t} &\approx \mu_0\left(-i\omega_0\mu\overrightarrow{H} + \beta_1\frac{\partial\overrightarrow{H}}{\partial t} + i\frac{\beta_2}{2}\frac{\partial^2\overrightarrow{H}}{\partial t^2} + \frac{\partial(\mu_{nl}\overrightarrow{H})}{\partial t} - i\omega_0\mu_{nl}\overrightarrow{H}\right)e^{-i\omega t}.
\end{aligned} \tag{2.5}$$

Indeed, after performing the curl of Eqs.(2.1), and neglecting vectorial terms such as $\nabla(\nabla.E) = 0$, and choosing appropriate variables for the measurement of time and spatial coordinates, that is $\xi = z$ and $\tau = t - \frac{1}{v_g}z$, where v_g is a real group velocity defined by $v_g = \left[\frac{\partial(n\omega)}{\partial\omega}\right]^{-1}$ and n is a negative-refractive index given by $n = -\sqrt{Re[\varepsilon\mu]} = k_r\frac{c}{\omega}$, with k_r being the negative wave vector's real part, one would obtain the following dynamical equation

$$\begin{aligned}
2ik\frac{\partial\overrightarrow{E}}{\partial\xi} + \Delta\overrightarrow{E} - \left(\frac{2}{v_g}\right)\frac{\partial^2\overrightarrow{E}}{\partial\xi\partial\tau} - \frac{W_2}{c^2}\frac{\partial^2\overrightarrow{E}}{\partial\tau^2} + i\frac{\omega_0^2}{c^2}Im[\varepsilon\mu]\overrightarrow{E} + \frac{\omega_0^2}{c^2}\mu\varepsilon_{nl}\overrightarrow{E} + i\frac{\omega_0}{c^2}(\mu+\beta_1)\frac{\partial(\varepsilon_{nl}\overrightarrow{E})}{\partial\tau}\\
- i\mu_0\frac{\partial(\mu_{nl}\overrightarrow{k}\times\overrightarrow{H})}{\partial\tau} - \mu_0\omega_0\mu_{nl}\overrightarrow{k}\times\overrightarrow{H} = 0,
\end{aligned} \tag{2.6a}$$

$$\begin{aligned}
2ik\frac{\partial\overrightarrow{H}}{\partial\xi} + \Delta\overrightarrow{H} - \left(\frac{2}{v_g}\right)\frac{\partial^2\overrightarrow{H}}{\partial\xi\partial\tau} - \frac{W_2}{c^2}\frac{\partial^2\overrightarrow{H}}{\partial\tau^2} + i\frac{\omega_0^2}{c^2}Im[\varepsilon\mu]\overrightarrow{H} + \frac{\omega_0^2}{c^2}\mu_{nl}\varepsilon\overrightarrow{H} + i\frac{\omega_0}{c^2}(\varepsilon+\alpha_1)\frac{\partial(\mu_{nl}\overrightarrow{H})}{\partial\tau}\\
+ i\varepsilon_0\frac{\partial(\varepsilon_{nl}\overrightarrow{k}\times\overrightarrow{E})}{\partial\tau} + \varepsilon_0\varepsilon_{nl}\omega_0\overrightarrow{k}\times\overrightarrow{E} = 0,
\end{aligned} \tag{2.6b}$$

where

$W_2 = -c^2v_g^{-2} + \frac{1}{2}\omega_0(\mu\alpha_2 + \varepsilon\beta_2) + \alpha_1\beta_1,$

These generalized complex (3+1)- dimensional equations describe dissipative effects in NIMs as well as in PIMs. Equations (Eqs.(2.6a)) and (Eqs.(2.6b)) are used in order to describe the dynamics of dissipative solitons in NIMs and to make the comparison with well-known soliton dynamics in PIMs modeled by usual the Ginzburg-Landau equation. The imaginary part of

linear permittivity ϵ_i , permeability μ_i , and wave vector k_i are considered small. To construct the ultrashort electromagnetic pulses in MMs for Eqs.(2.6), we assume both the electric and magnetic fields to propagate along the $z-$direction, with the linearly polarized fields

$$\begin{pmatrix} \overrightarrow{E} \\ \overrightarrow{H} \end{pmatrix} = \begin{pmatrix} \widehat{x}E \\ \widehat{y}H \end{pmatrix} \exp[i(\beta_0 z - \omega_0 t)] + c.c., \tag{2.7}$$

where ω_0 is the central frequency of the electromagnetic pulse, β_0 is the corresponding wave number, and *c.c.* denotes the complex conjugate. The nonlinear response of MMs is characterized by two different contributions. The first one is an intensity-dependent part of the effective dielectric permittivity of the MMs. The second contribution is the effective magnetic permeability which depends on the macroscopic magnetic field. We further illustrate high optical intensities by considering the following model expressions for both field-dependent dielectric permittivity and magnetic-permeability responses of the dispersive MMs of the form

$$\varepsilon_{nl}(|E|^2) = (\varepsilon_r^{(3)} + i\varepsilon_i^{(3)})|E|^2 - (\varepsilon_r^{(5)} + i\varepsilon_i^{(5)})|E|^4, \tag{2.8}$$

and

$$\mu_{nl}(|H|^2) = (\mu_r^{(3)} + i\mu_i^{(3)})|H|^2 - (\mu_r^{(5)} + i\mu_i^{(5)})|H|^4, \tag{2.9}$$

We further substitute Eq.(2.8) and Eq.(2.9) into Eq.(2.6a) to obtain for the electric field equation

$$\begin{aligned} &i\frac{\partial E}{\partial z} + \frac{1}{2n\varpi}\Delta_\perp E + \frac{1}{2n\varpi}\frac{\partial^2 E}{\partial z^2} - \left(\frac{c}{n\varpi v_g}\right)\frac{\partial^2 E}{\partial z \partial t} - \frac{W_2}{2n\omega}\frac{\partial^2 E}{\partial \tau^2} + i\frac{\varpi}{2n}Im[\varepsilon\mu]E + \\ &\quad \frac{\varpi}{2}\left[(\chi_r^{(3)} + i\chi_i^{(3)})|E|^2 E - (\chi_r^{(5)} + i\chi_i^{(5)})|E|^4 E\right] + \frac{i}{2}\left[\left(\chi_r^{(3)} + i\chi_i^{(3)}\right)\frac{\partial(|E|^2 E)}{\partial t} - (\chi_r^{(5)} + i\chi_i^{(5)})\frac{\partial(|E|^4 E)}{\partial t}\right] \\ &\quad = 0, \end{aligned} \tag{2.10}$$

in which we defined new normalized variables as [136]: $(\frac{c}{\omega_p})^2\Delta_\perp \to \Delta_\perp$, $\omega_p\tau \to t$, $(\frac{\omega_p}{c})\xi \to z$, $(\frac{\omega_0}{\omega_p}) \to \varpi$, where ω_p is the plasma frequency, and $\Delta_\perp = \frac{\partial^2}{\partial x^2} + \frac{\partial^2}{\partial y^2}$. The parameters $\chi^{(3)} = \varepsilon^{(3)}Z + \frac{\mu^{(W3)}}{Z^{(3)}}$ and $\chi^{(5)} = \varepsilon^{(5)}Z + \frac{\mu^{(5)}}{Z^{(5)}}$ are the cubic and quintic susceptibilities, respectively, with $Z = (\frac{\mu}{\varepsilon})^{\frac{1}{2}} = \frac{E}{H}$, being the medium impedance.

In order to calculate the first-order non-SVEA correction terms, we use Eq.(2.10) to evaluate $\frac{\partial^2 E}{\partial z^2}$ and $\frac{\partial^2 E}{\partial z \partial t}$. Consequently, omitting the higher order terms, which are assumed small, the above

derivatives can be approximately expressed by the following second-order partial differential equations

$$\begin{aligned} \frac{\partial^2 E}{\partial z^2} &\approx -C^2|E|^4E, \text{ and} \\ \frac{\partial^2 E}{\partial z \partial t} &\approx iC\frac{(|E|^2E)}{\partial t} - iQ\frac{\partial(|E|^4E)}{\partial t}, \end{aligned} \tag{2.11}$$

where, $C = \frac{\varpi}{2}\left(\chi_r^{(3)} + i\chi_i^{(3)}\right)$, $Q = \frac{\varpi}{2}\left(\chi_r^{(5)} + i\chi_i^{(5)}\right)$. Substituting Eqs.(2.11) into Eq.(2.10) and introducing the following normalization for Eq. (10), we obtain $\left(\sqrt{\frac{|2n\varpi|}{|Re[W]|}}\right) t \to t$, $\frac{\Delta_\perp}{2|n|\varpi} \to \Delta_\perp$, $\left(\frac{\sqrt{|\chi_r^{(3)}|\varpi}}{\sqrt{2}}\right) E \to E$,

$$\begin{aligned} i\frac{\partial E}{\partial z} + (\sigma_{r\perp})\Delta_\perp E - i\sigma_{i\perp}\nabla_\perp^2 E + (-k_{2r} - ik_{2i})\frac{\partial^2 E}{\partial t^2} + i\delta E + (N_{3r} + iN_{3i})|E|^2E + (N_{5r} + iN_{5i})|E|^4E \\ + (SS_{3r} + iSS_{3i})\frac{\partial(|E|^2E)}{\partial t} + (SS_{5r} + iSS_{5i})\frac{\partial(|E|^4E)}{\partial t} = 0, \end{aligned} \tag{2.12}$$

In the above equation, the different coefficients are given in the Appendix . The resulting nonlinear evolutionary equation (2.12) is the (3+1)D cubic-quintic CGL equation which models the propagation of ultrashort dissipative optical pulses in MMs, where $(\sigma_{r\perp} + \sigma_{i\perp})$ is the transverse complex coefficient, $k_{2r} + ik_{2i}$ is the complex group velocity dispersion (GVD). δ is related to the linear loss ($\delta < 0$) or gain ($\delta > 0$), while $(N_{3r} + iN_{3i})$ and $(N_{5r} + iN_{5i})$ are the cubic and quintic nonlinear complex coefficient, respectively. The complex parameters $(SS_{3r} + iSS_{3i})$ and $(SS_{5r} + iSS_{5i})$ characterize the so-called cubic and quintic self-steepening effects due to cubic and quintic nonlinear polarizations, The dielectric permittivity ϵ and magnetic permeability μ are, respectively, given by the lossy Drude model of free electron collisions (ν_ε and ν_μ) **[137, 138]**

$$\varepsilon(\omega) = 1 - \frac{\omega_p^2}{\omega^2 + i\omega\nu_\varepsilon}, \text{ and } \mu(\omega) = 1 - \frac{\omega_m^2}{\omega^2 + i\omega\nu_\mu}, \tag{2.13}$$

where ω_m is the magnetic plasma frequency.

2.2.2 The higher-order (3+1)-dimensional cubic-quintic-septic complex Ginzburg- Landau equation

♣ Higher-order dispersions

In the nonlinear regime, the possibility of ultrashort-pulse propagation has been investigated. It has also been shown that, under ultrashort-pulse propagation, a modification of the nonlinear Schrödinger equation, which is traditionally used for the theoretical description of nonlinear light propagation in optical metamaterial for the slowly varying envelope and which describes dispersion effects up to the second order and the self-phase modulation effect, is needed. For this purpose, various authors have considered the third-order dispersion effect **[139]** and the self-steepening effect **[140]**. Moreover, the real part as well as the imaginary part of the third-order nonlinear susceptibility has been taken into account in order to describe the Raman self-scattering effect **[141]**. In addition, a nonlinear wave equation that contains the third-order dispersion effect, self-steepening effect, Raman self-scattering effect, Stokes losses associated with the material excitations during the Raman self-scattering process and the dependence of the nonlinear effects and the fiber mode area on the light frequency, has been derived **[142]**. All the above-mentioned effects influence considerably the femtosecond soliton propagation. In particular, the possibility of obtaining high-quality pulses of less than 15 femtosecond duration by compression of fundamental solitons with approximately 100 femtosecond duration in fibers with slowly decreasing dispersion has been generated **[142]**.

It is well known that the theoretical description of the self-modulation of waves propagating in nonlinear magnetic metamaterials for the slowly varying envelope is governed by the nonlinear Schrödinger (NLS) equation **[11]**. The NLS equation has exact dark and bright soliton solutions that correspond to a balance between dispersion effects up to the second order and the self-phase modulation effect. For bright solitons, this balance should be with the positive nonlinearity in anomalous dispersive region or the negative nonlinearity in normal dispersive region, while for dark solitons, these conditions are opposite **[143]**. Higher-order harmonics can be selectively generated by introducing varactor diodes into the split-ring resonator circuit **[144]**. Let us recall that the interaction of light with nonlinear dispersive media depends on the physical and chemical structures of the metamaterial. Then, the desired linear and nonlinear properties

can be obtained, such as the dispersion in metamaterials which can be tailored by stacking a number of highly dispersive sheets of metamaterials. A number of studies have investigated the dispersive effect of metamaterial structures on pulse propagation. For this purpose, it has been shown that the dark soliton, which can transmit stably after the second-order dispersion and nonlinear cancellation, becomes unstable after adding the third-order dispersion (TOD) **[145]**. As the pulses become narrower in time, fourth-order dispersion (FOD) should also be taken into account. An exact dipole solitary wave solution has been derived in metamaterials with Kerr nonlinearity, TOD and FOD **[146]**. Dark, bright, combined dark?bright, singular, combined singular soliton, and singular periodic wave solutions are obtained in metamaterials with cubic-quintic nonlinearity, detuning intermodal dispersion, self- steepening effect and linear as well as nonlinear TOD and FOD terms **[147]**. Following Lagrangian variational method, stable dynamics of the dissipative soliton in metametarials has been demonstrated as a result of the interplay between various higher-order effects such as TOD and FOD terms as perturbation to the system. In particular, self-steepening effect and TOD can remove instabilities, while FOD always enhances the self-steepening effect induced temporal shift toward the trailing or leading edges of the pulse **[148]**. Parametric conditions for the existence of bright, dark and W-shaped solitary waves on the extended NLS equation with additional TOD and FOD terms, have been presented **[149]**. It has been found that TOD contributes none to MI **[150, 151]**, while FOD plays a major role in the critical MI frequency and leads to the appearance of new MI peaks that are experimentally observed instability regions **[152, 153, 154]**. Moreover, the evolution spectrum of the perturbed wave for different FOD coefficients in MMs has shown when the FOD coefficient increases, the period of modulation decreases, and the number of pulses increases **[155]**. The stabilizing effect of positive FOD as well as the strong destabilizing effect of negative FOG and TOD has been reported, and the nature of the instability in the vicinity of zero group-delay dispersion **[156]**. Generally speaking, as the group velocity reduces further, higher-order dispersive terms will start to play a role. Especially at these lower optical frequencies, it is well-known that the common approach to approximate the dispersive properties by a Taylor expansion, is only valid if many orders of the expansion are included. Indeed, it has been found that the effect of higher-order dispersion in a typical photonic crystal strongly increases when the group velocity decreases **[157]**.

They are expanded in the series around the carrying frequency up to the six order of the Eq.2.4, and we obtain the Eq.2.5 in the form

$$\begin{aligned}
&\frac{\partial \overrightarrow{D}}{\partial t} \approx \varepsilon_0(-i\omega_0\varepsilon\overrightarrow{E} + \alpha_1\frac{\partial \overrightarrow{E}}{\partial t} + i\frac{\alpha_2}{2}\frac{\partial^2 \overrightarrow{E}}{\partial t^2} - \frac{\alpha_3}{6}\frac{\partial^3 \overrightarrow{E}}{\partial t^3} - i\frac{\alpha_4}{24}\frac{\partial^4 \overrightarrow{E}}{\partial t^4} + \frac{\alpha_5}{120}\frac{\partial^5 \overrightarrow{E}}{\partial t^5} + i\frac{\alpha_6}{720}\frac{\partial^6 \overrightarrow{E}}{\partial t^6} \\
&+ \frac{\partial(\varepsilon_{nl}\overrightarrow{E})}{\partial t} - i\omega_0\varepsilon_{nl}\overrightarrow{E})e^{-i\omega t}, \\
&\frac{\partial \overrightarrow{B}}{\partial t} \approx \mu_0(-i\omega_0\mu\overrightarrow{H} + \beta_1\frac{\partial \overrightarrow{H}}{\partial t} + i\frac{\beta_2}{2}\frac{\partial^2 \overrightarrow{H}}{\partial t^2} - \frac{\beta_3}{6}\frac{\partial^3 \overrightarrow{H}}{\partial t^3} - i\frac{\beta_4}{24}\frac{\partial^4 \overrightarrow{H}}{\partial t^4} + \frac{\beta_5}{120}\frac{\partial^5 \overrightarrow{H}}{\partial t^5} + i\frac{\beta_6}{720}\frac{\partial^6 \overrightarrow{H}}{\partial t^6} \\
&+ \frac{\partial(\mu_{nl}\overrightarrow{H})}{\partial t} - i\omega_0\mu_{nl}\overrightarrow{H})e^{-i\omega t}.
\end{aligned} \tag{2.14}$$

♣ Higher-order nonlinearities

In fact, cubic (Kerr), quintic-septic (non-Kerr) nonlinearities can be well understood when considering the problem of soliton instabilities. Sometimes, these soliton instabilities lead to the collapse, and depend on the number of space dimensions and strength of nonlinearity, respectively. One of the principal direction in the studies of the collapse stabilization is the use of a weaker nonlinearity, such as saturable **[158]**, cubic-quintic **[159]**, quadratic (χ^2) **[160]**, or that induced by the self-induced transparency**[161]**. Remarkably, the connection between the use of a weaker nonlinearity and the collapse stabilization is that, as the intensity of the incident light field becomes stronger, non-Kerr nonlinear effects come into play. At the same time, when solving the problem of soliton instabilities leading to the collapse of waves, it is also important, for some applications in telecommunication and ultrafast signal routing systems, to increase the channel handling capacity and ultra high speed pulse. For this purpose, it is necessary to transmit dissipative solitons at a high bit rate ($\approx 1 - 10fs$) of ultrashort pulses, which can be seen in many applicative contexts such as high repetition pulse sources based on fiber as well as on doped fiber technology **[162]**. In addition, at high light intensities, the way through which the non-Kerr nonlinearities influence the dissipative soliton propagation in erbium doped fiber amplifiers has been described by the (3+1)-D complex Ginzburg-Landau equation with cubic-quintic-septic nonlinearities and higher degree dispersion terms **[17]**.

Specifically, it is well known that, the cubic (Kerr effect) nonlinearity is related to the value of third-order susceptibility (χ^3). Moreover, in a recent experiment, it has been established that the optical susceptibility of CdS_xSe_{1-x}-doped glass processes a considerable level

of fifth-order susceptibility (χ^5). In semiconductor doubled optical fibers **[95]**, the doping silica fibers with two appropriate semiconductor particles may lead to an increased value of thir-dorder susceptibility (χ^3) and a decreased value of (χ^5). However, when the saturation is very strong, a self-focusing (χ^7) is also needed. Quite recently, an experiment has been reported in material such as chalcogenide glass which exhibits not only third-order nonlinearities but even seventh-order nonlinearities **[163]**. In other words, chalcogenide glass can be classified as a cubic-quintic-septic nonlinear material. In the past few years, the higher-order nonlinear Schrödinger equation with cubic-quintic-septic nonlinearities were used, as a model equation for the propagation of ultrashort femtosecond optical pulse **[163]**. Thus, in order to investigate pulse propagation in such materials, it is necessary to consider higher-order nonlinearities in place of the usual Kerr nonlinearity. To the best of our knowledge, no work has been reported in the dynamics of dissipative light bullets in the nonlinear metamaterial, taking into account septic nonlinearity, self-steepening, fourth-, fifth- and sixth-order dispersion terms in the frame of the CGL equation. So we take Eq.2.8 and 2.9 in the form

$$\varepsilon_{nl}(|E|^2) = (\varepsilon_r^{(3)} + i\varepsilon_i^{(3)})|E|^2 - (\varepsilon_r^{(5)} + i\varepsilon_i^{(5)})|E|^4 + (\varepsilon_r^{(7)} + i\varepsilon_i^{(7)})|E|^6, \tag{2.15}$$

and

$$\mu_{nl}(|H|^2) = (\mu_r^{(3)} + i\mu_i^{(3)})|H|^2 - (\mu_r^{(5)} + i\mu_i^{(5)})|H|^4 + (\mu_r^{(7)} + i\mu_i^{(7)})|H|^6, \tag{2.16}$$

where in addition to the cubic Kerr-type dielectric nonlinearity, the quintic-septic non-Kerr nonlinear terms become important and should be incorporated when one increases the intensity of the incident light power to produce shorter pulses. As is well known in the study of soliton dynamics beyond Kerr nonlinearity, the minus sign of the quintic nonlinearity is to prevent pulse collapse.

Following the same procedure as in the previous section, we obtain

$$\begin{aligned} i\frac{\partial E}{\partial z} + (\sigma_{r\perp})\Delta_\perp E - i\sigma_{i\perp}\nabla_\perp^2 E + (-ik_{2i})\frac{\partial^2 E}{\partial t^2} - i(k_{3r} + ik_{3i})\frac{\partial^3 E}{\partial t^3} + (k_{4r} + ik_{4i})\frac{\partial^4 E}{\partial t^4} + i(k_{5r} + ik_{5i})\frac{\partial^5 E}{\partial t^5} \\ + (k_{6r} - ik_{6i})\frac{\partial^6 E}{\partial t^6} + i\delta E + (N_{3r} + iN_{3i})|E|^2 E + (N_{5r} + iN_{5i})|E|^4 E + (N_{7r} + iN_{7i})|E|^6 E + \\ (SS_{3r} + iSS_{3i})\frac{\partial(|E|^2 E)}{\partial t} + (SS_{5r} + iSS_{5i})\frac{\partial(|E|^4 E)}{\partial t} + (SS_{7r} + iSS_{7i})\frac{\partial(|E|^6 E)}{\partial t} = 0, \end{aligned} \tag{2.17}$$

In the above equation, the different coefficients are given in the Appendix B. The resulting nonlinear evolutionary equation ((2.17)) is the (3+1)D cubic-quintic-septic CGL equation which models the propagation of ultrashort dissipative optical light bullets in MMs in the few cycle regime, where $\sigma_\perp$ is the transverse complex coefficient, k_2 is the complex group velocity (GVD). δ is related to the linear loss ($\delta < 0$) or gain ($\delta > 0$), while N_3, N_5 and N_7 are the cubic, quintic and septic nonlinear complex coefficients, respectively. The complex parameters SS_3, SS_5 and SS_7 characterize the so-called cubic, quintic and septic self-steepening (SS) effects due to cubic, quintic and quintic nonlinear polarizations, respectively. Self steepening is a higher order nonlinear effect which results from the intensity dependence of the group velocity. It causes an asymmetry in the SPM broadened spectra of ultrashort pulses as the pulse moves at a lower speed than the wings of the pulse. Therefore, as the pulse propagates inside the system, the peak shifts towards the trailing edge and the trailing edge becomes steeper with increasing distance. Self steepening of the pulse creates an optical shock and is only important for short pulses. The complex quantities k_3, k_4, k_5, and k_6 account for the third-, fourth-, fifth- and sixth-order dispersion coefficients, respectively.

In our scaled units, we choose $\nu_\epsilon = \nu_\mu = 5.10^{-4}$, which results in negligible absorption **[164]**. In Figure 2. 1, we show ϵ, μ and the index of refraction n, when $\omega_m^2/\omega_p^2 = 0.64$.

Bright spatiotemporal solitons (i.e., light bullets) are generated whenever both diffraction and dispersion are compensated with saturating nonlinearity, having all the same sign **[14]**. As a consequence, as confirmed also by numerical simulations, light bullets may propagate only in NIMs with NGVD in the range $0.7 < \omega < 0.8$, for the choice of dissipative parameters $\sigma_{i\perp}$ and δ_i, contrary to PIMs where AGVD is required. Therefore, all real terms of CQS-CGL equation in NIMs have the opposite sign with respect to equivalent terms for PIMs, reflecting a "mirror" symmetry. The complementarity of both types of media corresponds essentially to a disjoint range of parameters in temporal domain. The obtained CQS-CGL equation, since it is not integrable, can be solved only numerically. However, some analytical approach is highly desirable.

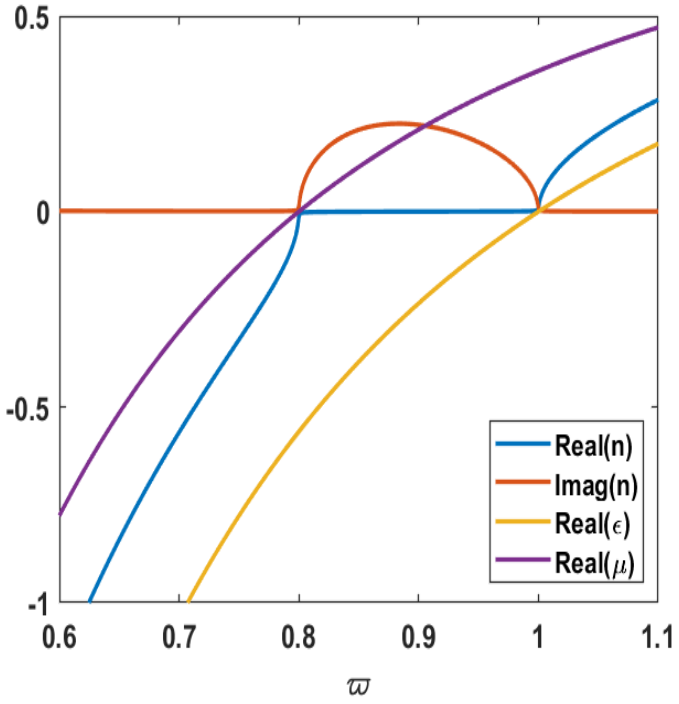

Figure 2.1: Dispersion of ϵ, μ, and resulting n. The region $0.8 \leq \omega/\omega_p \leq 1$ is characterized by metal-like reflections, as n becomes almost purely imaginary. $n < 0$ in the region $\omega/\omega_p \leq 0.8$.

2.3 Analytical methods

Before the discovery of solitons, mathematicians were under the impression that nonlinear partial differential equations could not be solved, at least not exactly. However, solitons lead to the recognition that through a combination of such diverse subjects as quantum physics and algebraic geometry, one can actually solve some nonlinear equations exactly, which opens up a wide window in the world of nonlinearity **[165]**. Since the concept of dromions was discovered and introduced by Boiti **[166]**, the study of soliton-like solutions in higher dimensions has attracted much attention. Now, several significant (2+1- and (3+1)-D models, such as (2+1)-D Kadomtsev-Petviashvili equation **[167]**, Davey-Stewartson equation **[168]**, generalized Korteweg-de Vries equation **[169]**, sine-Gordon equation **[170]**, (3+1)-D Korteweg-de Vries equation **[171]**, the nonlinear dispersion equation with compact structures **[172]**, the generalized Camassa-Holm (CH) equation **[172]**, the nonlinear elastic rod equation **[158-161]**, the coupled quadratic nonlinear equations **[177]**, the coupled Klein- Gordon-Schrödinger equations **[177]**, the coupled dispersionless system **[178]**, the similarity method **[179]**, and the method of

modulational instability **[180]**, the method of moments **[181]**, the method of collective coordinates **[167,169]**, the finite-difference time-domain method **[185]**, the effective-particle method **[186]**, the variational method **[187]**, the Lyapunov's method **[188, 189]** have been investigated and some special types of localized solutions for these have also been obtained by means of different approaches.

Solitons and localized structures have been intensively used during the recent years. The direct way to emerge solitons and localized structures from nonlinear systems is through the activation of MI. MI consists in the input of continuous wave (with a constant amplitude, but with an amplitude dependence of the dispersion relation) which propagates through the system, which can become unstable for a small perturbation under specific conditions.

In this thesis, a set of evolution equations have been derived using linear stability analysis method. We recall that this linear stability analysis method has been successfully used to address a variety of nonlinear problems. The motivations of our choice are based on the advantages of this method. Among them, we have: linear stability analysis gives a detailed qualitative picture of the role and mode of action of each perturbation (such as third-order dispersion, self-phase modulation, or self-steepening) on the pulse. In order to investigate new types of 3D dissipative optical light bullets, our consideration are based on the linear stability analysis.

• **Linear stability analysis method**

In a local nonlinear media(ker effet) the propagation of a slowly varying wave packet $A(z,t)$, along the z-axis is described by the nonlinear paraxial wave equation, that is, the 1D NLS equation that takes the following form **[190]**

$$i\frac{\partial A}{\partial z} = \frac{\beta_2}{2}\frac{\partial^2 A}{\partial T^2} - \gamma|A|^2 A, \tag{2.18}$$

where more precisely, $A(z,T)$ represents the amplitude of the pulse envelope, β_2 is the GVD parameter, and the nonlinear parameter γ is responsible for SPM. In the case of CW radiation, the amplitude A is independent of T at the input of the fiber at $z = 0$. Assuming that $A(z,T)$ remains time independent during propagation inside the fiber, Eq.(2.18) is readily solved to obtain the steady-state solution

$$A = \sqrt{P_0} exp(i\phi_{NL}), \tag{2.19}$$

where P_0 is the incident power and $\phi_{NL} = \gamma P_0 z$ is the nonlinear phase shift induced by SPM.

Eq.(2.19) implies that CW light should propagate through the fiber unchanged except for acquiring a power-dependent phase shift (and for reduction in power in the presence of fiber losses).

Before reaching this conclusion, however, we must ask whether the steady-state solution Eq.(2.19) is stable against small perturbations. To answer this question, we perturb the steady state slightly as follows

$$A = (\sqrt{P_0} + a)exp(i\phi_{NL}), \tag{2.20}$$

and examine evolution of the perturbation $a(z,T)$ using a linear stability analysis. Substituting Eq.(2.20) inEq.(2.18) and linearizing in a, we obtain

$$i\frac{\partial a}{\partial z} = \frac{\beta_2}{2}\frac{\partial^2 a}{\partial T^2} - \gamma P_0(a + a^*). \tag{2.21}$$

This linear equation can be solved easily in the frequency domain. However, because of the a^* term, the Fourier components at frequencies Ω and $-\Omega$ are coupled. Thus, we should consider its solution in the form

$$a(z,T) = a_1 exp[i(Kz - \Omega T)] + a_1 exp[-i(Kz - \Omega T)], \tag{2.22}$$

where K and Ω are the wave number and the frequency of perturbation, respectively. Equations (2.21) and (2.22) provide a set of two homogeneous equations for a_1 and a_2. This set has a nontrivial solution only when K and Ω satisfy the following dispersion relation

$$K = \pm\frac{1}{2}|\beta_2\Omega|[\Omega^2 + sgn(\beta_2\Omega_c^2)]^{1/2}, \tag{2.23}$$

where $sgn(\beta_2) = \pm 1$ depending on the sign of β_2, and

$$\Omega_c^2 = \frac{4\gamma P_0}{4}. \tag{2.24}$$

The dispersion relation (2.24) shows that steady-state stability depends critically on whether light experiences normal or anomalous GVD inside the fiber. In the case of normal GVD ($\beta_2 > 0$), the wave number K is real for all Ω, and the steady state is stable against small perturbations. By contrast, in the case of anomalous GVD ($\beta_2 < 0$), K becomes imaginary for $\Omega < \Omega_c$, and the perturbation $a(z,T)$ grows exponentially with z as seen from Eq.(2.22). As a

result, the CW solution ((2.20)) is inherently unstable for $\beta_2 < 0$. This instability is referred to as modulation instability because it leads to a spontaneous temporal modulation of the CW beam and transforms it into a pulse train.

The gain spectrum of modulation instability is obtained from Eq. ((2.23)) by $sgn(\beta_2) = 1$ and $g(\Omega) = 2Im(K)$, where the factor of 2 converts g to power gain. The gain given by

$$g(\Omega) = |\beta_2 \Omega|[\Omega_c^2 - \Omega^2]^{1/2}, \tag{2.25}$$

exists only if $\Omega < \Omega_c$.

2.4 Numerical Methods

A numerical approach is therefore often necessary for an understanding of nonlinear effects in dissipative systems. A large number of numerical methods can be used for this purpose **[191, 192]**. These can be classified into two broad categories known as: (i) the finite-difference methods; and (ii) the pseudospectral methods. Generally speaking, pseudospectral methods are faster by up to an order of magnitude to achieve the same accuracy **[193]**. The one method that has been used extensively to solve the pulse-propagation problem in nonlinear dispersive or dissipative media is the split-step Fourier method **[194, 195]**. The relative speed of this method compared with most finite-difference schemes can be attributed in part to the use of the finite-Fourier-transform (FFT) algorithm **[196]**. This section describes various numerical techniques used to study the pulse-propagation problem with emphasis on the split-step Fourier method and its modifications.

• **Split-step Fourier method**

The Split-step method is based on the pseudo-spectral method. This method involves calculating the dispersive and nonlinear terms in the dynamical equations governing the propagation of ultrashort dissipative optical bullets in highly nonlinear metamaterials. In numerical analysis, the split-step Fourier method is a pseudo-spectral numerical method used to solve nonlinear partial differential equations like the NLS equation. The name arises for two reasons. First, the method relies on computing the solution in small steps, and treating the linear and the nonlinear steps separately (see Fig. 2.2). Second, it is necessary to Fourier transform back and

forth because the linear step is made in the frequency domain, while the nonlinear step is made in the time domain. An example of usage of this method is in the field of light pulse propagation in optical fibers, where the interaction of linear and nonlinear mechanisms makes it difficult to find general analytical solutions. However, the split-step method provides a numerical solution to the problem. It is the most popular algorithm because of its good accuracy and relatively modest computing cost. Here, below, is the description of the method.

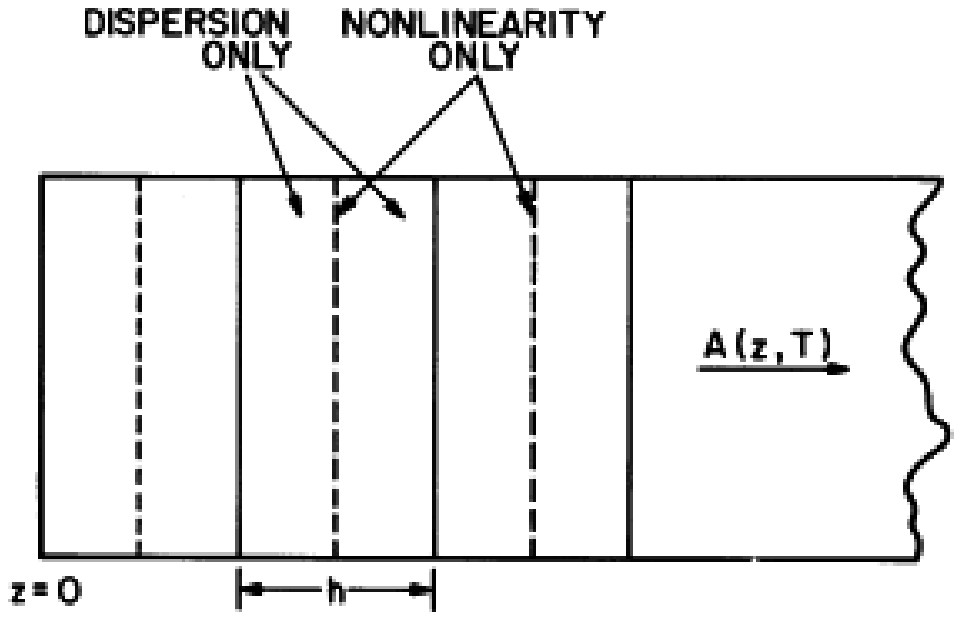

Figure 2.2: Split-step Fourier method algorithm.

Let us, Consider for example, the NLS equation

$$i\frac{\partial A}{\partial z} - \frac{\beta}{2}\frac{\partial^2 A}{\partial t^2} + \gamma|A|^2 A = 0, \tag{2.26}$$

where $A(t, x)$ describes the pulse envelope in time t at the spatial position x. We rewrite this equation as

$$i\frac{\partial A}{\partial z} - \frac{\beta}{2}\frac{\partial^2 A}{\partial t^2} + \gamma|A|^2 A = [\widehat{D} + \widehat{N}]A. \tag{2.27}$$

This equation (2.26) can be split into a linear part,

$$-\frac{\beta}{2}\frac{\partial^2 A_D}{\partial t^2} = \widehat{D}A_D, \tag{2.28}$$

and a nonlinear part,

$$\gamma|A|^2 A_N = \widehat{N} A_N. \tag{2.29}$$

Both the linear and the nonlinear parts have analytical solutions. However, if only a small step h is taken along z, then, the two parts can be treated separately with only a small numerical error. One can, therefore, first take a small nonlinear step,

$$A_N(t, z+h) = exp[i\gamma|A|^2 h]A(t, z), \tag{2.30}$$

using the analytical solution. The dispersion step has an analytical solution in the frequency domain, so it is first necessary to Fourier transform AD using

$$\widetilde{A_D}(\omega, z) = \int_{-\infty}^{+\infty} A_D(t, z) exp[i(\omega - \omega_0)t]dt, \tag{2.31}$$

where ω_0 is the center frequency of the pulse. It can be shown that using the above definition of the Fourier transform, the analytical solution to the linear step is

$$\widetilde{A_D}(\omega, z+h) = exp[i\frac{\beta}{2}(\omega - \omega_0)^2 h]A_D(\omega, z). \tag{2.32}$$

By taking the inverse Fourier transform of $\widetilde{A_D}(\omega, z+h)$, one obtains $A_D(t, z+h)$; the pulse has thus been propagated a small step h. By repeating the above N times, the pulse can be propagated over a length of Nh.

The above shows how to use the method to propagate a solution forward in space. However, many physics applications, such as studying the evolution of a wave packet describing a particle, require one to propagate the solution forward in time rather than in space. The nonlinear Schrödinger equation, when used to govern the time evolution of a wave function, takes the form

$$i\frac{\partial\psi}{\partial t} = -\frac{\hbar^2}{2m}\frac{\partial^2\psi}{\partial x^2} + \gamma|\psi|^2\psi = [\widehat{D} + \widehat{N}]A, \tag{2.33}$$

where $\widehat{D} = -\frac{\hbar^2}{2m}\frac{\partial^2\psi}{\partial x^2}$, and $\widehat{N} = \gamma|\psi|^2\psi$, and that, m is the mass of the particle and $\hbar$ is Planck's constant.

The formal solution to this equation is a complex exponential

$$\psi(x, t) = e^{it(\widehat{D}+\widehat{N})\psi(x,0)}. \tag{2.34}$$

Since $\widehat{D}$ and $\widehat{N}$ are operators, they do not in general commute. However, the Baker-Hausdorff formula can be applied to show that the error from treating them as if they do will be of order dt^2, if we are taking a small but finite time step dt. We, therefore, can write

$$\psi(x, t + dt) \approx e^{idt\widehat{D}} e^{idt\widehat{N}} \psi(x, t). \tag{2.35}$$

The part of this equation involving $\widehat{N}$ can be computed directly using the wave function at time t, but to compute the exponential involving $\widehat{D}$, we use the fact that in frequency space, the partial derivative operator can be converted into a number by substituting ik for $\frac{\partial}{\partial x}$, where k is the frequency (or more properly, wave number, as we are dealing with a spatial variable and thus transforming to a space of spatial frequencies, i.e. wave numbers) associated with the Fourier transform of whatever is being operated on. Thus, we take the Fourier transform of e^{idtk^2}, recover the associated wave number, compute the quantity e^{-idtk^2} and use it to find the product of the complex exponentials involving and in frequency space as below:

$e^{-idtk^2} F[e^{idt\widehat{N}} \psi(x, t)]$, where F denotes a Fourier transform. We then use the inverse Fourier transform of this expression to find the final result in physical space, yielding the final expression

$$\psi(x, t + dt) = F^{-1}[e^{idtk^2} F[e^{idt\widehat{N}} \psi(x, t)]]. \tag{2.36}$$

A variation on this method is the symmetrized split-step Fourier method, which takes half a time step using one operator, then takes a full time step with only the other, and then takes a second half time step again with only the first. This method is an improvement upon the generic split-step Fourier method because its error is of order dt^3 for a time step dt. The Fourier transforms of this algorithm can be computed relatively fast using the Fast Fourier Transform (FFT). Compared to the typical finite difference methods **[197]**, the split-step Fourier method can therefore be much faster.

2.5 Conclusion

This chapter was devoted to the methods used in this thesis. Helped by the Maxwell's equations, we have derivatived the $(3 + 1)$D CQS-CGL equation. Other analytical methods (linear stability analysis method) and numerical methods (the Split-Step Fourier) have been presented, and

some of these methods have been used to study the dynamics of the signal in the nonlinear metamaterial. The numerical methods are used to consolidate the analytical results. In the next chapter, we will present our results together with discussions.

Chapter III

Results and Discussions

3.1 Introduction

The preceding chapters were devoted to generalities on the nonlinear metamaterials, soliton, dissipative soliton and vortex soliton in dissipative optical systems (nonlinear metamaterials) modeled by CGL equations. From the Maxwell's equations, we have derived a new equation which models the propagation of the optical soliton in the nonlinear metamaterials, called "the (3+1)-D CQS-CGL equation". This new model which takes into account higher-order dispersion terms up to six, cubic-quintic-septic nonlinearities and higher-order effects such as self-steepening effects, is an originality in the study of dissipative solitons propagation based on CGL models. It is nowadays, the most advanced model in this field of study and represents our first contribution in this thesis.

In order to reach other objectives, such as different results derived from this model, we has pointed out analytical treatment which have been proposed to describe the main characteristics of the pulse evolution such as the linear stability analysis. To confirm the analytical methods and to plot the different curves, we carried out numerical simulations of the higher-order (3+1)D CQS-CGL equation based on the split-step Fourier method. There are a lot of works on the spatiotemporal dissipative soliton, but this thesis focuses on the investigation of modulational instability phenomena and the new families of spatiotemporal dissipative optical bullets by the (3+1)D CQS-CGL equation, which can overcome the bandwidth challenge currently faced by industrial sectors like information and communication technologies, space, security, and defense.

3.2 Modulational instability in the (3+1)-dimensional cubic-quintic CGL equation for MMs

Modulation instability (MI) is a well known and most ubiquitous and widespread type of instability that appears in most nonlinear systems **[198]**. In fact, a search on the Internet with the term "Modulation instability" returns millions of hits! In Physics, it appears in many branches of physics such as hydrodynamics, plasma physics, and electrodynamics, low temperature physics, and quite obviously in nonlinear optics **[198]**. It is very difficult to say who started MI research first. However, Benjamin and Feir was the first to observe the MI process on deep water waves in 1967 **[199]**. Since then, MI is also sometimes known as Benjamin-Feir instability. MI has been experimentally observed for electromagnetic waves in radio-wave signal by Zagryadskaya and Ostrovsky in 1969 **[200]**. Later, numerous studies on MI has been carried out in the field of nonlinear optics **[198]**. In optics, the interest in MI stems from its possible applications and relevance in ultrafast pulse generation with high repetition rate, ultra-broadband super continuum generation etc.**[201]**. MI is useful to generate ultrashort pulses whose repetition rate could be externally controlled. Nowadays, MI is used as a technique to generate ultra-short pulses with repetition rate higher than those attainable from mode locked-laser **[198]**. Also, MI is now widely recognized as the precursor of soliton formation. In the context of nonlinear fiber optics, the possibility of MI was predicted theoretically in optical fiber by Hasegawa in 1984 **[202]** and have been experimentally verified by Tai et al **[203]**. In general, MI occurs in the anomalous group velocity dispersion (GVD) regime for a focusing nonlinearity **[198]**. MI is possible in the normal GVD regime also but it is limited to some special cases only **[204]**. It is interesting to know that, recently, the study of MI process has even been extended to oceanography, to understand the phenomena behind the generation of the so-called rogue waves **[205]**.

3.2.1 Linear stability analysis and gain spectrum

Physical, engineering, and biological sciences are continuously generating problems of either theoretical or practical interest. The necessary investigations of these problems involve models that, very often, are mathematically expressed as ordinary differential equations (ODEs). In this respect, solving ODEs constitutes an important research activity which is ever attracting a

great deal of attention. For instance, approximate solutions can be obtained analytically using various perturbation techniques for nonlinear ODEs which contain a small parameter. Problems with two or more scales of variation can be analyzed using the method of multiple scales **[206]** or the method of averaging **[207]**. In general, the starting point is the motivation in the choice of the ansatz. When a small parameter is zero, ODE has a sine or cosine periodic solution with the amplitude and phase constants. For small values of the small parameter, we expect the same form of the solution to be approximately valid, but now the amplitude and phase are expected to be slowly varying functions of time. The natural question is how the behavior of the amplitude and phase of the wave has been approached in PDEs.

Usually, the study of the linear stability starts by considering a plane-wave solution, especially in the case of MI. In this framework, we assume that Eq. (2.12), gets the exact CW solution

$$E(z,x,y,t) = Me^{i(k_1 x + l_1 y + k_z z - \omega_1 t)}, \tag{3.1}$$

where $|M|$ is positive real number representing the amplitude of the plane wave $E(z,x,y,t)$. k_1, l_1, and k_z are real numbers representing the wave vectors. ω_1 is real number representing the natural angular frequency of the plane wave. Making use of the above into Eq.(2.12), and setting both imaginary and real parts to zero, we obtain the dispersion relations

$$\begin{aligned} &k_z - \sigma_{r\perp}(k_1^2 + l_1^2) - \omega_1^2\sigma_r + \delta_r + M^2(N_{3r} + M^2 N_{5r}) + \omega_1 M^2(SS_{3i} + M^2 SS_{5i}) = 0, \\ &- \sigma_{i\perp}(k_1^2 + l_1^2) - \omega_1^2\sigma_i + \delta_i + M^2(N_{3i} + M^2 N_{5i}) - \omega_1 M^2(SS_{3r} + M^2 SS_{5r}) = 0. \end{aligned} \tag{3.2}$$

The linear stability of the CW solution can be examined by introducing a small perturbation in the amplitude or in the phase or in both. Nevertheless, it has been shown in several occasions that even when amplitude and phase perturbations are simultaneously considered, the growth rate of instability mainly depends on the amplitude of the plane wave but it is independent of its wave vector and its frequency **[64, 208]**. The latter relies on the fact that in the linearization process of the perturbed wave around the unperturbed one, there is always a possibility of finding a linear relationship between the phase and amplitude of the perturbation, which easily allows to control the emergence of instability around an amplitude threshold **[64, 208]**. Zhao et al. **[209]**, adopting the same procedure, confirmed that the emergence of nonlinear spin waves in an atomic chain of spinor Bose-Einstein condensates under MI, mainly depends on the

amplitude perturbation, even when both the phase and amplitude are perturbed. This finds real applications in the field of gravitational waves, for example, where the carrier frequency is extremely high so that the subperiod power cannot be measured. In such conditions, the only measurable quantity remains the slowly varying amplitude of modulation **[210]**. Interestingly, phase and frequency modulation can indubitably become detectable only if converted into amplitude modulation **[210]**. Therefore, in the rest of this work, we consider an amplitude perturbation so that solution (3.1) becomes

$$E(z,x,y,t) = (M + a(z,x,y,t))e^{i(k_1 x + l_1 y + k_z z - \omega_1 t)}, \tag{3.3}$$

where the complex field $a(x,y,z,t)$ is small perturbations of the carrier waves, i.e., $|a(x,y,z,t)| << |M|$. Next, we substitute Eq.(3.3) into Eq.(2.12) and keep only the terms that are linear in $a(x,y,z,t)$, which leads to the linearized equation of the perturbed field

$$\begin{aligned} i\frac{\partial a}{\partial z} + \sigma_\perp\left(\Delta_\perp a + 2i\left(k_1 K\frac{\partial a}{\partial x} + l_1 L\frac{\partial a}{\partial y}\right)\right) + \sigma\frac{\partial^2 a}{\partial t^2} - 2i\omega_1\sigma\frac{\partial a}{\partial t} + M^2(N_3 + 2M^2N_5)(a + a^*) \\ + M^2(2SS_3 + 3M^2SS_5)\frac{\partial a}{\partial t} + M^2(SS_3 + 2M^2SS_5)\frac{\partial a^*}{\partial t} - i\omega_1 M^2(SS_3 + 2M^2SS_5)(a + a^*) = 0. \end{aligned} \tag{3.4}$$

Here, $a^*(x,y,z,t)$ is the complex conjugate of the perturbed field, assumed to be of the form

$$a(z,x,y,t) = a_1 e^{i(Kx + Ly + K_z z - \Omega t)} + a_2^* e^{-i(Kx + Ly + K_z z - \Omega^* t)}, \tag{3.5}$$

where K , L and K_z are the perturbation wave numbers, Ω is the frequency of the perturbation modulating the carrier signal, and the parameters a_1 and a_2^* are constant complex amplitudes. The substitution of Eq.(3.5) into Eq.(3.4) gives a linear homogeneous system of equations in terms of a_1 and a_2

$$\begin{pmatrix} K_z + a_{11} & a_{12} \\ a_{21} & K_z + a_{22} \end{pmatrix}\begin{pmatrix} a_1 \\ a_2 \end{pmatrix} = \begin{pmatrix} 0 \\ 0 \end{pmatrix}, \tag{3.6}$$

where,

$$a_{11} = \sigma_\perp(K^2 + L^2 + 2k_1K + 2l_1L) + \sigma(\Omega^2 + 2\Omega\omega_1) - M^2(N_3 + 2M^2N_5) + iM^2\Omega(2SS_3 + 3M^2SS_5)$$
$$+ i\omega_1M^2(SS_3 + 2M^2SS_5),$$
$$a_{12} = -M^2(N_3 + 2M^2N_5) + iM^2\Omega(SS_3 + 2M^2SS_5) + i\omega_1M^2(SS_3 + 2M^2SS_5),$$
$$a_{21} = M^2(N_3^* + 2M^2N_5^*) - iM^2\Omega(SS_3^* + 2M^2SS_5^*) + i\omega_1M^2(SS_3^* + 2M^2SS_5^*),$$
$$a_{22} = -\sigma_\perp^*(K^2 + L^2 - 2k_1K - 2l_1L) - \sigma^*(\Omega^2 - 2\Omega\omega_1) + M^2(N_3^* + 2M^2N_5^*) - iM^2\Omega(2SS_3^* + 3M^2SS_5^*)$$
$$+ i\omega_1M^2(SS_3^* + 2M^2SS_5^*). \tag{3.7}$$

The condition for the existence of nontrivial solution for the system (3.6) gives rise to a second-order polynomial equation for the wave number K_z that represents the dispersion law for the perturbation, i.e.,

$$K_z^2 + sK_z + p = 0, \tag{3.8}$$

in which $s = a_{11} + a_{22}$ and $p = a_{11}a_{22} - a_{12}a_{21}$. We study the sign of the imaginary part of the roots of Eq.(3.8) and we investigate the gain or loss spectrum or the MI regions. This equation has two roots given by

$$K_z^\pm = \frac{1}{2}\left(-s \pm \sqrt{s^2 - 4p}\right). \tag{3.9}$$

The steady-state solution becomes unstable whenever the wave numbers $K_z^\pm$ have a nonzero imaginary part, since the perturbed amplitude grows exponentially along the NIM.The quantities $K_z^\pm$ depend on the values of the parameters that make the coefficients of the dispersion relation. Therefore, MI in NIMs, with the presence of the wave numbers K and L of the perturbed mode, the wave number of the continuous wave k_1, cubic-quintic nonlinearities and, cubic and quintic self-steepening effects, can be controlled. The regions of instability are called MI gain spectrums and are regions where the gain $G_+ = 2\mathrm{Im}(K_z^+) > 0$, or $G_- = 2\mathrm{Im}(K_z^-) > 0$, where $\mathrm{Im}(K_z^\pm)$) represents the imaginary part of $K_z^\pm$.

Fig. 3.1 displays some bounded regions of MI, with finite gains $G_- > 0$, and their corresponding density plots, versus the wave number K and k_1 of the perturbation and CW, respectively. The parameters used in the calculations are: $\Omega = 0.6$, $\omega_1 = 0.8$, $L = -K$, $l_1 = 0.8$, $k_1 = 0.8$, $\sigma_\perp = -1 + i0.005$, $\sigma_i = 0.19$, $\delta = -i0.081$, $SS_3 = -1 - i0.1$, $SS_{5r} = 1$. In regions

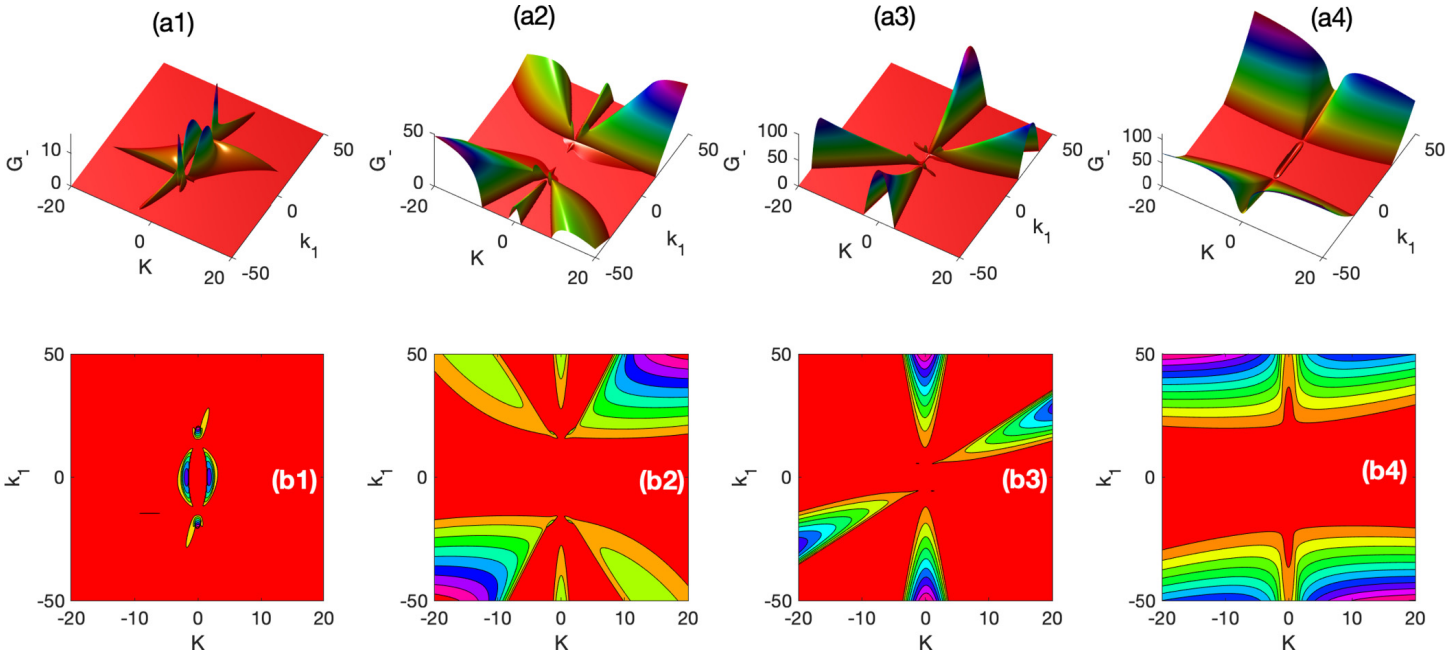

Figure 3.1: Modulational instabilty gain associated with the solution G_{-} as a function of the wave number of the perturbation mode K and the wave number of the continuous wave k_1. Panels in $(\mathrm{aj})_{j=1,2,3,4}$ show bounded gains of MI, and the corresponding density plots in Panels $(\mathrm{bj})_{j=1,2,3,4}$, for $\Omega = 0.6$, $\omega_1 = 0.8$, $L = -K$, $l_1 = 0.8$, $k_1 = 0.8$, $\sigma_{r\perp} = -1$, $\sigma_{i\perp} = 0.005$, $\sigma_i = 1.98$, $\delta_r = 0$, $\delta_i = -0.081$, $SS_{3r} = -0.4$, $SS_{3i} = 1.2$, $SS_{5r} = 0.5$, $SS_{5i} = -0.9$. Panels (a1)-(b1): normal-GVD regime of self-focusing negative-index MMs, $\sigma_{r\perp} = -1$, $\sigma_r = 1$, $N_{3r} = 1$, $N_{3i} = -0.12$, $N_{5r} = -1$, $N_{5i} = 0.075$. Panels (a2)-(b2): anomalous-GVD regime of self-defocusing negative-index MMs, $\sigma_{r\perp} = -1$, $\sigma_r = 1$, $N_{3r} = -1$, $N_{3i} = 0.12$, $N_{5r} = 1$, $N_{5i} = -0.075$. Panels (a3)-(b3): normal-GVD regime of self-defocusing negative-index MMs, $\sigma_{r\perp} = -1$, $\sigma_r = 1$,$N_{3r} = -1$, $N_{3i} = 0.12$, $N_{5r} = 1$, $N_{5i} = -0.075$. Panels (a4)-(b4): anomalous-GVD regime of self-defocusing positive-index MMs, $\sigma_{r\perp} = 1$, $\sigma_r = -1$, $N_{3r} = -1$, $N_{3i} = 0.12$, $N_{5r} = 1$, $N_{5i} = -0.075$.

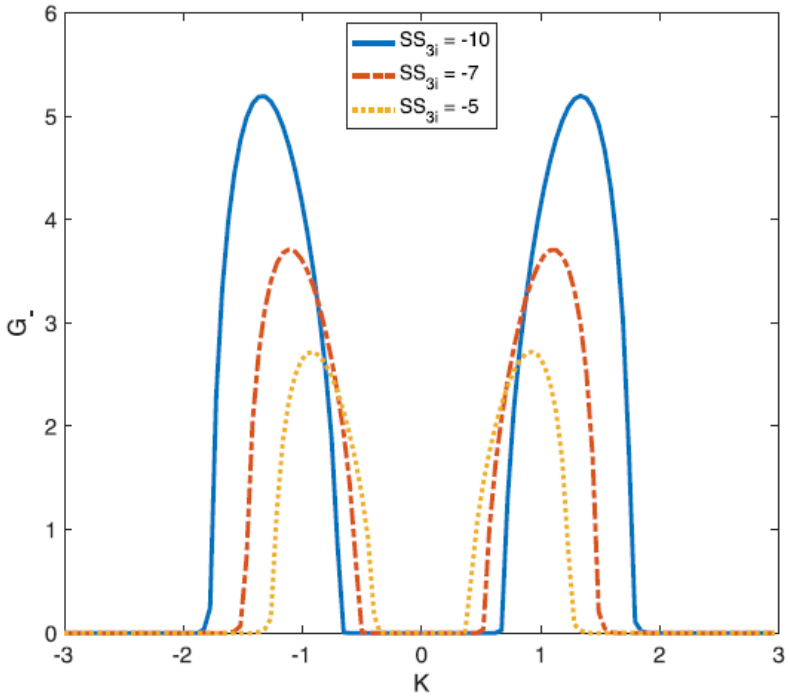

Figure 3.2: Plots of MI gain associated with solution G_{-}, versus K, for different values of SS_{3i}, for $\Omega = 0.6$, $\omega_1 = 0.8$, $L = -K$, $l_1 = 0.8$, $k_1 = 0.8$, $\sigma_{r\perp} = -1$, $\sigma_{i\perp} = 0.005$, $\sigma_r = -1$, $\sigma_i = 0.19$, $\delta_i = -0.081$, $N_{3r} = -1$, $N_{3i} = 0.12$, $N_{5r} = 1$, $N_{5i} = -0.075$, $\delta_r = 0$, $SS_{3r} = -1$, $SS_{5r} = 1$ and $SS_{5i} = -0.44$.

where $G_{-} > 0$, the plane wave will be expected to break-up into nonlinear patterns and solitonic objects. Otherwise, the plane wave will remain stable under modulation. Such features of instability/stability are importantly modified by the changes in system parameters such as the cubic and quintic self-steepening coefficients. A good illustration of such effects is given by Fig.3.2, where the MI gain G_{-} is plotted against the perturbation wave number K, with the cubic self-steepening coefficient SS_{3i} changing. In general, the MI gain spectrum is illustrated by two identical and symmetric lobes which get expanded when SS_{3i} decreases. This also affects the band-gap which also grows when SS_{3i} decreases, while the MI gain decreases under the same effect. To remind, Fig.3.2 has been plotted for $SS_{5i} = -0.44$, a value which does not give full information on how the MI gain can be affected by the quintic self-steepening term. This is illustrated in Fig. 3.3, where G_{-} is plotted versus K and SS_{5i}, both under anomalous- and normal-GVD regimes, with $SS_{3i} = -0.1$. As in Fig. 3.2, the MI gain is characterized by two symmetric and identical lobes and, in general, G_{-} is a decreasing function of SS_{5i}. How-

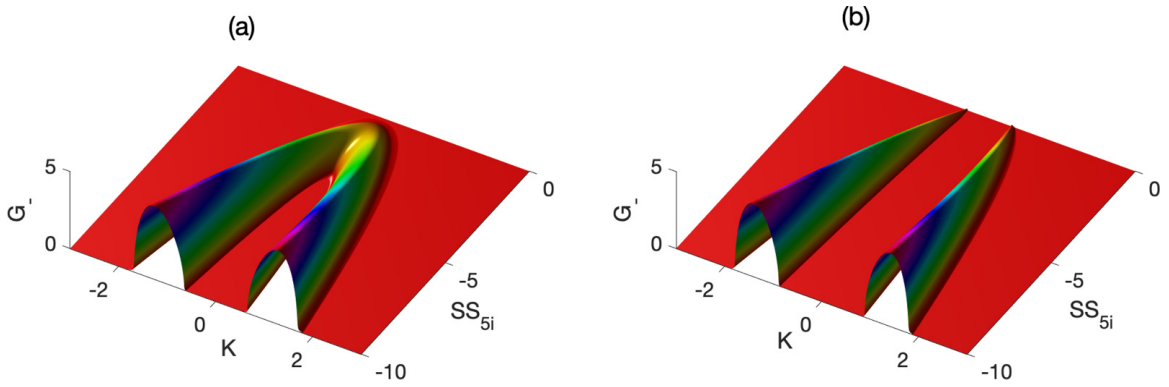

Figure 3.3: Regions of MI illustrating gain associated with solution G_{-} against K, the wave number of perturbation, and the quintic self-steepening imaginary coefficient SS_{5i}, for $\Omega = 0.6$, $\omega_1 = 0.8$, $L = -K$, $l_1 = 0.8$, $k_1 = 0.8$, $\sigma_{r\perp} = -1$, $\sigma_{i\perp} = 0.005$, $\sigma_i = 0.19$, $\delta_r = 0$, $\delta_i = -0.081$, $N_{3i} = 0.12$, $N_{5r} = 1$, $N_{5i} = -0.075$, $SS_{3r} = -1$, $SS_{3i} = -0.1$, $SS_{5r} = 1$. Panel (a): anomalous-GVD regime of self-defocusing negative-index MMs, $\sigma_r = -1$ and $N_{3r} = -1$. Panel (b): normal-GVD regime of self-defocusing negative-index MMs, $\sigma_r = 1$ and $N_{3r} = -1$.

ever, in the anomalous regime (see Fig. 3.3(a)), the band-gap reduces with SS_{5i} increasing and solitons are not likely to exist when $SS_{5i} = 0$. On the other side, the normal-GVD regime supports solitonic structures for $SS_{5i} = 0$ and the MI bad-gap is not considerable affected as in the anomalous-GVD case. Indeed, this is contrary to what was already reported by Wen et al.**[10]**. In fact, they showed, using a (3+1)D NLS equation for ultrashort pulse propagation, that there was bandwidth amplification with increasing the cubic self-steepening parameter, in absence of the quintic nonlinear coefficient and the quintic self-steepening term. Moreover, the proposed model, which contains essentially complex coefficient, is a generalized case, which, when $\sigma_i = \sigma_{i\perp} = \delta_I = \delta_r = N_{3i} = N_{5r} = N_{5i} = SS_{3r} = SS_{5i} = SS_{5r} = 0$, the NLS equation is recovered. Obviously, the balance between such new effects can modify the gain and be responsible for the emergence of more suitable patterns under long-time evolution.

3.2.2 Numerical experiment

The linear stability analysis, which is based on the linearization around the unperturbed plane wave, is valid only when the amplitude of the perturbation is small compared to that of the carrier wave. More precisely, the linear approximation should not be valid at large time scales,

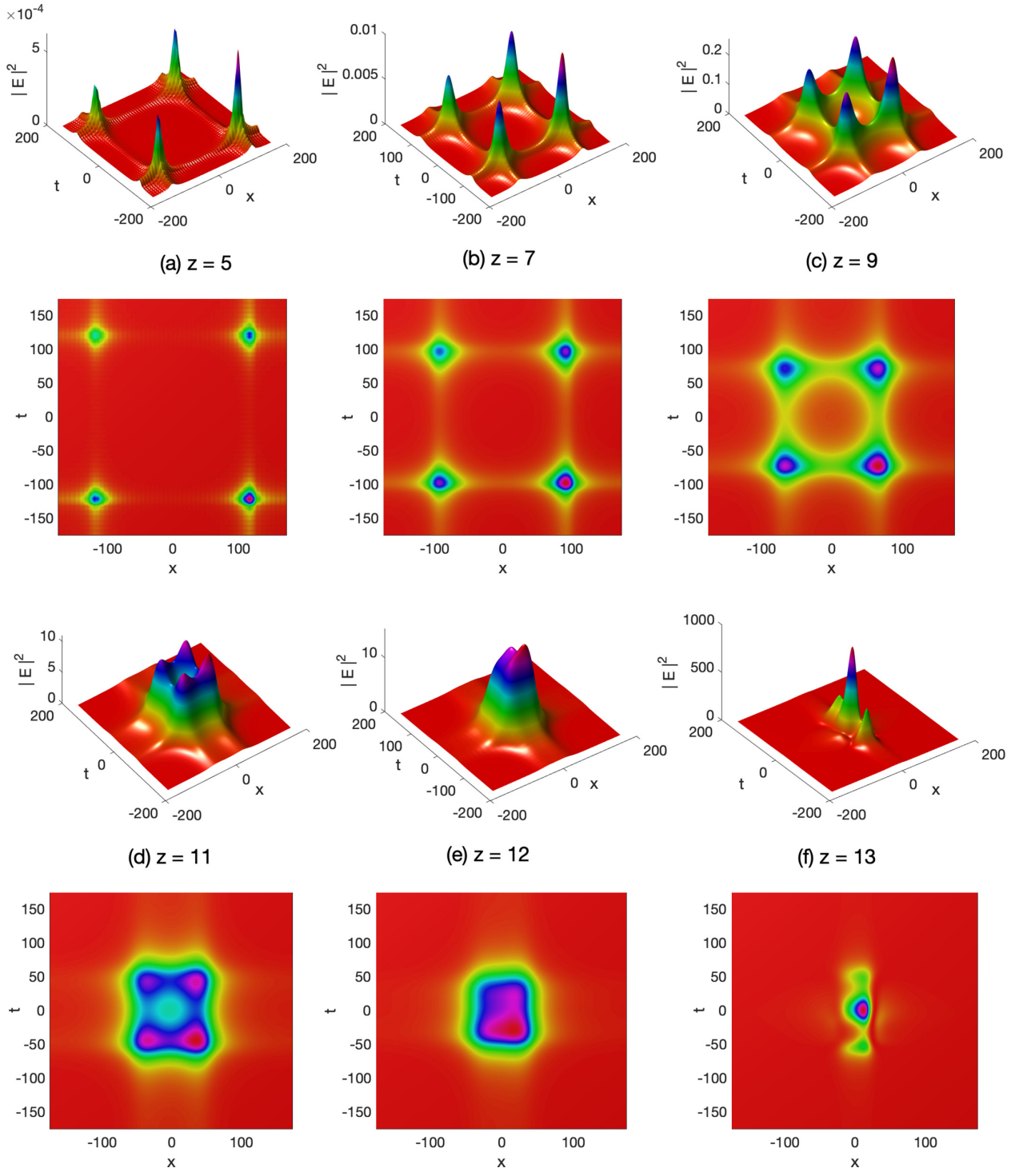

Figure 3.4: Panels (a)-(f) show the structure of the beam intensity for a cluster of four fundamental solitons for different values of the longitudinal distance z, and the corresponding density plots. Panel (a): $z = 7$. Panel (b): $z = 8$. Panel (c): $z = 10$; panel (d): $z = 11$. The other parameter values are $A = 0.001$, $\Omega_1 = \Omega_2 = 0.5$, $\omega_1 = \omega_2 = 0.41$, $\sigma_{r\perp} = -2.71$, $\sigma_{i\perp} = 0.5$, $\sigma_r = 2.57$, $\sigma_i = 0.5$, $\delta_r = 0$, $\delta_r = -0.0079$, $N_{3r} = -1$, $N_{3i} = 0.12$, $N_{5r} = 1$, $N_{5i} = -0.65$, $SS_{3r} = -0.2$, $SS_{3i} = -0.6$, $SS_{5r} = 0.42$ and $SS_{5i} = -0.5$.

since the amplitude of an unstable sideband grows exponentially. Therefore, the long-time evolution of the modulated plane wave requires full numerical simulations of the generic equation. This is, in fact, a way of confronting the analytical predictions and, in our context, pulse propagation in NIM is carried out via the split-step Fourier method on Eq.(2.12). In order to examine the accuracy of the performed digital experiment, different space and time steps are tested. 256 space Fourier modes are used with the space period of 8, and in time, the number of Fourier modes is also 256, with a similar period of 8. Additionally, the numbers of grid points in space and time are 350 and 350, respectively, with the mesh size $\Delta x = \Delta y = 0.005$ and $\Delta t = 0.005$. The split-step Fourier method is then applied considering $y = 0$, with z constant, with the initial signal being of the form

$$E(x,t,0) = M(1 + Asin(2\pi(\Omega_1 x + \Omega_2 t)))e^{-i(\omega_1 x + \omega_2 t)}, \tag{3.10}$$

where A is the modulation amplitude, Ω_1 and Ω_2 are the frequencies of weak sinusoidal modulations imposed on the continuous waves in the x direction and time t, respectively.

According to features of Figs. 3.1-3.3, the development of MI depends on both the wavenumbers K and self-steepening parameter values, which implies that right values of such parameters should be chosen to expect the appearance of soliton-like objects. We used the parameter values $A = 0.001$, $\Omega_1 = \Omega_2 = 0.5$, $\omega_1 = \omega_2 = 0.41$, $\sigma_{r\perp} = -2.71$, $\sigma_{i\perp} = 0.5$, $\sigma_r = 2.57$, $\sigma_i = 0.5$, $\delta_r = 0$, $\delta_i = -0.0079$, $N_{3r} = -1$, $N_{3i} = 0.12$, $N_{5r} = 1$, $N_{5i} = -0.65$, $SS_{3r} = -0.2$, $SS_{5r} = 0.42$,. Calculations are initiated for $SS_{3i} = -0.6$ and $SS_{5i} = -0.5$, which results to the MI behaviors summarized in Fig. 3.4, where, at distance $z = 5$, one clearly sees the appearance of a cluster of four fundamental solitons as the result of the interplay between nonlinear and dispersive effects. This, indeed, shows the accuracy of our analytical predictions and confirms that MI is a direct mechanism for soliton formation in nonlinear media. The most interesting aspect of the present numerical experiment is that the emerging entities are found to be moving as z increases, and their interaction leads to a complex molecular soliton (see Figs. 3.4(e) and (f)), which concentrates all the energies carry by individual solitons. Also, this brings out another main effect of MI, which is the creation of localized pulses and energy localization. In the last decades, different kinds of solitons have been discussed in the literature, along with their relationship with MI, including Bragg solitons, vortex solitons, discrete solitons and cavity solitons **[86]**, just to name a few. They are however few, the contributions that discuss the appearance of cluster solitons

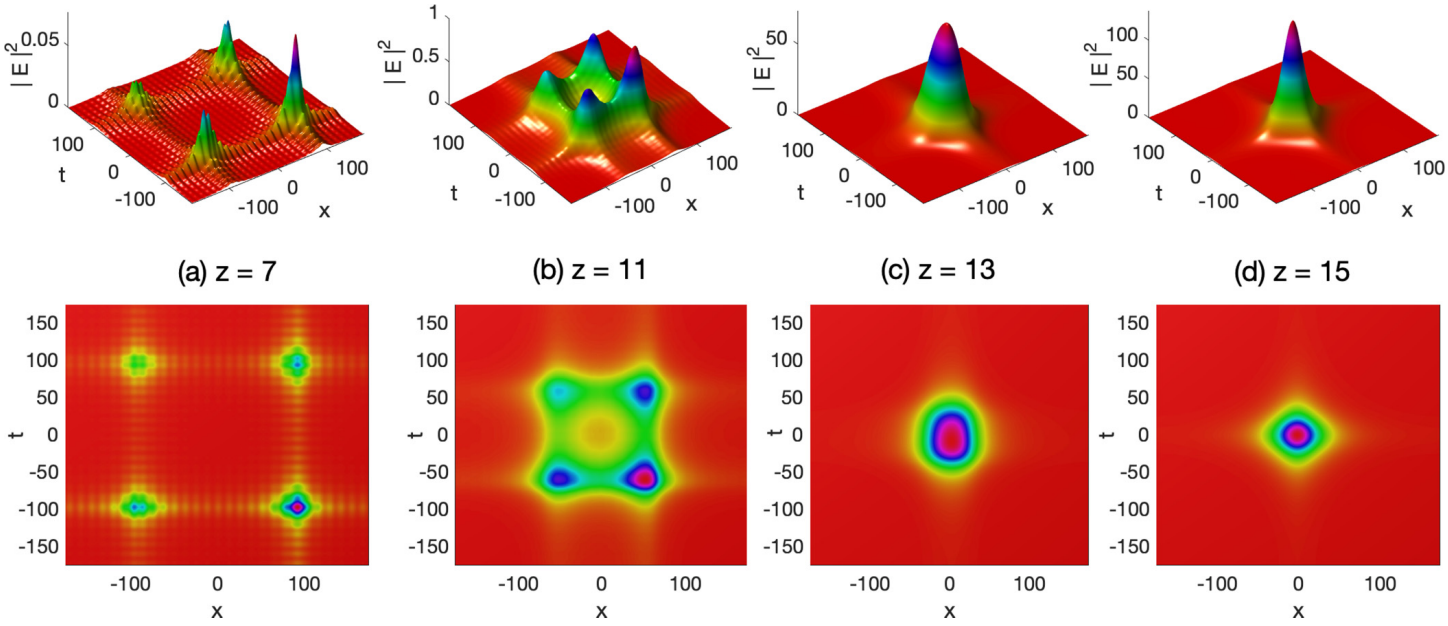

Figure 3.5: Panels (a)-(d) show the structure of the beam intensity for a cluster of four fundamental solitons for different values of the longitudinal distance z, and their corresponding density plots. Panel (a): $z = 7$. Panel (b): $z = 11$. Panel (c): $z = 13$. Panel (d): $z = 15$. The other parameter values used here are $A = 0.001$, $\Omega_1 = \Omega_2 = 0.5$, $\omega_1 = \omega_2 = 0.41$, $\sigma_{r\perp} = -2.71$, $\sigma_{i\perp} = 0.5$, $\sigma_r = 2.57$, $\sigma_i = 0.5$, $\delta_r = 0$, $\delta_r = -0.0079$, $N_{3r} = -1$, $N_{3i} = 0.12$, $N_{5r} = 1$, $N_{5i} = -0.65$, $SS_{3r} = -0.2$, $SS_{3i} = -0.6$, $SS_{5r} = 0.42$ and $SS_{5i} = -2$.

as the consequence of MI, a phenomenon that has, for instance, been related to azimuthal MI by Petroski et al.**[211]**. We should however stress that intensive numerical studies have pointed out the fact that the stability of such structures is very sensitive to noise input**[105]**, depending on the number of solitons composing the cluster, the angular quantum number of the azimuthal instability and the corresponding largest growth rate of MI. Nevertheless, noise effects being not considered in the present paper, other aspects can be regarded as done in Fig. 3.5, where we have decreased the imaginary quintic self- steepening parameter to $SS_{5i} = -2$. As previously, the initial plane wave breaks into a four-wave cluster of moving solitons which, as distance increases, merge into a unique structure (see Fig. 3.5(c)), gets more localized from distance $z = 15$ (see Fig. 3.5(d)). Compared to the molecular structure of Fig. 3.4(f), which contains some humps, the unique molecular soliton of Fig. 3.5(d) displays some features of dromions that are well known in the literature**[212, 213]**. As a whole, the numerical results discussed above show the strengths and weaknesses of our linear stability analysis of the MI in the (3+1)D CQ

CGL equation. It gives a correct conclusion about the analytical predictions, at least at the onset stage of wave evolution for a short distance of propagation. Indeed, for a sufficiently long distance and time, the linear stability analysis fails and the modulation can lead the system to the formation of localized patterns, spontaneously generated via wave-mixing processes during propagation and interaction. Indeed, such interaction, when they are inelastic, give rise to the complex molecular entities obtained from the model under study. From the physical point of view, the phenomenon displayed by Figs. 3.4(f) and 3.5(d) may result from the fact that the cubic and quintic self-steepening terms bring about additional nonlinear effects, which, because of the well-balanced effects between self-defocussing nonlinearity and dispersion, cause the rapid increase of pulse intensity, leading to maximum peaks. There are however two interesting behaviors of such maximum peak intensities, depending on the quintic self-steepening strength, that are pulse splitting in the temporal domain and compression in the spatial domain, on the one hand, and symmetric shrinking in both temporal and spatial domains, with the highest intensity being located at $(x = 0, t = 0)$ in both cases in the other hand. In some other contexts, such behaviors may predict the emergence of spatial ring solitons that were reported in MMs by Zhang et al.**[105]** using a (3+1)D NLS equation, with simultaneous cubic electric and magnetic nonlinearity, by means of the variational method.

3.3 Propagation of dissipative light bullet in Kerr and non-Kerr negative-refractive-index materials

Up to now, all studies on MMs have been concerned with only CQ nonlinearities, and there have been no studies on the properties of dissipative solitons in 3D dissipative optical metamaterials with cubic-quintic-septic nonlinearities. In particular, the generalized CQ CGL equation modeling dissipative spatiotemporal solitons in NIMs has been derived, and the simultaneous cross-compensation of saturating nonlinearity excess with losses that are balanced by gain generates dissipative light bullets, transforming the medium into an active dissipationless composite metamaterial **[15]**.

In this section, we chose a set of parameters that allows us to generate stable dissipative light bullets propagation characterized by different topological charges, namely fundamental

vortex, necklace, and azimuthon in MMs displaying optical nonlinearities up to the seventh order, with (3+1)D CQS-CGL equation with competing effects of dispersion, diffraction, gain, loss, cubic-quintic- septic nonlinearities, and cubic, quintic, and septic self-steepening terms.

Dynamics of dissipative optical solitons is described by the higher-order (3+1)-D CQS-CGL equation for the normalized complex envelope of the optical field:

$$\begin{aligned} i\frac{\partial E}{\partial z} + (\sigma_{r\perp})\Delta_\perp E - i\sigma_{i\perp}\nabla_\perp^2 E + (-ik_{2i})\frac{\partial^2 E}{\partial t^2} - i(k_{3r}+ik_{3i})\frac{\partial^3 E}{\partial t^3} + (k_{4r}+ik_{4i})\frac{\partial^4 E}{\partial t^4} + i(k_{5r}+ik_{5i})\frac{\partial^5 E}{\partial t^5} \\ + (k_{6r}-ik_{6i})\frac{\partial^6 E}{\partial t^6} + i\delta E + (N_{3r}+iN_{3i})|E|^2 E + (N_{5r}+iN_{5i})|E|^4 E + (N_{7r}+iN_{7i})|E|^6 E + \\ (SS_{3r}+iSS_{3i})\frac{\partial(|E|^2 E)}{\partial t} + (SS_{5r}+iSS_{5i})\frac{\partial(|E|^4 E)}{\partial t} + (SS_{7r}+iSS_{7i})\frac{\partial(|E|^6 E)}{\partial t} = 0, \end{aligned} \tag{3.11}$$

We show that families of spatiotemporal dissipative optical ligth bullets, including simple vortex, necklace-ring and azimuthon solitons, uniformrig beam, sphericals distributions of ligth bullets are possible in Eq.(3.11), where the time-dependent Laplacian is $\Delta_\perp = \nabla_\perp^2 + k_{2r}\frac{\partial^2}{\partial t^2}$. Here, k_{2r} is the normal GVD. Normalizing reduced time $t = \frac{t}{\sqrt{k_{2r}}}$, one obtains the laplacian $\Delta_\perp = \frac{\partial^2}{\partial x^2} + \frac{\partial^2}{\partial y^2} + \frac{\partial^2}{\partial t^2}$, which is completely symmetrical with respect to spacial coordinates x, y and time coordinate t. Metamaterials possessing a negative refractive index can display both negative and positive self-steepening effects, which govern the dimensions of the SRR circuit, unlike regular materials with a positive refractive index. Research has demonstrated that nonlinear dispersive parameters (self-steepening) cause a time delay in the system while the soliton progresses. The influence of higher-order dispersion on the soliton, where the light bullet permits the suppression or enhancement of this temporal delay caused by the self-steepening.

One of the critical issues in studying the emergence of light bullets and vortices in nonlinear systems is the choice of the appropriate initial conditions. Most of such initial conditions, used in several contributions, were derived as analytical solutions of single and coupled (2+1)D and (3+1)D NLS equations, using different methods among which the Hirotas bilinear method **[214]**, the self-similarity method **[215]**, and so on. It was shown that an azimuthally periodically modulated bright ring necklace beam could self-trap in a (2+1)D cubic NLS equation **[216]**. This was generalized to a (2+1)D cubic-quintic CGL equation, where necklace-shaped arrays of localized spatial beams were shown to merge into stable fundamental or vortex solitons due to

the competition between cubic and quintic nonlinearities **[217]**. Numerical simulations were also performed in spherical coordinates using incident soliton shape derived in Refs.**[17, 216, 217]** and given by:

$$E(z=o,r,\varphi)=E_0 sech[(r-R_0)/r_0][cos(n\varphi)+iq\ \ sin(n\varphi)]e^{im\varphi}, \tag{3.12}$$

with E_0 being the amplitude factor, R_0 being the mean initial radius, r_0 being the width. The parameter q, with $0 \leq q \leq 1$, determines the azimuthal modulation depth **[218, 219, 220]** and m and $2n$ stand for the number of topological charge(TC) and necklace beads in the input beam, respectively. $r=(x^2+y^2+t^2)^{1/2}$ and $\varphi = arctan(y/x)$. In general, the beam given by Eq.(3.12) can be perceived as a combination of two vortices with respective $m+n$ and $m-n$, which is expressed as

$$E(z=o,r,\varphi)=\frac{E_0}{2}(1+q)sech[(r-R_0)/r_0]e^{[i(m+n)\varphi]}+\frac{E_0}{2}(1-q)sech[(r-R_0)/r_0]e^{[i(m-n)\varphi]}, \tag{3.13}$$

Numerical studies of vortices formation are carried out via the split-step Fourier algorithm applied to Eq.(3.11). In what follows, we have adopted the following approach in order to allow a good understanding of the method applied to Eq.(3.11). To succeed, it is useful to write Eq.(3.11) formally in the form:

$$\frac{\partial E}{\partial z}=(\widehat{D}+\widehat{N})E, \tag{3.14}$$

where $\widehat{D}$ is the linear differential operator that accounts for dispersion in a linear medium and $\widehat{N}$ is a nonlinear operator that governs the effect of nonlinearities.

Taking the case where the nonlinearities have to offset the dispersion terms, these operators are given by:

$$\widehat{D}=i\sigma_{r\perp}\Delta_\perp+\sigma_{i\perp}\nabla^2_\perp+k_{2i}\frac{\partial^2}{\partial t^2}+(k_{3r}+ik_{3i})\frac{\partial^3}{\partial t^3}+i(k_{4r}+ik_{4i})\frac{\partial^4}{\partial t^4}-(k_{5r}+ik_{5i})\frac{\partial^5}{\partial t^5}+i(k_{6r}-ik_{6i})\frac{\partial^6}{\partial t^6}-\delta, \tag{3.15}$$

and

$$\widehat{N} = i(N_{3r} + iN_{3i})|E|^2 + i(N_{5r} + iN_{5i})|E|^4 + i(N_{7r} + iN_{7i})|E|^6 + i(SS_{3r} + iSS_{3i})\frac{\partial(|E|^2E)}{|E|\partial t} + i(SS_{5r} + iSS_{5i})\frac{\partial(|E|^4E)}{|E|\partial t} + i(SS_{7r} + iSS_{7i})\frac{\partial(|E|^6E)}{|E|\partial t}. \tag{3.16}$$

The split-step Fourier method obtains an approximate solution by assuming that in propagating the optical field over a small distance h, the dispersion and nonlinear effects can be pretended to act independently. More specifically, propagation from z to $z+h$ is carried out in two steps. In the first step, the nonlinearity acts alone, and $\widehat{D} = 0$ in Eq.(3.14). In the second step, dispersion acts alone, and $\widehat{N} = 0$ in Eq. (3.14). Mathematically, the integration of Eq. ((3.14) gives

$$E(z + h, x, y, t) = exp(h\widehat{D})exp(h\widehat{N})E(z, x, y, t). \tag{3.17}$$

The exponential operator $exp(h\widehat{D})$ can be evaluated in the Fourier domain using the prescription:

$$exp(h\widehat{D})E(z, x, y, t) = F_T^{-1}exp[h\widehat{D}(ik_x, ik_y, -i\omega)]F_T E(z, x, y, t), \tag{3.18}$$

where F_T denotes the Fourier-transform operation. Operator $\widehat{D}(ik_x, ik_y, -i\omega)$ is obtained from Eq. (3.15) by replacing the differential operator $\frac{\partial^2}{\partial x^2} = (ik_x)^2$, $\frac{\partial^2}{\partial y^2} = (ik_y)^2$ in k space and $\frac{\partial^m}{\partial t^2}$ by $(-i\omega)^m$, and ω is the frequency in the Fourier domain.

In order to be used, the self-steepening have to be transformed as follows:

$$\frac{(SS_{3r} + iSS_{3i})}{E}F_T^{-1}((-i\omega(F_T((abs(E)^2)E)))) + \frac{(SS_{5r} + iSS_{5i})}{E}F_T^{-1}((-i\omega(F_T((abs(E)^2)E)))) + \frac{(SS_{7r} + iSS_{7i})}{E}F_T^{-1}((-i\omega(F_T((abs(E)^2)E)))). \tag{3.19}$$

3.3.1 Simple light bullet($n = 0$ or $q = 1$)

We have used the longitudinal step size $\triangle\ z = 0.01$, being adopted for all cases. Moreover, numerical calculations are made using the following relevant parameters of the studied metamaterial: $\sigma_{r\perp} = -1$, $\sigma_{i\perp} = 0.25$, $k_{2i} = 0.5$, $k_3 = 0.01 + i0.21$, $k_4 = 0.1 + i0.001$, $k_5 = 0.21 + i0.01$, $k_6 = 2.1 + i0.66$, $\delta = -0.0079$, $N_3 = -1 + i0.12$, $N_5 = 1 - i2.65$, $N_7 = -0.05 + i0.02$,

$SS_3 = -0.0001 - i0.02$, $SS_5 = 0.1 - i0.01$, $SS_7 = 0.2 - i0.2$, while the initial beam (3.13) is characterized by the set of parameters $E_0 = 1.2$, $R_0 = 5mm$ and $r_0 = 4mm$.

To start, the fundamental light bullet is obtained in Fig. 3.6 , where the upper row (a) shows the evolution of the light bullet propagating without changing its shape over different propagation distances and the lower row (b) displays the evolution of the amplitude related to this light bullet. It appears that the optical intensity distribution does not depend on the number of topological charges nor on the number of beads of the necklace and the azimuthal modulation. Obviously, the light bullet?s amplitude, shape and radial radius decrease during the propagation. Such features, obtain for $m = n = 0$ and $q = 0$, may change depending on the choice of the azimuthal modulation, the topological charge, and necklace beads in the input beam

Based on the above, propagation features of such a fundamental light bullet are given in in Fig. 3.7, where $q = 1$ and $n = 0$, with $m = -6$, where the upper row (a) depicts the evolution of the light bullet propagating by changing its shape on different propagation distances and the lower row (b) shows the phase distribution related to that of the light bullet. We see that the shape of the light bullets can change depending on the choice of the azimuthal modulation, the topological load and the necklace beads in the input beam. In this case, the optical intensity distribution does not depend on the parameter n and has radial symmetry in the transverse plane. This is due to the condition $q = 1$. We notice the initial light ball, which, at $z = 10$, presents chains of ring-modulated solitons with 6 layers. With increasing distance, the fundamental light bullet, using the indicated set of parameter values, appears as a ring that gradually disintegrates into individual solitonic fragments. This is due to the non-linearities that are too weak to balance the dispersions and diffraction. Interestingly, the stability of such a structure is obtained in in Fig. 3.8, where the bullets are stable over a large propagation distance. Here, the upper row (a) shows us the evolution of the light ball propagating in a stable way without changing its shape on different propagation distances, while the lower row (b) shows the phase distribution related to this light bullet. The stability achieved is attributed to the competing nonlinearities, which create a nearly stable profile. This is a result of the heightened third, fourth, and fifth-order dispersive parameters and third and fifth-order nonlinear dispersive parameters. Furthermore, these nonlinear dispersive parameters are increased to balance the

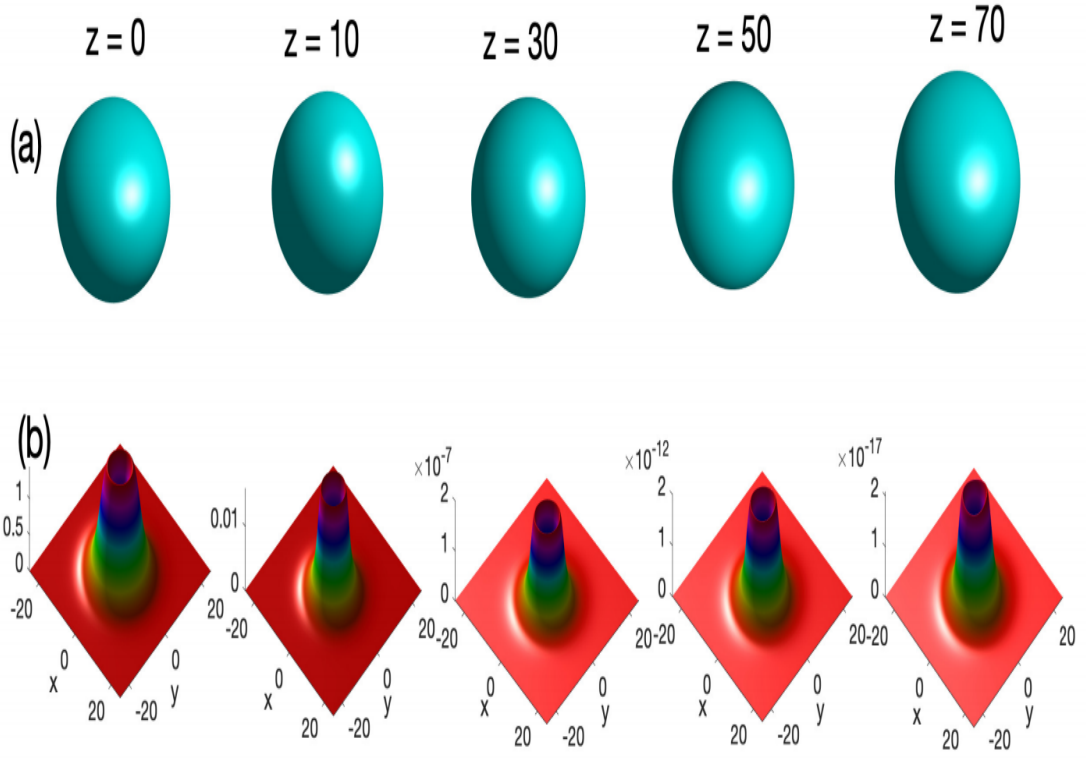

Figure 3.6: The upper row (a) shows the isosurface evolution of a fundamental 3D light bullet for $n = m = q = 0$ at different distances $z = 0$, $z = 10$, $z = 30$, $z = 50$ and $z = 70$, respectively, from left to right. The lower row (b) shows the corresponding wave amplitude. The values of parameters are: $\sigma_{r\perp} = -1$, $\sigma_{i\perp} = 0.25$, $k_{2i} = 0.5$, $k_3 = 0.01 + i0.21$, $k_4 = 0.1 + i0.001$, $k_5 = 0.21 + i0.1$, $k_6 = 2.1 + i0.66$, $\delta = -0.0079$, $N_3 = -1 + i0.12$, $N_5 = 1 - i2.65$, $N_7 = -0.05 + i0.02$, $SS_3 = -0.0001 - i0.02$, $SS_5 = 0.1 - i0.01$, and $SS_7 = 0.2 - i0.2$.

dispersions, resulting in cubic and septic nonlinearity in other physical terms. In fact, higher-order dispersions help maintain stability over a large propagation distance compared to the stabilization of light bullets in nonlinear MM waveguides discussed in Ref. **[221]**. In general, the increase in the strength of dispersion reveals some hidden phenomena of the system which did not appear when we were at the lower orders. This can be better understood either by demonstrating the stability or the instability of the system, which can later lead to the collapse of the system. In this article, we describe the phenomenon of propagation and stability that appears thanks to its higher orders. However, in in Fig. 3.8, the higher order terms allow us to put in stability and prevent a collapse of the structure at a large propagation distance. The above results from in Fig. 3.7 and in Fig. 3.8 are also confirmed by the evolution of the amuplides of Fig. 3.9 of the built structures. There, observations show that the unstable fundamental light ball experiences a decrease in amplitude as it propagates and simultaneously gets expanded radially. In contrast, the stable fundamental light bullet maintains a constant amplitude and radius at the same distance of propagation. The scenario is supported by a clockwise rotation of the optical vortex around the origin [see row (b) of Fig. 3.7], which differs from that of materials with a positive refractive index **[222]**.

Additionally, the sign of the topological charge imposes the rotation direction of the azimuthons, which is related to the negative diffraction in MMs. This is, for example, illustrated in Fig. 3.10, where $m = -6$ in panel (a) and $m = 6$ in panel (b). This, once more, confirms the main characteristic of vortex and solitons, which is accompanied by phase dislocation and nonzero angular momentum.

3.3.2 Necklace-ring solitons ($(n \neq 0$ or $q = 0)$

The optical wave packet described by Eq. ((3.13) becomes the necklace beams when $n \neq 0$ and $q = 0$, in which $2n$ determines the number of input lobes. In Fig. 3.8, it is confirmed that the number of azimuthal modes, for a multipole light bullet is $2n$, as we have fixed $n = 1$, $q = 0$ and $m = -6$. The light bullet, which exhibits six notches at $z = 10$, progressively merges into one structure, while notches disappear with increasing distance. The amplitude and the phase distribution show an initial presence of a dipole-type azimuth whose collective rotation leads to a single structure. In the rotational frame , there is a presence of six, then four lobes, probably

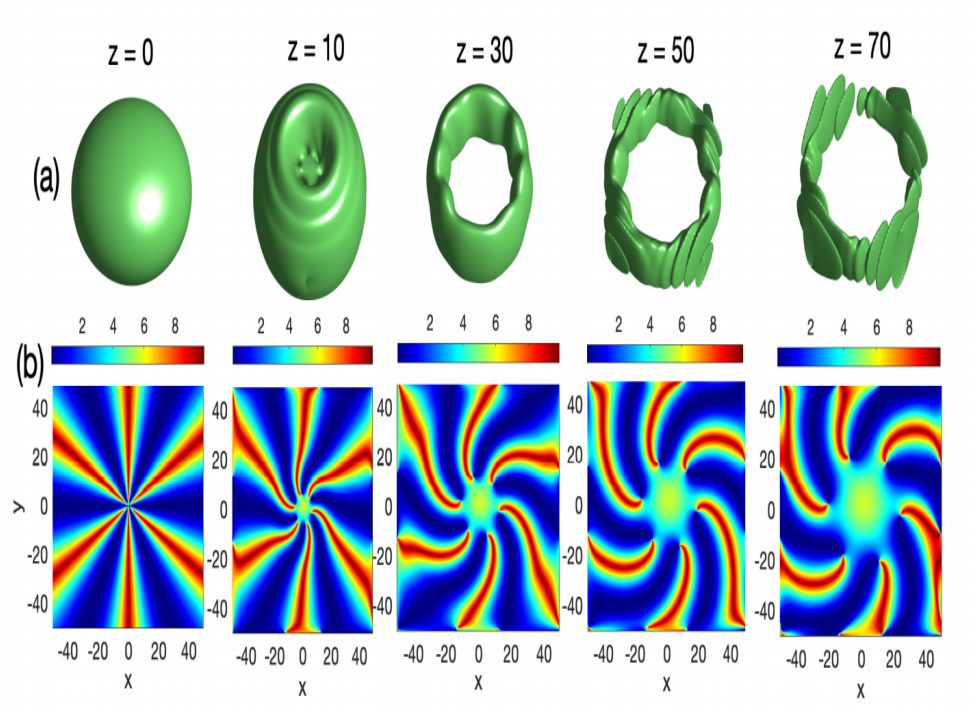

Figure 3.7: The upper row (a) shows the 3D isosurface evolution and progressive collapse of the fundamental light bullet with distance, for $m = -6$, $n = 0$ and $q = 1$, at $timet = 10$ and distances $z = 0$, $z = 10$, $z = 30$, $z = 50$ and $z = 70$, while the lower row (b) show the corresponding phase distribution in the (x, y)-plane. The parameters are: $\sigma_{r\perp} = -1$, $\sigma_{i\perp} = 0.25$, $k_{2i} = 0.5$, $k_3 = 0.01 + i0.21$, $k_4 = 0.1 + i0.001$, $k_5 = 0.21 + i0.1$, $k_6 = 2.1 + i0.66$, $\delta = -0.0079$, $N_3 = -1 + i0.12$, $N_5 = 1 - i2.65$, $N_7 = -0.05 + i0.02$, $SS_3 = -0.0001 - i0.02$, $SS_5 = 0.1 - i0.01$, and $SS_7 = 0.2 - i0.2$.

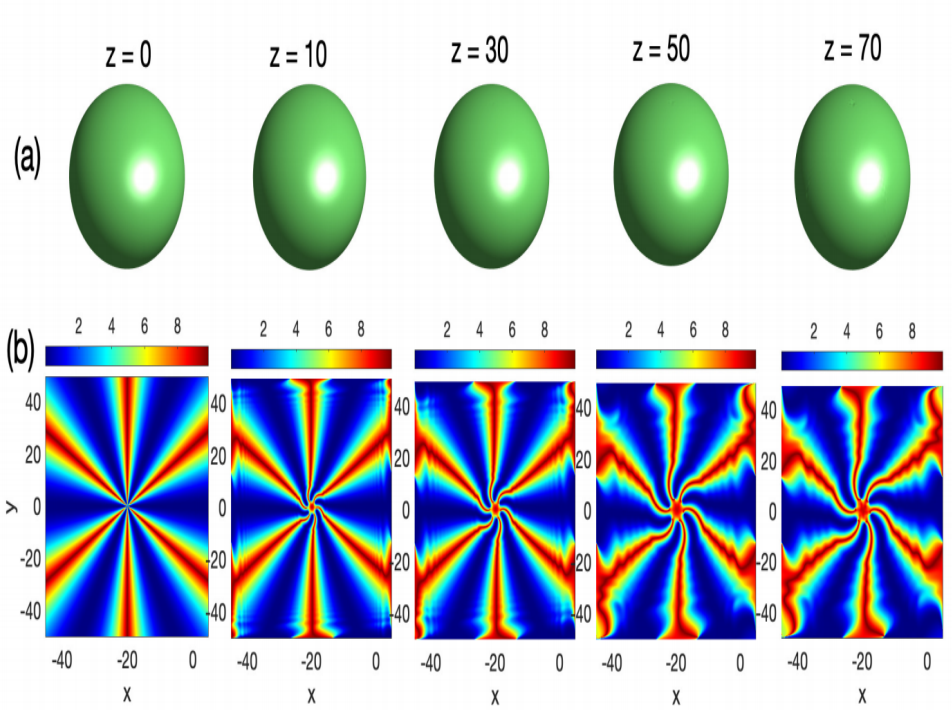

Figure 3.8: The upper row (a) shows the 3D isosurface evolution of the stabilized fundamental light bullet, for $m = -6$, $n = 0$ and $q = 1$, at time $t = 10$ and distances $z = 0$, $z = 10$, $z = 30$, $z = 50$ and $z = 70$, while the lower row (b) show the corresponding phase distribution in the (x, y)-plane. The parameters are: $\sigma_{r\perp} = -0.1$, $\sigma_{i\perp} = 0.25$, $k_{2i} = 0.5$, $k_3 = 3.1 + i2.21$, $k_4 = 0.1 + i0.01$, $k_5 = 2.21 + i0.1$, $k_6 = 0.1 + i0.66$, $\delta = -0.0079$, $N_3 =?1 + i0.12$, $N_5 = 1 - i2.65$, $N_7 = -0.05 + i0.02$, $SS_3 = -0.001 - i0.0001$, $SS_5 = 0.1 - i0.01$, and $SS_7 = -0.2 - i0.2$.

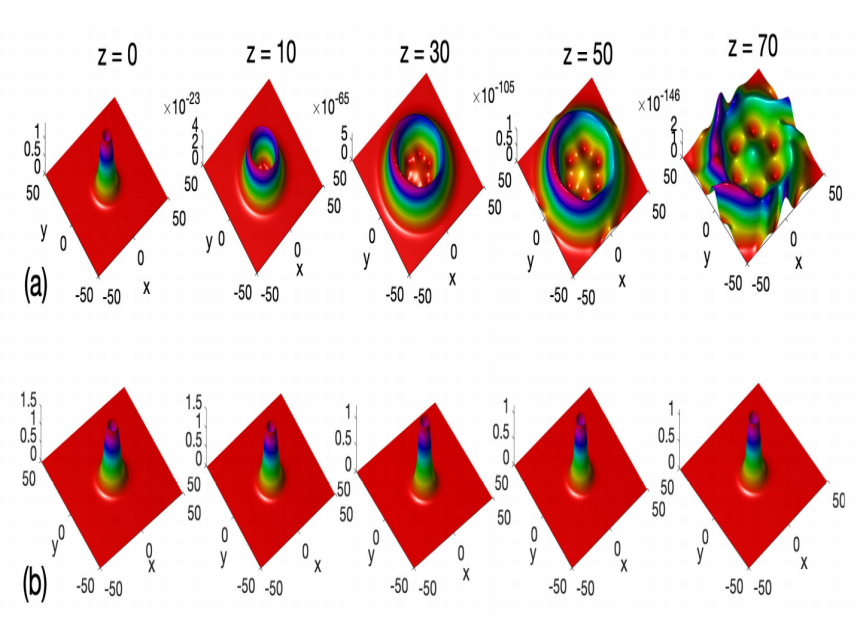

Figure 3.9: The upper row (a) corresponds to the amplitude evolution of the unstable light bullet of Fig. 3.7, while the lower row (b) displays the amplitude evolution of the stable fundamental light bullet of Fig. 3.8, with columns from left to right corresponding to the respective distances $z = 0$, $z = 10$, $z = 30$, $z = 50$ and $z = 70$.

induced by the notches appearing from a distance $z = 10$. To remind, azimuthons constitute a new class of optical beams spatially located in nonlinear media .

3.3.3 Azimuthon incidence($n \neq 0$ or $q \neq 1$)

Azimuthons are a new class of optical beams spatially located in nonlinear media introduced in Ref.**[224]**. They provide an important link between radially symmetrical vortices and soliton clusters rotating through the azimuthal modulation q defined Eq.(13). Azimuthons are characterized by two independent integers or azimuthal indices: the topological load m and the number of intensity peaks n. However, the visible rotation of azimutons can be directed along or opposite to the direction of the energy determined by the sign of the topological charge m, see **[225]**. Note that in MMs, the direction of azimuthons will always be opposed to that of materials with a positive refractive index due to negative diffraction in MMs.

The number of notches can be concluded to be determined by $\mathbf{min}|m \pm n|$, while the formation of nonzero TC rotates in different directions as presented in the corresponding phase

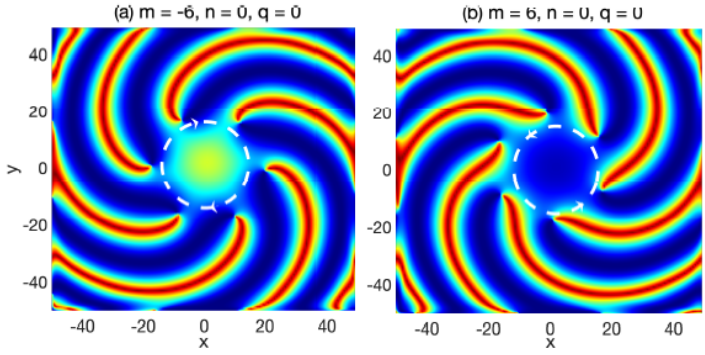

Figure 3.10: The panels show phase distributions of light bullets corresponding to opposite signs of the topological charge. This imposes opposite rotative frames of the azimuthons, as expected in negative-index metamaterials. For panel (a): $m = -6$, $n = 0$ and $q = 0$, while for (b): $m = 6$, $n = 0$ and $q = 0$, with the other parameters keeping their values.

distributions. This is illustrated by the features of Fig. 3.12, where, in the propagative frame, the hexapole light bullet rotates with the distance increasing until the unstable state of the fundamental light bullet is reached. This effectively corroborates the findings of Ref. **[226]**, which suggested the spontaneous formation of a cluster of four fundamental solitons in a cubic-quintic CGL equation in addition to the cubic and quintic self-steepening effects. However, for consistency, the panels of Fig. 3.13 show the propagation of a stable hexapole, under the same conditions where the light bullet of Fig. 3.8 was stabilized. Once more, the strong impact of the balance between higherorder dispersions and the rest of the parameters is emphasized, which once more confirms the importance of higher-order terms in the proposed model. Moreover, it was also confirmed that such structures had the tendency to merge into a single soliton as a final state, with some features of dromion. The same study revealed that the spatial expansion and the transition from vortex to azimuthon are very sensitive to system parameters, with exceptionally high self-steepening effects. Combined with the competition between nonlinearity and dispersion, loss, and gain, such effects may indeed affect the azimuthal modulation process with substantial consequences on the stability/instability of the propagating light bullet. An excellent example of such is summarized in Fig. 3.12. The amplitude evolution, displayed in Fig. 3.14, row (a), confirms the instability of such a structure, where the six notches progres-

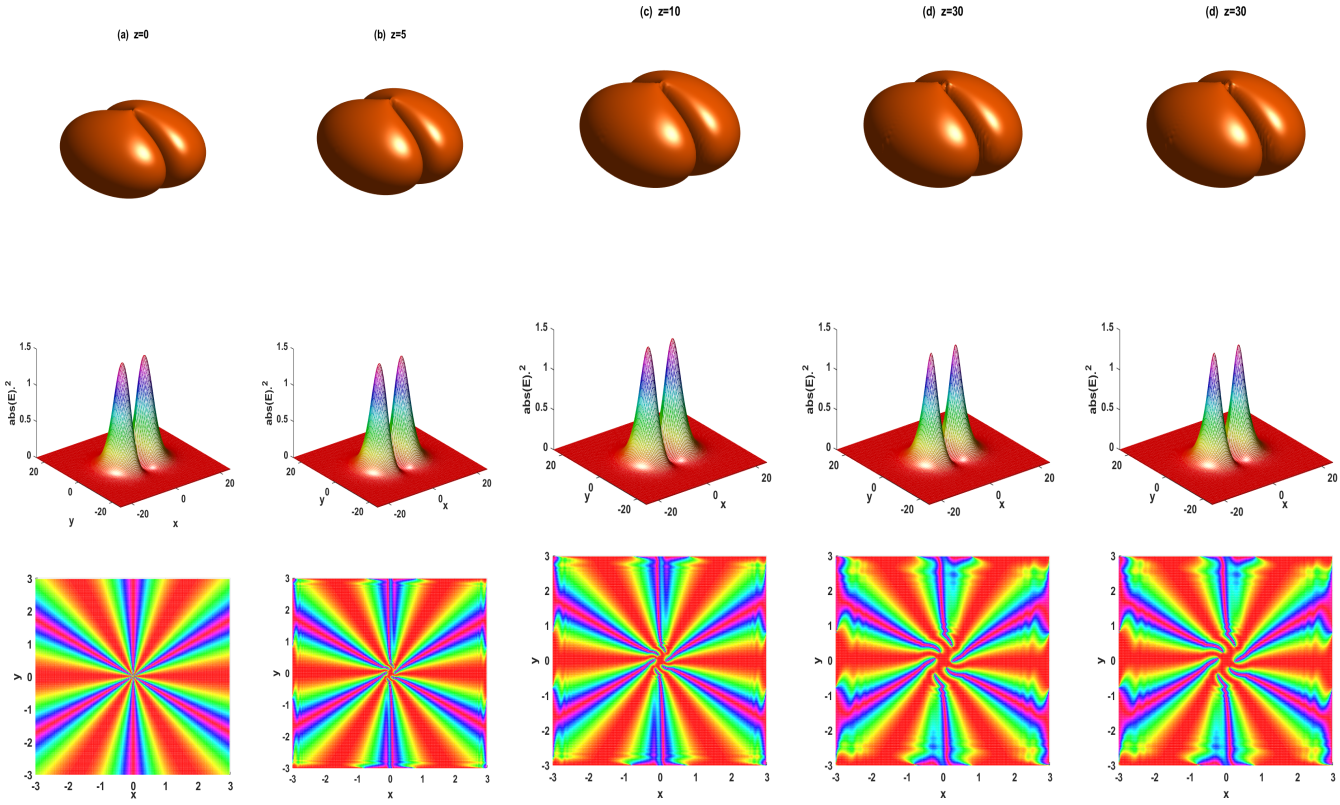

Figure 3.11: The upper row shows the evolution of a dipolar light bullet for $q = 0$, $n = 1$ and $m = -6$, at different propagation distances $z = 0$, $z = 5$, $z = 10$, $z = 30$ and $z = 50$,respectively. The lower rows display the amplitude $|E|^2$, and their corresponding phase distributions of the dipolar light bullet at time $t = 10$.

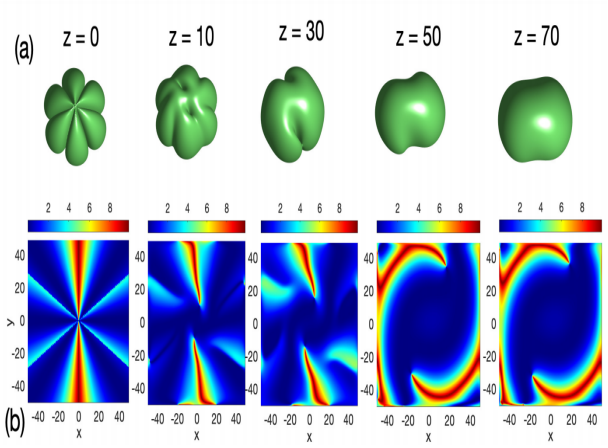

Figure 3.12: The upper row (a) shows the 3D isosurface evolution and progressive disintegration of a hexapole light bullet with distance, for $q = 0.5$, $n = 3$ and $m = 4$, at time $t = 10$ and distances $z = 0$, $z = 10$, $z = 30$, $z = 50$ and $z = 70$, while the lower row (b) show the corresponding phase distribution in the (x, y)-plane. The parameters are: $\sigma_{r\perp} = -0.1$, $\sigma_{i\perp} = 0.25$, $k_{2i} = 0.5$, $k_3 = 0.01 + i0.21$, $k_4 = 0.1 + i0.01$, $k_5 = 0.21 + i0.1$, $k_6 = 2.1 + i0.66$, $\delta = -0.0079$, $N_3 = -1 + i0.12$, $N_5 = 1 - i2.65$, $N_7 = -0.05 + i0.02$, $SS_3 = -0.0001 - i0.02$, $SS_5 = 0.1 - i0.01$, and $SS_7 = 0.2 - i0.2$.

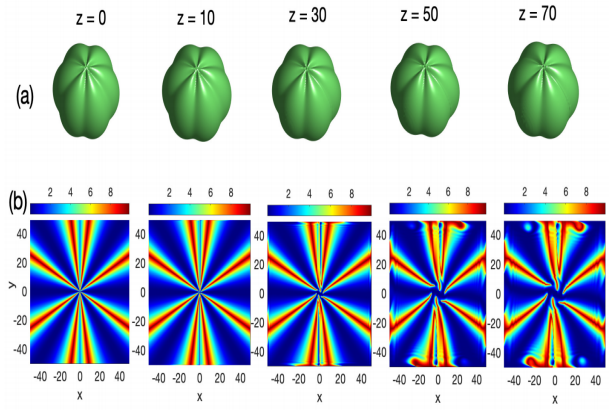

Figure 3.13: The upper row (a) shows the 3D isosurface evolution of a stabilized hexapole light bullet, for $m = 4$, $n = 3$ and $q = 0.5$, at time $t = 10$ and distances $z = 0$, $z = 10$, $z = 30$, $z = 50$ and $z = 70$, while the lower row (b) show the corresponding phase distribution in the (x, y)-plane. The parameters are: $\sigma_{r\perp} = -0.1$, $\sigma_{i\perp} = 0.01$, $k_{2i} = 0.5$, $k_3 = 3.1 + i2.21$, $k_4 = 0.1 + i0.1$, $k_5 = 2.21 + i1.01$, $k_6 = 0.1 + i0.66$, $\delta = -1.59$, $N_3 = -1 + i0.12$, $N_5 = 1 - i2.65$, $N_7 = -0.5 + i0.2$, $SS_3 = -0.001 - i0.00001$, $SS_5 = 0.1 - i0.01$, and $SS_7 = -0.2 - i0.2$.

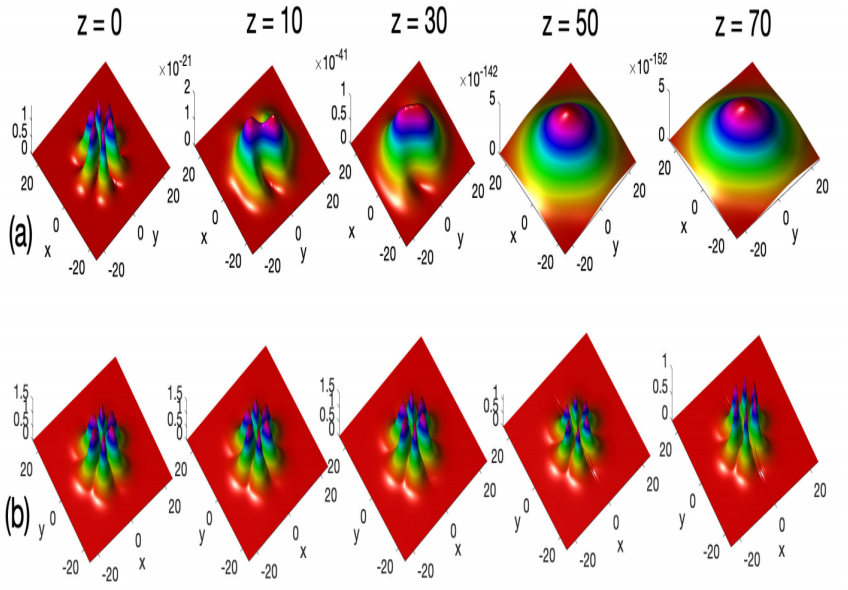

Figure 3.14: he upper row (a) corresponds to the amplitude evolution of the unstable hexapole light bullet of Fig. 3.12, while the lower row (b) displays the amplitude evolution of the stable hexapole light bullet of Fig. 3.13, with columns from left to right corresponding to the respective distances $z = 0$, $z = 10$, $z = 30$, $z = 50$ and $z = 70$.

sively merge into one structure, with the amplitude drastically dropping, as already noticed in Fig. 3.7. However, for positive real and negative imaginary parts of the septic self-steepening coefficient SS7, one gets a stable hexapole, that propagates without being disintegrated by distance, as noticed earlier. In another context, one instability figure, where the vortex does not get disintegrated, but the beam rather shrinks radially during propagation while its intensity tends to be localized on one leaf, is obtained by changing the value of the imaginary part of the septic self-steepening coefficient SS7 to -2 [see Fig. 3.15]. This may imply some energy concentration necessary to secure residual energy in the system. The appearance of a non-symmetric set of leaves in the light bullet distribution may result from low energy input, as argued by Eilenberger et al. **[228]**, which may require new stability properties necessary when higherorder dispersive nonlinearities are considered. The natural question that comes in mind is how the sixth-order dispersion (SOD) can completely compensate the septic nonlinearity in the formation conditions and existence regions of the solitary wave properties in MMs in the context of the Drude model, when the pulse width is below 10 fs.

The answer to such a question is important both for the fundamental physics and practical

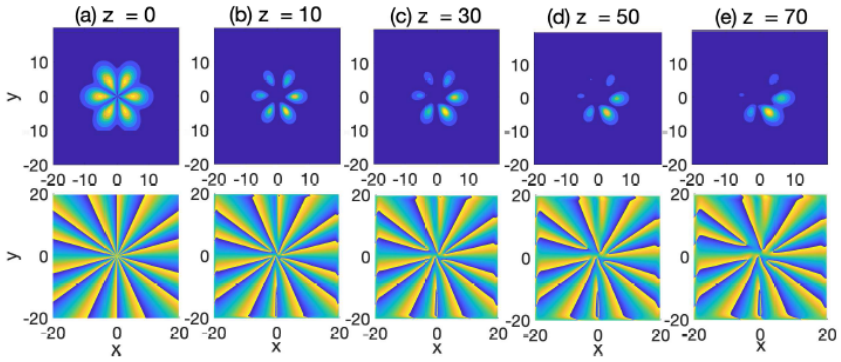

Figure 3.15: The upper panels show the dynamical disintegration of the vortex azimuthon related to Fig. 3.14 due to change of the value of the septic self-steepening coefficient. The lower row shows the corresponding phase distribution, at time $t = 10$, with $q = 0.5$, $n = 3$ and $m = 4$.

applications, since it has been proven experimentally by Cristiani et al. **[229]** that the inclusion of the higher-order dispersion terms up to thirteen allows a reliable description of the fiber dispersion behavior over a wide wavelength range and leads to a more accurate result. The presence of higher-order dispersion will represent new regimes for the generation of dispersive waves by soliton-like pulses propagating in the normal dispersion regime as well as in the anomalous dispersion regime in nonlinear fiber optics, and may provide important insights into the initial stages of supercontinuum generation. Additionally, they might provide a basis for finding further novel forms of solitary waves in MMs, and ensure their stability under suitable balance with the septic nonlinearity concomitantly with the other dispersive nonlinear contributions offered by our model, which couples with recent advances and future perspectives, therefore opening a new route for potential applications, for nanoscience and nanotechnology, in the emerging field of plasmonic MMs, for example.

3.4 conclusion

In this chapter, we have performed a detailed analytical and numerical study of modulational instability modeled by the CQ CGL equation with self steepening. Following the standard procedure of linear stability analysis, the expression for the MI gain has been proposed and the

effect of some key parameters, such as the cubic and quintic self-steepening parameters, on the occurrence of MI has been addressed, both under anomalous and normal GVD regimes. As the cubic and quintic self-steepening parameters, on the occurrence of MI has been addressed, both under anomalous and normal GVD regimes. The gain spectrum has revealed itself to be very sensitive to both self-steepening effects, which has been confirmed by direct numerical simulation, on the CQ CGL equation, using the split-step Fourier method. Initially, the MI manifested itself by cluster of four fundamental pulses, which, with increasing distance, displayed some features of inelastic collision, leading to a single complex solitonic object. However, with decreasing the quintic self-steepening parameter, the resulting solitonic complex has been found to be more coherent, with a dromion-like shape. The model equation that we have derived yields a corrected expression for the SVEA SS parameter, which essentially improves the description of the MI predicted by the improved growth rate spectrum for realistic MMs. In consequence, the obtained results, especially the emergence of clusters of localized pulses and their fusion over long propagation distance, make it possible to infer that a combination of competing cubic and quintic self-steepening terms can give rise to more complex behaviors, especially when there exists a suitable balance between such effects and dispersion, diffraction, loss, gain and cubic and quintic nonlinearities, some of the consequences being the formation of light bullets that constitute a hot topic in nonlinear optics nowadays.

We investigated the propagation in terms of simple vortex-necklace- and azimuthon shaped beams with higher-order nonlinearities and high-order dispersion. Under different configurations of the topological charge, the azimuthal modulation, and the number of input lobes. We have explored the behaviors of a fundamental light bullet, which has been found to disintegrate into new structures, whose implications have been discussed comprehensively, along with their rotational features in the phase distribution.

Chapter IV

General Conclusion

In this thesis, we have theoretically investigated the formation, the propagation of new classes of 3D spatiotemporal optical dissipative solitons in nonlinear MMs. In our contribution, we have started with the Maxwell's equations describing the response of the nonlinear medium to an electromagnetic wave. Then we have reported on the derivation of the (3+1)D cubic-quintic CGL equation, as well as the (3+1)D cubic-quintic-septic CGL equation, beyond the SVEA,includes the effects of two-dimensional transverse diffraction , the dispersion. The higher-order terms that are taen into account in the nonlinear dynamical model include: third-, fourth-, fifth and sixth-order dispersions, self-steepening effect in addition to septic nonlinearity. To understand the process of the formation and propagation of solitons, it was necessary to explain in detail the different notions that we have used in our investigations.

The thesis has been organized in three parts: In chapter I, we have presented the literature review on the metamaterials, the different types of metamaterials, electromagnetic properties of metamaterials, dissipative solitons and vortex soliton . In the second chapter, we have derived some new models and have presented the analytical method based on linear stability analysis,in the frame work. Details on the numerical methods used to achieve our goals have been provided. The last chapter has been devoted for the results of our investigations. Firstly, we have investigated, analytically and numerically, MI in nonlinear media. The contributions of cubic and quintic self-steepening parameters, on the occurrence of MI has been addressed, both under anomalous and normal GVD regimes. The gain spectrum has revealed to be very sensitive to both self-steepening effects, which has been confirmed by direct numerical simulation, on the CQ CGL equation, using the split-step Fourier method. Initially, the MI manifested itself by cluster of four fundamental pulses, which, with increasing distance, displayed some features of inelastic collision, leading to a single complex solitonic object. However, with decreasing the

quintic self-steepening parameter, the resulting solitonic complex has been found to be more coherent, with a dromion-like shape. Finally, simple vortex-necklace- and azimuthon shaped beams, using a generalized (3+1)D cubic-quintic-septic CGL equation with up to sixth-order dispersion and septic self-steepening, have been investigated. Under different configurations of the topological charge, azimuthal modulation, and the number of input lobes, we have explored the behaviors of a fundamental light bullet, which has been found to disintegrate into new structures, whose implications have been discussed comprehensively, along with their rotational features in the phase distribution. Based on that, clockwise and counterclockwise rotations of light bullet dynamics have been discussed with a specific interest in multipole light bullets. We have, for example, found that in the rotation frame, dipole, quadruple, and hexapole light bullets had the tendency to merge into one single structure: the fundamental light bullet. In addition, the sensitivity of such structures to changes in parameter values has been debated. It has been found that even though the shape of the wave object was conserved, the septic self-steepening may significantly affect energy distribution among individual solitons of the molecular structures.

This work may be interesting for all those, whether professionals or not, who want to refresh their knowledge and to obtain information or to find the appropriate keys for the better understanding of dissipative light bullets in nonlinear metamaterials.

Future directions

• This thesis does not address the important issue of the stability of solitary waves in the nonlinear optical systems considered. It could be one of the extremely potential areas of investigation in future and we will use the variational method for the azimuthon stability.

• We will investigate the modulational instability and bifurcation soliton with (3+1)D complex Ginzburg-Landau equation with the aim to generate the supercontinuum and study the cascading phenomena.

• Understanding and controlling the properties of optical vortices could lead to applications in the near future, ranging from optical communications and data storage to the trapping, control, and manipulation of particles and cold atoms.

• We will study evolution of this model and stationary homogeneous solutions for electric and magnetic field amplitudes in a ring cavity with flat mirrors.

APPENDIX

The value of parameters of Eq.(2.12)

$$\sigma_\perp = sgn(n) + 2i\frac{-k_i}{k_r^2},$$
$$k_{2r} = sgn\left(-\frac{Re[W_2]}{n\varpi}\right),$$
$$k_{2i} = \frac{Im[W_2]}{n\varpi}\left|\frac{n\varpi}{Re[W_2]}\right|,$$
$$k_{3r} = \frac{3}{6}\left(\left|\frac{n\varpi}{Re[W_2]}\right|\right)^{\frac{3}{2}}\left(\omega_p\frac{Re[W_3]}{n\varpi} - \frac{Re[W_2]c}{n^2\varpi^2 v_g}\right),$$
$$k_{3i} = \frac{3}{6}\left(\left|\frac{n\varpi}{Re[W_2]}\right|\right)^{\frac{3}{2}}\left(\omega_p\frac{Im[W_3]}{n\varpi} - \frac{Im[W_2]c}{n^2\varpi^2 v_g}\right),$$
$$k_{4r} = \frac{12}{24}\left(\left|\frac{n\varpi}{Re[W_2]}\right|\right)^{2}\left(\omega_p^2\frac{Re[W_4]}{n\varpi} - \frac{(Re[W_2])^2-(Im[W_2])^2}{4n^2\varpi^2} - \omega_p c\frac{Re[W_3]}{n^2\varpi^2 v_g}\right),$$
$$k_{4i} = \frac{12}{24}\left(\left|\frac{n\varpi}{Re[W_2]}\right|\right)^{2}\left(\omega_p^2\frac{Im[W_4]}{n\varpi} - \frac{Re[W_2]Im[W_2]}{2n^2\varpi^2} - \omega_p c\frac{Im[W_3]}{n^2\varpi^2 v_g}\right),$$
$$k_{5r} = \frac{60}{120}\left(\left|\frac{n\varpi}{Re[W_2]}\right|\right)^{\frac{5}{2}}\left(\omega_p^3\frac{Re[W_5]}{n\varpi} - \omega_p^2 c\frac{Re[W_4]}{n^2\varpi^2 v_g} - \omega_p\frac{(Re[W_2]Im[W_3]+Im[W_2]Re[W_3])}{n^3\varpi^3}\right),$$
$$k_{5i} = \frac{60}{120}\left(\left|\frac{n\varpi}{Re[W_2]}\right|\right)^{\frac{5}{2}}\left(\omega_p^3\frac{Im[W_5]}{n\varpi} - \omega_p^2 c\frac{Im[W_4]}{n^2\varpi^2 v_g} - \omega_p\frac{(Re[W_2]Re[W_3]-Im[W_2]Im[W_3])}{n^3\varpi^3}\right),$$
$$k_{6r} = \frac{360}{720}\left(\left|\frac{n\varpi}{Re[W_2]}\right|\right)^{3}\left(-\omega_p^4\frac{Re[W_6]}{n\varpi}+\omega_p^2\left(\frac{Re[W_2]Re[W_4]-Im[W_2]Im[W_4]}{4n^3\varpi^3}\right)+\omega_p^2\frac{Re[W_3]^2-Im[W_3]^2}{4n^3\varpi^3}+\omega_p^3 c\frac{Re[W_5]}{n^2\varpi^2 v_g}\right),$$
$$k_{6i} = \frac{360}{720}\left(\left|\frac{n\varpi}{Re[W_2]}\right|\right)^{3}\left(-\omega_p^4\frac{Im[W_6]}{n\varpi} + \omega_p^2\left(\frac{Re[W_2]Im[W_4]+Im[W_2]Re[W_4]}{4n^3\varpi^3}\right) + \omega_p^2\frac{Re[W_3]Im[W_3]}{2n^3\varpi^3} - \omega_p^3 c\frac{Im[W_5]}{n^2\varpi^2 v_g}\right),$$

$\delta = i\frac{\varpi}{2n}Im[\varepsilon\mu]$,

$$N_3 = sgn(\chi_r^{(3)}) + i\frac{\chi_i^{(3)}}{|\chi_r^{(3)}|},$$
$$N_5 = \frac{-\chi_r^{(5)}}{|\chi_r^{(3)}|} - \frac{\chi_r^{(3)}\chi_r^{(3)}-\chi_i^{(3)}\chi_i^{(3)}}{4n|\chi_r^{(3)}|} + i\left(\frac{-\chi_i^{(5)}}{|\chi_r^{(3)}|} - \frac{2\chi_r^{(3)}\chi_i^{(3)}}{4n|\chi_r^{(3)}|}\right),$$
$$N_7 = \frac{\chi_r^{(7)}}{|\chi_r^{(3)}|} + \frac{\chi_r^{(3)}\chi_r^{(5)}-\chi_i^{(3)}\chi_i^{(5)}}{4n|\chi_r^{(3)}|} + i\left(\frac{\chi_i^{(7)}}{|\chi_r^{(3)}|} + \frac{\chi_r^{(3)}\chi_i^{(5)}+\chi_r^{(5)}\chi_i^{(3)}}{4n|\chi_r^{(3)}|}\right),$$
$$SS_3 = -\frac{1}{\varpi}\left(1+\frac{1}{2nv_g}\right)\frac{\chi_i^{(3)}}{\left|\left(-\frac{\chi_r^{(3)}Re[W]}{n\varpi}\right)\right|} + i\left(\frac{1}{\varpi}\left(1+\frac{1}{2nv_g}\right)\frac{sgn(\chi_r^{(3)})}{\left|\left(-\frac{Re[W]}{n\varpi}\right)\right|}\right),$$
$$SS_5 = -\frac{1}{\varpi}\left(1+\frac{1}{2nv_g}\right)\frac{\chi_i^{(5)}}{\left|\left(-\frac{Re[W]}{n\varpi}\right)\right||\chi_r^{(3)}|} + i\left(\frac{1}{\varpi}\left(1+\frac{1}{2nv_g}\right)\frac{\chi_r^{(5)}}{\left|\left(-\frac{Re[W]}{n\varpi}\right)\right||\chi_r^{(3)}|}\right).$$
$$SS_7 = -\frac{1}{\varpi}\left(1+\frac{1}{2nv_g}\right)\frac{\chi_i^{(7)}}{\left|\left(-\frac{Re[W]}{n\varpi}\right)\right||\chi_r^{(3)}|} + i\left(\frac{1}{\varpi}\left(1+\frac{1}{2nv_g}\right)\frac{\chi_r^{(7)}}{\left|\left(-\frac{Re[W]}{n\varpi}\right)\right||\chi_r^{(3)}|}\right).$$

Bibliography

[1] S. A. Ramakrishna and T. M. Grzegorczyk, Physics and Applications of Negative Refractive Index Materials, CRC Press, 2009.

[2] W. Cai and Shalaev, Optical Metamaterials, Springer, 2010.

[3] V. G. Veselago, "The Electrodynamics of Substances with Simultaneously Negative Values of ϵ and μ" Soviet Physics Uspekhi, **10**, 509-514, (1968).

[4] D. Smith, W. Padilla, D. Vier, S. Nemat-Nasser, and S. Schultz, "Composite medium with simultaneously negative permeability and permittivity," Phys. Rev. Lett, **84**, 4184, (2000).

[5] J. Pendry, D. Schurig, and D. Smith, "Controlling electromagnetic fields," Science, **312**, 1780, (2006).

[6] W. T. Lu, J. B. Sokoloff, and S. Sridhar, "Refraction of electromagnetic energy for wave packets incident on a negative-index medium is always negative", Phys. Rev. E **69**, 026604 (2004).

[7] X. Huang and W. L. Schaich "Wavepacket propagation into a negative index medium", Am. J. Phys.**72**, 1232 (2004).

[8] A. A.Zharov, I. V. Shadrivov, and Y. S. Kivshar, "Nonlinear properties of left-handed meta-materials", Phys. Rev. Lett. **91**, 037401 (2003).

[9] M. Scalora, M. S. Syrchin, N. Akozbek, E. Y. Poliakov, G. D'Aguanno, N. Mattiucci, M. J. Bloemer, and A. M. Zheltikov, "Generalized nonlinear Schrodinger equation for dispersive susceptibility and permeability: application to negative index materials," Phys. Rev. Lett. **95**, 013902 (2005).

[10] S. Wen, Y. Wang, W. Su, Y. Xiang, and X. Fu, "Modulation instability in nonlinear negative-index material," Phys. Rev. E **73**, 036617 (2006).

[11] I. Kourakis, N. Lazarides, and G. P. Tsironis, Phys. Rev. E **75**, 067601 (2007).

[12] I. S. Aranson and L. Kramer, Rev. Mod. Phys. **74**, 99 (2002).

[13] N. N. Akhmediev and A. A. Ankiewicz, Solitons, Nonlinear Pulses and Beams (Chapman and Hall, London, 1997); Yu. S. Kivshar and B. A. Malomed, Rev. Mod. Phys. **61**, 763 (1989).

[14] V. Skarka and N. B. Aleksi´c, Phys. Rev. Lett. **96**, 013903 (2006); N. B. Aleksi´c, V. Skarka, D. V. Timotijevi´c, and D. Gauthier, Phys. Rev. A **75**, 061802(R) (2007); V. Skarka, D. V. Timotijevi´c, and N. B. Aleksi´c, J. Opt. A: Pure Appl. Opt. **10**, 075102 (2008).

[15] V. Skarka, N. B. Aleksic, and V. I. Berezhiani, Phys. Rev. A **81**, 045803 (2010).

[16] Z. Wu and Z. Wang, Nonlinear Dyn (2018). https://doi.org/10.1007/s11071-018-4494-5.

[17] M. Djoko, C. B. Tabi, and T. C. Kofané, Phys. Scr. **94**, 075501 (2019).

[18] G. P. Agrawal, Nonlinear Fiber Optics, Optics and Photonics, Academic Press, 2001.

[19] G. B. Whitham, Proc. Roy. Soc. London **283**, 238 (1965).

[20] T. B. Benjamin and J. E. Feir, J. Fluid Mech. **27**, 417 (1967).

[21] V. I. Bespalov and V. I. Talanov, JETP Lett. **3**, 307 (1966).

[22] V. I. Karpman, JETP Lett. **6**, 277 (1967).

[23] T. Taniuti and H. Washimi, Phys. Rev. Lett. **21**, 209 (1968).

[24] K. Tai, A. Hasegawa, and A. Tomita, Phys. Rev. Lett. **56**, 135 (1986).

[25] W. P. Hong, Optics Commun. **213**, 178 (2002).

[26] J. M. Soto-Crespo, N. Ahkmediev, and G. Town, J. Opt. Soc. Amer. B. **19**, 234 (2002).

[27] J. E. Rothenberg, Opt. Lett. **17**, 1340 (1992).

[28] B. L. Holian, R. Blumenfeld, and P. Gumbsch, Phys. Rev. Lett. **78**, 78 (1997).

[29] J. Pendry, A. Holden, W. Stewart, and I. Youngs, "Extremely low frequency plasmons in metallic mesostructures," Phys. Rev. Lett, **76**, 4773, (1996).

[30] J. Pendry, A. Holden, D. Robbins, and W. Stewart, "Low frequency plasmons in thin-wire structures," Journal of Physics : Condensed Matter, **10**, 4785, (1998).

[31] J. Pendry, A. Holden, D. Robbins, and W. Stewart, "Magnetism from conductors and enhanced nonlinear phenomena," IEEE transactions on microwave theory and techniques, **47**, 2075, (1999).

[32] R. A. Shelby, D. R. Smith, and S. Schultz, "Experimental verification of a negative index of refraction."Science, **292**, 77, (2001).

[33] J. Pendry, "Negative refraction makes a perfect lens," Phys. Rev. Lett. **85**, 3966, (2000).

[34] D. R. Smith, J. B. Pendry, and M. C. K. Wiltshire, "Metamaterials and negative refractive index," Science, vol. **305**, no. 5685, pp. 788 -792, 2004.

[35] J.Brown, "Artificial dielectrics having refractive indices less than unity," Proceedings of the IEEPart IV : Institution Monographs, **100**, 51, (1953).

[36] W. Rotman, "Plasma simulation by artificial dielectrics and parallel-plate media," Antennas and Propagation, IRE Transactions on, **10**, 82, (1962).

[37] W. Hardy and L. Whitehead, "Split-ring resonator for use in magnetic resonance from 200-2000 MHz," Review of Scientific Instruments, **52**, 213, (1981).

[38] S. Linden, C. Enkrich, M. Wegener, J. Zhou, T. Koschny, and C. Soukoulis, "Magnetic response of metamaterials at 100 terahertz," Science, **306**, 1351, (2004).

[39] C. Enkrich, M.Wegener, S. Linden, S. Burger, L. Zschiedrich, F. Schmidt, J. Zhou, T. Koschny, and C. Soukoulis, "Magnetic metamaterials at telecommunication and visible frequencies," Phys. Rev. Lett. **95**, 203901, (2005).

[40] S. Zhang, W. Fan, B. Minhas, A. Frauenglass, K. Malloy, and S. Brueck, "Midinfrared resonant magnetic nanostructures exhibiting a negative permeability," Phys. Rev. Lett. **94**, 37402, (2005).

[41] P. Gay-Balmaz and O. J. F. Martin, " Efficient isotropic magnetic resonators ", App. Phys. Lett.**5**, 939, (2002).

[42] Shah Nawaz BUROKUR, " Mise en oeuvre de métamatériaux en vue d'application aux circuits microonde et aux antennes ", Thèse de Doctorat, Novembre 2005.

[43] Christophe Caloz, Tatsuo Itoh, " Electromagnetic metamaterials : Transmission line theory and microwave applications ", 2, (2006).

[44] Badreddine Ouagague. Etude théorique et expérimentale et experimentale des métamatériaux et des thechnique d'agilité (MEmS, BST) pour la conception RF miniatures et reconfigurables. Micro et nanotechnologies/ Microélectronique. université Paul Sabatier-Toulousse III. tel-01071682.

[45] C. Caloz and T. Itoh, Electromagnetic Metamaterials: Transmission line theory and Microwave applications, Wiley Interscience, 2006.

[46] S. H. Lee, C. M. Park, Y. Mun Seo and C. K. Kim, "Reversed Doppler effect in double negative Metamaterials", Phys. Rev. B **81**, 241102 (2010).

[47] . S. Xi, H. Chen, T. Jiang, L. Ran, J. Huangfu,, B-I Wu , J. A. Kong, and M. Chen, "Experimental verification of reversed Cherenkov Radiation in Left-Handed Metamaterial", Phys. Rev.Lett. **103**, 194801 (2009).

[48] A. Lakhtakia, "On Planewave Remittances and Goos-Hänchen Shifts of Planar Slabs with Negative Real Permittivity and Permeability", Electromagnetics **23**, 71(2005).

[49] N. J. Zabusky and M. D. Kruskal, "Interaction of Solitons in a collisionless plasma and the recurrence of initial states", Phys. Rev. Lett. **15**, 240 (1965).

[50] J. Scott Russell, Report of 14th Meeting of the British Association for Advancement of Science, NewYork, September 311 (1844).

[51] G. B. Airy, "Tides and waves", In Hugh James Rose, et al. Encyclopaedia Metropolitana. Mixed Sciences **3**, 1817 (1841).

[52] G. G. Stokes, "On the theory of oscillatory waves", Transactions of the Cambridge Philosophical Society **8**, 441 (1847).

[53] H. Bazin, Recherches experimentales relatives aux remoux et a la propagation des ondes, in Recherches Hydrauliques, ed. By H. Darcy and H. Bazin.(1865).

[54] J. Boussinesq, "Théorie de l'intumescence liquide, applelée onde solitaire ou de translation, se propageant dans un canal rectangulaire", Comptes Rendus de l'Academie des Sciences **72**, 755 (1871).

[55] L. Rayleigh , "On waves", Phil. Mag. **1**, 257 (1876).

[56] D. J. Korteweg, G. de Vries, (1895), "On the change of form of long waves advancing in a eectangular canal, and on a new type of long stationary waves", Philosophical Magazine **39**, 422(1895).

[57] E. Fermi, J. Pasta, S. Ulam, "Studies of Nonlinear Problems", Los Alamos Sci. Lab. Rep., LA-1940 (1955).

[58] C. S. Gardner, J. M. Greene, M. D. Kruskal, and R. M. Miura, "Method for solving the Korteweg-de Vries equation", Phys. Rev. Lett. **91**, 1095 (1967).

[59] P. Lax, "Integrals of nonlinear equations of evolution and solitary waves", Comm. Pure Applied Math. **21**, 467 (1968).

[60] V. E. Zakharov and A. B. Shabat, "Exact theory of two-dimensional self-focusing and one dimensional self-modulation of waves in nonlinear media", Sov. Phys. JETP **37**, 823 (1972).

[61] A. Hasegawa and F. Tappert, "Transmission of stationary nonlinear optical pulses in dispersive dielectric fibers. I. Anomalous dispersion", Appl. Phys. Lett. **23**, 142 (1973).

[62] L. F. Mollenauer, R. H. Stolen, and J. P. Gordon, "Experimental observation of picosecond pulse narrowing and solitons in optical fibers", Phys. Rev. Lett. **45**, 1095 (1980).

[63] R. H. Stolen, L. F. Mollenauer, and W. J. Tomlinson, "Observation of pulse restoration at the soliton period in optical fibers", Opt. Lett. **8**, 186 (1983).

[64] T. Dauxois and M. Peyrard, "Physics of Solitons", Cambrige University Press (2006).

[65] A. Hasegawa and Y. Kodama, Solitons in Optical Communications, (Clarendon, Oxford University Press, Oxford, (1995)).

[66] H. A. Haus and W. S. Wong, Rev. Mod. Phys. **68**, 423 (1996).

[67] A. D. Boardman, O. Hess, R. C. Mitchell-Thomas and L.Velasco see front matter 2010 Elsevier B.V. doi:10.1016/j.photonics.2010.05.001.

[68] R.C. Yang, X. Min, J.P. Tian, W. Xue, W. Zhang, "New types of exact quasi-soliton solutions in metamaterials", Phys. Scr. **91**, 025201 (2016).

[69] M. Marklund, P. K. Shukla, L. Stenflo, "Ultrashort solitons and kinetic effects in nonlinear metamaterials", Phys. Rev. E **75** 037601 (2006).

[70] A. Ankiewicz, J.M. Soto-Crespo, N. Akhmediev, "Rogue waves and rational solutions of the Hirota equation", Phys. Rev. E **81**, 046602 (2010).

[71] J. R. de Oliveira, Marco A. de Moura, J. Miguel Hickmann, A. S. L. Gomes, "Self-steepening of optical pulses in dispersive media", J. Opt. Soc. Amer. B **9** 2025 (1992).

[72] D. J. Kaup, A. C. Newell," An exact solution for a derivative nonlinear Schrödinger equational", J. Math. Phys.**19**, 798,(1978).

[73] J.-d. He, J. Zhang, M.Y. Zhang, C.Q. Dai, "Analytical nonautonomous soliton solutions for the cubic-quintic nonlinear Schrödinger equation with distributed coefficients", Opt. Commun. **285** 755, (2012).

[74] J. Belmonte-Beitia, G. F. Calvo, "Exact solutions for the quintic nonlinear Schrödinger equation with time and space modulated nonlinearities and potentials", Phys. Lett. A, **373**, 448, (2009).

[75] A. K. Sarma Eur. Phys. J. D **62** 421, (2011).

[76] W. J. Liu , J. H. Xiao , J. Y. Yan and B. Tian Phys. Lett. A **376** 1344, (2012) .

[77] A. B. Kozyrev and D. W. Van der Weide Appl. Phys. Lett. **91** 254111 (2007).

[78] A. B. Kozyrev and D. W. Van der Weide J. Phys. D: Appl. Phys. **41** 173001 (2008).

[79] A. B. Kozyrev , I. V. Shadrivov and Y. S. Kivshar Appl. Phys. Lett. **104** 084105 (2014).

[80] Z. Wang , Y. Feng , B. Zhu , J. Zhao and T. J. Jiang. Appl. Phys. **107** 094907 (2010).

[81] Y. R. Shen, Principles of Nonlinear Optics (Wiley, New York, 1984).

[82] P. N. Butcher and D. N. Cotter, The Elements of Nonlinear Optics (Cambridge University Press, Cambridge, UK, 1990).

[83] R. W. Boyd, Nonlinear Optics (Academic Press, San Diego, CA, 1992).

[84] G. P. Agrawal, Fiber-Optic Communication Systems, (3rd Ed. New York: Wiley, (2002)).

[85] R. Y. Chiao, E. Garmire and C. H. Townes: Phys. Rev. Lett. **13** 479 (1964).

[86] Y. S. Kivshar and G. P. Agrawal, Optical solitons (2003).

[87] V. E. Zakharov, and A. B. Sharab, Exact theory of two-dimensional self-focosing and one-dimensional self-modulation of waves in nonlinear media. Sov. Phys. JETP, **34**, 62 (1972).

[88] V. N. Tsytovich, and R. Bingham, Arrest of wave collaps and transitional damping, Comments Plasma Phys. Controlled Fusion **14**, 361 (1992).

[89] G. Fibich, and G. Papanicolaou, Self-focusing in the perturbed and unperturbed nonlinear Schrödinger equation in critical dimension, SIAM J. Appl. Math. **60** 183 (1999).

[90] O. Bang, D. Edmundson, and W. Krolikowski, Collapse of incoherent light beam in inertial bulk Kerr media, Phys. Rev. Lett. **83** 5479 (1999).

[91] J. T. Manassah, Collapse of the two-dimensional spatial soliton in a parabolic-index media, Opt. Lett. **17** 1259 (1992).

[92] C. Sun, C. Barsi, and J. W. Fleischeur, Peakon profiles and collapse-bounce cycles in sef-focusing Spatial beamd, Opt. Express**16** 20676 (2008).

[93] C. Sulem and P. L. Sulem, The nonlinear Schrödinger equation: self-focusing and wave collapse,(Springer-Verlag, New York, (1999)).

[94] Y. Silberberg, Collapse of optical pulses, Opt. Lett.**15**, 1282 (1990).

[95] X. Liu, K. Beckwitt, and F.W. Wise, Two-dimensional optical spatiotemporal solitons in quadratic media, Phys. Rev. E **62**, 1328 (2000).

[96] X. Liu, L.J. Qian, and F.W. Wise, Generation of optical spatiotemporal solitons, Phys. Rev. Lett. **82**, 4631 (1999).

[97] Y. Linzon, I. Ilsar, D. Cheskis, R. Morandotti, J. S. Aitchison, and S. Bar-Ad, Near-¯eld imaging of nonlinear pulse propagation in planar silica waveguides, Phys. Rev. E **72**, 066607 (2005).

[98] B.A. Malomed, D. Mihalache, F. Wise, and L. Torner, Spatiotemporal optical solitons, J. Opt. B **7**, R53 (2005).

[99] Partha P. Banerjee and G. Nehmetallah, J. Opt. Soc. Am. B 23, 2348 (2006).

[100] A. Joseph and K. Porsezian, Phys. Rev. A **81** , 023805 (2010).

[101] Partha P. Banerjee and G. Nehmetallah, J. Opt. Soc.Am. B **24** , A69 (2007).

[102] M. Marklund, P. K. Shukla, and L. Stenflo, Phys. Rev.E **73** , 037601 (2006).

[103] Y. Xiang, X. Dai, S. Wen, J. Guo and D. Fan, "Controllable Raman soliton self- frequency shift in nonlinear Metamaterials", Phys. Rev. E **84**, 033815 (2011).

[104] P. Li, R. Yang, and Z. Xu, Phys. Rev. E **82** , 046603 (2010).

[105] J. Zhang, S. Wen, Y. Xiang, Y. Wang and H. Luo, "Spatiotemporal electromagnetic soliton and spatial ring formation in nonlinear Metamaterials", Phys. Rev. A **81**, 023829 (2010).

[106] J. Zhang, Y. Xiang, S. Wen and Y. Li, J. Opt. Soc. Am.B **31** , 45 (2014).

[107] V. K. Sharma , A. Goyal , T. S. Raju and C.N. Kumar, J. Mod. Opt. **60** , 836 (2013).

[108] N. N. Rosanov, Spatial Hysteresis and Optical Patterns (Springer, Berlin, (2002), Chap. 6).

[109] H. Haken, Synergetics, (Springer-Verlag, Berlin, 1983).

[110] N. Akhmediev, A. Ankiewicz, Dissipative Solitons, Springer, Berlin, 2005.

[111] H. Sakaguchi, D. V. Skryabin, Boris A. Malomed, Opt. Lett. **43**, 2688 (2018).

[112] N. N. Rosanov, N. V. Vysotina, A. N. Shatsev, D.V. Shadrivov, D.A. Powell, Y.S. Kivshar, Opt. Express **19**, 26500 (2011).

[113] N. N. Rosanov, N. V. Vysotina, A. N. Shatsev, A. S. Desyatnikov, Y.S. Kivshar, Phys. Rev. Lett. **108**, 133902 (2012).

[114] N. Lazarides, G. P. Tsironis, Phys. Rev. E **98** (2018) 012207.

[115] M. Lax, W. H. Louisell, and W. B. McKnight, Phys. Rev. A 11, 1365 (1975).

[116] G. P. Agrawal and D. N. Pattanayak, J. Opt. Soc. Am. A 69, 575 (1979).

[117] M. Couture and P. A. Belanger, Phys. Rev. A 24, 355 (1981).

[118] T. Takenaka, M. Yokota, and O. Fukumitsu, J. Opt. Soc. Am. A 2, 826 (1985).

[119] A. Wunsche, J. Opt. Soc. Am. A 9, 765 (1992).

[120] R. Borghi, M. Santarsiero, and M. A. Porras, J. Opt. Soc. Am. A 18, 1618 (2001).

[121] S. R. Seshadri, J. Opt. Soc. Am. A 19, 2136 (2002).

[122] S. R. Seshadri, J. Opt. Soc. Am. A 25, 2156 (2008).

[123] B. Crosignani, P. D. Porto, and A. Yariv, Opt. Lett. 22, 778 (1997).

[124] G. Baruch, G. Fibich and S. Tsynkov, Opt. Express 16, 13323 (2008).

[125] H. Wang and W. She, opt. Commun. 254, 145 (2005).

[126] F. Biancalana and C. Creatore, Opt. Express 16, 14882 (2008).

[127] S. I. Fewo, H. Moussambi, and T. C. Kofane, Phys. Scr. 84, 035002 (2011).

[128] P. Chamorro-Posada, G. S. McDonald, and G. H. C. New 45, 1111 (1198).

[129] M. D. Feit and J. A. Fleck, J. Opt. Soc. Am. B 5, 633 (1988).

[130] N. Akhmediev, A. Ankiewicz, and J. M. Soto Crespo, Opt. Lett. 18, 411 (1993).

[131] A. D. Boardman, K. Marinov, D. I. Pushkarov and A. Shivarova, Opt. and Quant. Electr. 32, 49 (2000).

[132] S. Chi and Q. Guo, Opt. Lett. 20, 1598 (1995).

[133] K. Marinov, D. I. Pushkarov and A. Shivarova, Phys. Scripta T84, 197 (2000).

[134] M. S. Syrchin, A. M. Zheltikov , and M. Scalora, Phys. Rev. A 69, 053803 (2004).

[135] T Brabec and F. Krausz, Phys. Rev. Lett. 78, 3282 (1997).

[136] V. Skarka, N. B. Aleksic, and V. I. Berezhiani, Phys. Rev. A **81**, 045803 (2010).

[137] A. A. Zharov, I. V. Shadrivov, and Y. S. Kivshar, Phys. Rev. Lett. **91**, 037401 (2003).

[138] A. Maluckov, Lj. Hadzievski, N. Lazarides, and G. P. Tsironis, Phys. Rev. E **77**, 046607 (2008).

[139] V. A. Vysloukh, Kvant. Elektron. (Moscow) **10**, 1688 (1983).

[140] N. Tzoar, and M. Jain, Phys. Rev. A **23**,1266 (1981).

[141] E. M. Dianov, A. Ya. Karasik, P. V. Mamyshev, A. M. Prokhorov, V. N. Serkin, M. F. Stel'makh, and A. A. Fomichev, Pis?ma Zh. Eksp. Teor. Fiz. **41**, 242 (1985).

[142] P. V. Mamyshev and S. V. Chernikov, Opt. Lett. **15**, 1076 (1990).

[143] H. Liu and S. Wen Acta Optica Sinica **56**, 6473 (2007).

[144] I.V. Shadrivov, A.B. Kozyrev, D.W. van der Weide, Y.S. Kivshar, Appl. Phys. Lett. **93** (2008) 161903.

[145] F. Yang and Y. Xue, J. of Phys: Conference Series **1815**, 012027 (2021).

[146] X. Min, R. Yang, J. Tian, W. Xue and J. M. Christian, Journal of Modern Optics **63**, S44 (2016).

[147] T. Mathanaranjan, D. Kumar, H. Rezazadeh, and L. Akinyemi, Opt. and Quant. Electron. **271** (2022).

[148] A.K. S. Ali , M. Z. Ullah , M. Lakshmanan, Phys. Lett. A **384**, 126744 (2020).

[8]

[149] I. Bendahmane et al. , Superlattices and Microstructures **114**, 53 (2018).

[150] V. A. Vysloukh, N. A. Sukhotskova, Sov. J. Quantum Electron. **17**, 1509 (1987).

[151] M. J. Potasek, Opt. Lett. **12**, 921 (1987).

[152] A. Hook, M. Karlsson, Opt. Lett. **18**, 1388 (1993).

[153] M. N. Z. Abou?ou, P. T. Dinda, C. M. Ngabireng, B. Kibler, and F. J. Smektala, Opt. Soc. Am. B **28**, 1518 (2011).

[154] M. Droques et al. Opt. Lett. **38**, 3464 (2013).

[155] C. G. Latchio Tiofack , A. Mohamadou , Alim , K. Porsezian and T. C. Kofane, J. Modern Opt. **59**, 972 (2012).

[156] V. L. Kalashnikov, A. Fernandez, and A. Apolonski, Opt. Express **16**, 4206 (2008).

[157] R. J. P. Engelen, Opt. Express **14**, 1658 (2006).

[158] H. Enns, and S. S. Rangnekar, Phys. Rev. A. **45**, 3354 (1992).

[159] A. Desyatnikov, A. Maimistov, and B. A. Malomed, Phys. Rev. E **61**, 3107 (2000).

[160] D. Mihalache, D. Mazilu, L-C. Crasovan, I. Towers, B. A. Malomed, A. V. Buryak, L. Torner, and F. Lederer, Phys. Rev. Lett. **88**, 073902 (2002).

[161] D. Mihalache, D. Mazilu, L.-C. Crasovan, B. A. Malomed, and F. Lederer, Phys. Rev. E **61**, 7142 (2000).

[162] S.Hädrich, J. Rothhardt, M. Krebs, F. Tavella, A. Willner, J. Limpert, A. Tünnermann, Optics Express **18**, 0242 (2010).

[163] Y. Chen, K. Beckwitt, F. Wise, B. Aiken, J. Sanghera, and I. D. Aggarwal, J. Opt. Soc. Am. B. **23**, 347 (2006).

[164] R.W. Ziolkowski, Opt. Express **11**, 662 (2003); R.W. Ziolkowski and A. D. Kipple, Phys. Rev. E **68**, 026615 (2003).

[165] M. Antonova, A. Biswas, "Adiabatic parameter dynamics of perturbed solitary waves", Commun. Nonlinear Sci. Numer. Simul. **14**, 734 (2009).

[166] M. Boiti, L. M. Martiona, F. Pempinelli, "Scattering of localized solitons in the plane", Phys. Lett. A **132**, 116 (1988).

[167] B. B. Kadomtsov, V. I. Petviashvilli, "On the stability of solitary waves in weakly dispersive media", Sov. Phys. Dokl. **15**, 539 (1970).

[168] A. Davey, K. Stewartson, "On three-dimensional packets of surface waves", Proc. R. Soc. London A **338** 101-117 (1974).

[169] R. Radha, M. Lakshmanan, "Dromion like structures in the (2 + 1)-dimensional breaking soliton equation", J. Math. Phys. **35** 4746 (1994).

[170] B. G. Konopelchenko, C. Rogers, "On (2 + 1)-dimensional nonlinear systems of Loewner type", Phys. Lett. A **158** 391 (1991).

[171] S. Y. Lou, "Dromion-like structures in a (3 + 1)-dimensional KdV-type equation, J. Phys. A **29** 5989 (1996).

[172] B. B. Thomas, B. Gambo, K. V. Kuetche, T. C. Kofane , "On periodic wave solutions to (1 + 1)-dimensional nonlinear physical models using the sine-cosine method", Acta Appl. Math. **110**, 945 (2010).

[173] J. Li, Y. Zhang, "Exact travelling wave solutions in a nonlinear elastic rod equation", Appl. Math. Comput. **202**, 504 (2008).

[174] W. Zhuang, S. Y. Zhang, "The strain solitary waves in a nonlinear elastic rod", Acta Mech. Sin. **20**20, 58 (1988).

[175] W. Zhuang, G. T. Zhang, "The propagation of solitary waves in a nonlinear elastic rod", Appl. Math. Mech. **7** 615 (1986).

[176] W. S. Duan, J. B. Zhao, "Solitary waves in a quadric nonlinear elastic rod", Chaos Solitons Fract. **11** 1265 (2000).

[177] B. Gambo, B. B. Thomas, K. V. Kuetche, T. C. Kofane, "Explicit series solutions to nonlinear evolution equations the sine-cosine method", Appl. Math. Comput. **215** , 4239 (2010).

[178] B. Gambo, B. B. Thomas, K. V. Kuetche, T. C. Kofane, "Dynamical system approach to a coupled dispersionless system: localized and periodic traveling waves", Chin. Phys. Lett. **26**, 060503 (2009).

[179] A. P. Sergey and G. P. Agrawal, "Do solitonlike Self-Similar Waves Exist in Nonlinear Optical Media?", Phys. Rev. Lett. **97**, 013901 (2006).

[180] S. R. Nodari, M. Conforti, G. Dujardins, "Modulational instability in dispersion-kicked optical fibers", Phys. Rev. A **92**, 013810 (2015).

[181] P. T. Dinda, A. B. Moubissi, K. Nakkeeran, Phys Rev E **64**, 016608 (2001).

[182] B. G. Onana Essama, J. Atangana, F. B. Motto, B. Mokhtari, E. C. Noureddine , and T. C. Kofane, Phys. Rev. E **90**, 032911 (2014).

[183] J. Fan, S. Jiang, Appl. Math. Lett. **16**, 435 (2003).

[184] G. D. Montesinos, M. I. Rodas-Verde, V. M. Pérez-García, M. Humberto, chao **15**, 033501 (2005).

[185] A. Ankiewicz, N. Akhmediev, and N. Devine, Optical Fiber Technology 13, **91** (2007).

[186] P. M. Morse, H. Feshbach, methods of Theoretical Physics, McGraw-Hill, (1953).

[187] V. Skarka and N. B. Aleksic, Phys. Rev. Lett. **96** 013903 (2006).

[188] Stephen Lynch Dynamical Systems with Applications using Matlab, Manchester, UK (2010).

[189] E. A. Kuznetsov and F. Dias, Bifurcations of solitons and their stability, (2011).

[190] G. P. Agrawal, Nonlinear Fiber Optics (Academic, San Diego, CA (1989).

[191] V. I. Karpman and E. M. Krushkal, Sov. Phys. JETP **28**, 277 (1969).

[192] Q. Chang, E. Jia, and W. Sun, J. Comput. Phys. 148, 397 (1999).

[193] T. R. Taha and M. J. Ablowitz, J. Comput. Phys. **55**, 203 (1984).

[194] R. H. Hardin and F. D. Tappert, SIAM Rev. Chronicle **15**, 423 (1973).

[195] R. A. Fisher andW. K. Bischel, Appl. Phys. Lett. **23**, 661 (1973); J. Appl. Phys. **46**, 4921 (1975).

[196] J. W. Cooley and J. W. Tukey, Math. Comput. **19**, 297 (1965).

[197] K. S. Yee, IEEE Trans. Antennas Propagat., **AP-14**, 302 (1966).

[198] G. P. Agrawal, Nonlinear Fiber Optics, 4th ed. Academic, New York 2007.

[199] T. B. Benjamin, J. E. Feir, "The disintegration of wave trains on deep water. Part 1. Theory", Journal of Fluid Mechanics **27**, 417 (1967).

[200] L. I. Zagryadskaya, L. A. Ostrovskii, "Observed self-influence of modulated waves in a nonlinear line", Transl. Radiophys. and Quantum Electronics **11**, 548 (1969).

[201] S. Sudo, H. Itoh, K. Okamoto, K. Kubodera, "Generation of 5 THz repetition optical pulses by modulation instability in optical fibers", Appl. Phys. Lett. **54** , 993 (1989).

[202] A. Hasegawa, "Generation of a train of soliton pulses by induced modulational instability in optical fibers", Opt. let. **9**, 288 (1984).

[203] K. Tai, A. Hasegawa and A. Tomita, "Observation of modulational instability in optical fibers", Phy.Rev. Lett **56**,135 (1986).

[204] A. Höök and M. Karlsson, "Ultrashort solitons at the minimum-dispersion wavelength: effects of fourth-order dispersion", Opt. Lett. **18**, 1388 (1993).

[205] A. R. Osborne, Nonlinear Ocean Waves and the Inverse Scattering Transform, Academic Press, New York 2010.

[206] A. H. Nayfeh, Introduction to Perturbation Techniques (Wiley, New York, 1981).

[207] J. A. Sanders, F. Verhulst, and J. Murdock, Averaging Methods in Nonlinear Dynamical Systems (Springer, New York, 2007).

[208] A. Kenfack Jiotsa and T. C. Kofané, J. Phys. Soc. Jpn. **72**, 1800 (2003).

[209] X.-D. Zhao, Z.W. Xie, and W. Zhang, Phys. Rev. B **76**, 214408 (2007).

[210] A. Freise, K. Strain, D. Brown, and C. Bond, Living Rev. Relat. **13**, 1 (2010).

[211] M. M. Petroski, M. S. Petrovi´c, and M. R. Belić, Opt. Commun. **279**, 196 (2007).

[212] C. S. Panguetna, C. B. Tabi, and T. C. Kofané, Phys. Plasmas **24**, 092114 (2017).

[213] W. Liu, Y. Zhang, Z. Luan, Q. Zhou, M. Mirzazadeh, M. Ekici, and A. Biswas, Nonlin. Dyn. **196**, 729 (2019).

[214] W.-P. Zhong, M. R. Beli´c, G. Assanto, B. A. Malomed, and T. Huang, Phys. Rev. E **83**, 043833 (2011).

[215] S.-L. Xu, G.-P. Zhao, M. R. Beli´c, J.-R. He, and L. Xue, Opt. Express **25**, 9094 (2017).

[216] M. Soljacić, S. Sears, and M. Segev, Phys. Rev. Lett. **81**, 4851 (1998)

[217] Y. J. He, B. A. Malomed, and H. Z. Wang, Opt. Express **15**, 17502 (2007).

[218] Y. Q. Zhang, S. Skupin, F. Maucher, A. G. Pour, K. Q. Lu, and W. Królikowski, Opt. Express **18**, 27846 (2010).

[219] D. Buccoliero, A. S. Desyatnikov, W. Krolikowski, and Y. S. Kivshar, Phys. Rev. Lett. **98**, 053901 (2007).

[220] Z. K. Wu, Z. P. Wang, H. Guo, W. Wang, and Y. Z. Gu, Opt. Express **25**, 30468 (2017).

[221] Shafeeque Ali, A. K., Govindarajan, A., Lakshmanan, M.: Stabilization of light bullets in nonlinear metamaterial waveguides. Phys. Rev. A **105**, 033516 (2022).

[222] Wu, Z., Wang, Z.: Optical vortices in the GinzburgLandau equation with cubic-quintic nonlinearity. Nonl.Dyn. **94**, 2363 (2018).

[223] Z. Wu and Z. Wang, Nonl. Dyn. **94**, 2363 (2018).

[224] S. Gatz and J. Herrmann, Opt. Lett. **17** 484 (1992).

[225] L. Coutaz and M. Kull, J. Opt. Soc. Am. B **8** (1991) 99.

[226] L. T. Megne, C. B. Tabi, and T. C. Kofane, Phys. Rev. E **102**, 042207 (2020).

[227] F. Eilenberger, K. Prater, S. Minardi, R. Geiss, U. Röpke, J. Kobelke, K. Schuster, H. Bartelt, S. Nolte, A. Tünnermann, and T. Pertsch, Phys. Rev. X **3**, 041031 (2013)

[228] Eilenberger, F., Prater, K., Minardi, S., Geiss, R., Röpke, U., Kobelke, J., Schuster, K., Bartelt, H., Nolte S., Tünnermann, A., Pertsch, T.: Observation of discrete, vortex light bullets. Phys. Rev. X **3**, 041031 (2013).

[229] I. Cristiani, R. Tediosi, L. Tartara, and V. Degiorgio, Opt Express **12**, 124 (2004).

List of Publications

[1] Laure Tiam Megne, Conrad B. Tabi and Timoléon C. Kofané, "*Modulation instability in nonlinear metamaterials modeled by a cubic-quintic complex Ginzburg-Landau equation beyond the slowly varying envelope approximation*", PhysRevE. **102**, 042207 (2020).